Carbon Dioxide Sequestration in Cement-Based Materials: Carbonation Treatment of Recycled Concrete Powder

Kay Farrugia

Dissertation submitted to the Faculty for the Built Environment, University of Malta in part of fulfilment of the requirements for the attainment of the degree of Master in Engineering (Structural Engineering)

December 2025

DEDICATED TO MY FAMILY and KEITH

Acknowledgements

I would like to express my sincere gratitude to Professor Ruben Paul Borg, my supervisor, for his expert guidance and invaluable feedback during the course of this research and dissertation writing.

I would also like to express my appreciation to Mr. Nicholas Azzopardi and Mr. Alex Falzon, the Laboratory Technicians from the Faculty for the Built Environment, for their assistance and technical support during the experimental procedures.

Special thanks go to Dr. Marie Christine Scicluna, and Prof. Ulrich Baisch, Department of Chemistry – CrEMa Laboratories for the provision of solid-state analytical data, Dr. Roderick Abdilla, Mr. Mark Zerafa, Mr. Jonathan Spiteri from the Department of Chemistry, and Ing. James Camilleri from the Department of Metallurgy and Materials Engineering for providing essential research resources.

Finally, I thank my family and Keith, for their unwavering belief, encouragement and continuous moral support.

L-Università ta' Malta

FACULTY/INSTITUTE/CENTRE/SCHOOL for the Built Environment

DECLARATIONS BY POSTGRADUATE STUDENTS

(a) Authenticity of Dissertation

I hereby declare that I am the legitimate author of this Dissertation and that it is my original work.

No portion of this work has been submitted in support of an application for another degree or qualification of this or any other university or institution of higher education.

I hold the University of Malta harmless against any third party claims with regard to copyright violation, breach of confidentiality, defamation and any other third party right infringement.

(b) Research Code of Practice and Ethics Review Procedures

I declare that I have abided by the University's Research Ethics Review Procedures. Research Ethics & Data Protection form code BEN-2024-00109.

As a Master's student, as per Regulation 77 of the General Regulations for University Postgraduate Awards 2021, I accept that should my dissertation be awarded a Grade A, it will be made publicly available on the University of Malta Institutional Repository.

This dissertation utilises materials and methods produced and developed by Prof. Ruben Paul Borg. These innovations are currently being registered as Intellectual Property through the University of Malta's Knowledge Transfer Office (KTO).

All information in this dissertation is confidential. It may not be shared or used without written permission from both the supervisor and the KTO.

Abstract

Urbanisation growth has brought about (i) an increased use of concrete and consequently an increase in Cem I production which is a major contributor to carbon dioxide (CO_2) emissions and (ii) an increase of construction and demolition waste (C&DW).

The objective of this study is to explore ways of how to provide a partial Cem I replacement whilst mitigating the problems mentioned above, namely by (i) reducing CO_2 emissions by using CO_2 captured during cement production in a process to produce supplementary cementitious material and (ii) using recycled concrete from construction and demolition waste in the afore-mentioned process to produce supplementary cementitious material (SCM).

This dissertation focuses on the production of recycled concrete powder (RCP) and its activation via different treatment methods, to identify the process which yields the best supplementary cementitious material. Treatment processes researched in this dissertation included calcination, dry carbonation, aqueous carbonation, calcination followed by dry carbonation, calcination followed by aqueous carbonation and limewater soaking followed by dry carbonation.

Initially, characteristic testing was done on the various treated powders to determine their physical and chemical properties. This was followed by the assessment of these treated powders when introduced as a 20% cement replacement within the mix design of paste and mortar samples, to determine their fresh, mechanical and durability properties.

Calcination treatment achieved a material with the highest pozzolanic activity, as XRD results showed it to have the highest percentages of portlandite, tobermorite, gismondine, and belite at 17.4%, 12%, 2.1% and 17.2% respectively, when compared to the other treated samples. Through XRD, compressive strength and durability testing, it was determined that both dry and aqueous carbonation treatments also yielded materials with potential to be suitable supplementary cementitious material.

The combined calcination and carbonation treatments yielded the best chemical and mechanical results due to the formation of both calcite and hydrated phases, creating materials of increased reactivity and strength. The dry carbonation in the calcination and dry carbonation process contributed to produce a material with better properties than that produced in the calcination and aqueous carbonation treatment. In fact, calcination followed by dry carbonation achieved the highest compressive strength of 114.90 MPa at 21 days, surpassing that of the cement control.

Keywords: CO_2 Sequestration, Construction and Demolition Waste, Recycled Concrete Powder, Supplementary Cementitious Material, CO_2 Treatment, Dry Carbonation, CO_2 Concentration, Aqueous Carbonation, CO_2 Flow Rate, Heat Treatment, Calcite, Compressive Strength

Table of Contents

List of Tables

List of Figures

Abbreviations

AFm	Aluminate-Ferrite-Monosulfate (Monosulfate)
AFt	Aluminate-Ferrite-Trisulfate (Ettringite)
Al_2O_3	Aluminium Oxide (Alumina)
As_2O_3	Arsenic Trioxide
B/S Ratio	Binder to Sand Ratio
Br	Bromine
C&DW	Construction and Demolition Waste
C_3A	Tricalcium Aluminate
C_3S	Tricalcium Silicate (Alite)
C_4AF	Tetracalcium Aluminoferrite (Ferrite)
$Ca(OH)_2$	Calcium Hydroxide (Portlandite)
Ca/Si Ratio	Calcium/Silicon Ratio
$CaCO_3$	Calcium Carbonate (Calcite)
CaO	Calcium Oxide
C-A-S-H	Calcium Aluminosilicate Hydrate (Gismondine)
CdO	Cadmium Oxide
Cl	Chlorine
CO_2	Carbon Dioxide
CoO	Cobalt (II) Oxide
Cr_2O_3	Chromium (III) Oxide
C-S-H	Calcium Silicate Hydrate (Tobermorite)
CuO	Copper (II) Oxide
Fe_2O_3	Iron (III) Oxide
FTIR	Fourier-Transform Infrared Spectroscopy
Ga_2O_3	Gallium Trioxide
GeO_2	Germanium Dioxide
GGBF	Ground Granulated Blast Furnace
H^+	Hydrogen Ion
H_2O	Dihydrogen Monoxide (Water)
HCO_3^-	Bicarbonate Ion
HCP	Hydrated Cement Paste
K_20	Potassium Oxide
KBr	Potassium Bromide
MgO	Magnesium Oxide
MnO	Manganese (II) Oxide
Na_20	Sodium Oxide
NiO	Nickel (II) Oxide
NMR Testing	Nuclear Magnetic Resonance Testing
OPC	Ordinary Portland Cement

P_2O_5	Phosphorus Pentoxide
PSD	Particle Size Distribution
Rb_2O	Rubidium Oxide
RCA	Recycled Concrete Aggregate
RCP	Recycled Concrete Powder
rpm	Revolution per Minute
SCM	Supplementary Cementitious Material
SEM	Scanning Electron Microscope
SeO_2	Selenium Dioxide
Si-O frequency	Silicon Oxygen Stretching Frequency
SiO_2	Silicon Dioxide (Silica)
SnO_2	Tin (IV) Oxide
SO_3	Sulphur Trioxide
SP	Superplasticizer
SrO	Strontium Oxide
TiO_2	Titanium Dioxide
V_2O_5	Vanadium Pentoxide
W/B Ratio	Water to Binder Ratio
XRD	X-Ray Diffraction
XRF	X-Ray Fluorescence
Y_2O_3	Yttrium (III) Oxide
ZnO	Zinc Oxide
ZrO_2	Zirconium Dioxide
β-C_2S	Dicalcium Silicate (Belite)
S.	Satisfied
N.S.	Not Satisfied

CHAPTER 1 - Introduction

1.1 Motivation Behind Research

Over the last 65 years there has been rapid population and urbanization growth attributed to the changes and/or improvements in the world's economy, in combination with political, technological and medical advancements. During this period the percentage of the world's population residing within urban context has increased from 30% to 54%. It is estimated that within the next 35 years this percentage will rise to 66%, equivalent to a 2.5 billion increase in urban area population (Miller et al., 2016).

This population and urban expansion has led to a high strain on the world's natural resources, causing drastic climate change concerns. Atmospheric Carbon Dioxide - a greenhouse gas within the global atmosphere - has increased drastically since the 18th century due to human activities, which is one of the main factors for such climate change issues (Wu et al., 2024).

A statistical study found that approximately 36.8 billion tons of carbon dioxide (CO_2) were emitted in 2022, 5-8% of which were a result of the construction industry (Wu et al., 2024). Increased urbanization has brought about a larger demand for infrastructure development (Miller et al., 2016), leading to an increase in construction material consumption. The majority of the material being used is concrete, having an annual production of approximately 30 billion tons (Kazemian & Shafei, 2023). The main component that makes up concrete is Cem I, production of which results in approximately one ton of CO_2 released per 1 ton production of Cem I, making it the main problematic source (Kazemian & Shafei, 2023). Additionally, the disposal of the large quantities of construction and demolition waste (C&DW) are also posing environmental problems (J. Li et al., 2024).

Thus, carbon peak and neutrality strategies within the construction materials industry have become a worldwide sustainability goal (J. Li et al., 2024). These strategies are also intended to reach the targets set out by the United Nations' Sustainable Development Goals namely Targets 9.4 and 9.5 aimed at upgrading industry infrastructure coupled by enhanced scientific research to provide a cleaner and more efficient industrial process, Targets 12.2, 12.4 and 12.5 aimed at the sustainable and efficient use of natural resources and waste, and Target 13.2.2 specifically aimed at reducing the total greenhouse gas emissions.

1.2 Problem Mitigation

The use of concrete and hence Cem I within the construction industry is of major importance and cannot simply be omitted. Alternative solutions to reduce the use of cement are required as a means for the reduction in CO_2 emissions.

In past years, research has focused on finding or creating a viable enough material that possesses cementitious properties, that could potentially be used as a full replacement or complement to Cem I. Studies on materials such as fly ash and ground granulated blast furnace and their viability to be used as a supplementary cementitious material (SCM) have grown in popularity. However, recent studies have attempted to focus on other alternative materials, such as recycled concrete that may produce adequate results.

In the meantime, the construction industry is facing issues with regards to the continuously increasing amounts of waste material produced from demolition. A potential mitigation measure for this problem is to transform C&DW into a suitable SCM, such as recycled concrete powder (RCP). Research on such an application is growing. However, due to RCP being a non-highly reactive material, its viability as a

sufficient SCM is still questionable. Thus, attempts to increase the reactivity of RCP are being studied but the research is still limited (Al-Janabi et al., 2024).

Another solution to the reduction in the carbon footprint is CO_2 sequestration. More specifically, studies are focusing on capturing and storing carbon dioxide prior to its release, to be used as a treatment process within concrete production (Kazemian & Shafei, 2023). Research has explored the use of carbonation to improve properties of concrete as well as other cementitious materials, and more recently, the stabilizing effect carbonation treatment has on construction waste material (Kazemian & Shafei, 2023).

Hence, carbonation treatment has gained increasing interest in solving both problems mentioned previously: reduction in CO_2 emissions and increasing the reactivity of RCP.

1.3 Scope and Objectives

The scope of this research is to reduce the amount of C&DW being disposed of and making beneficial use of the CO_2 produced during cement production. This shall be achieved by utilizing the captured CO_2 to perform a carbonation treatment process, which aims to transform and stabilize recycled concrete obtained from C&DW into a sufficient and reactive SCM, such as RCP.

The aim of such a process is to reduce the overall amount of cement required for concrete production and hence, the CO_2 emissions it brings with it, all the while extracting already produced CO_2 and creating a useful material out if it.

1.4 Layout of Dissertation

The dissertation is split into 4 main chapters, which include:

Chapter 2:

explores the reasoning and theory behind the scope and objectives of this dissertation. It does so through the review of literature, where the background of carbonation of RCP and its development and beneficial properties and characteristics produced, is understood. It also explores the use of other treatment processes and their explanation, that may result in a more improved material once combined with carbonation treatment. Finally, this chapter describes how the parameters chosen for treatment conditions, curing conditions, water to cement ratio, and the percentage cement replacement chosen, may affect the final characteristics of the product.

Chapter 3:

covers the research methodology used. It outlines the material production and preparation process involving the applied treatments on the raw material, then delves into the mix design and sample preparation of both pastes and mortar. Additionally, this chapter explains the testing procedures applied to all cast samples.

Chapter 4:

presents and explains the test results obtained. This chapter identifies any data patterns found within the results and analyses them. Such analysis helps identify influencing factors that might affect the results both positively and negatively.

Chapter 5:

presents the main conclusions obtained from the results' analysis and provides research limitations and recommendations for improved results within future studies.

CHAPTER 2 – Data Mining & Literature Review

PART 1: Data Mining Analysis Exercise

The initial process of reviewing various literature and gathering research regarding carbon dioxide sequestration was done in collaboration with foreign researchers whose expertise lies in concrete science and the development of machine learning for construction materials. These researchers were carrying out a data mining analysis exercise, towards which the data gathering and input also contributed.

This study having the title 'Optimization of CO_2 Curing Conditions for Sustainable Cementitious Materials using Machine Learning Approach' by Seongho Han, Jayon Kim, Kay Farrugia, Heejung Jun, Ruben Paul Borg, Jae Hong Kim and Jinyoung Yoon was eventually submitted for publication.

The objective of this research focused on predicting and optimising compressive strength and CO_2 uptake within cement-based materials using the Least Squares Boosting approach.

This required gathering information from various selected published literature on topics related to CO_2 sequestration using CO_2 curing and various SCM's. This data gathering included the compilation of data relating to binder type (including binder combination percentages), binder composition (through XRF testing), mixture proportions, pre-conditioning parameters, and CO_2 curing parameters.

Such data was then used to analyse the effects that relative humidity percentage, CO_2 concentration, curing duration and binder type have on compressive strength and CO_2 uptake. It was determined that compressive strength is influenced by the water to binder ratio, Steinour formula, curing duration and total curing age, while CO_2 uptake is dependant on relative humidity, CO_2 concentration and exposure time. The optimal curing conditions were obtained, and the corresponding results were found to be as follows:

- CO_2 Concentration = Above 15%
- Curing Duration = 72 hours
- Relative Humidity = Above 60%

This data mining exercise broadened the understanding on the variety of research that has been carried out on carbon dioxide sequestration and provided the initial background information that helped with streamlining the research topic of this dissertation. Complemented with additional research, the above-mentioned exercise was useful for the acquirement of knowledge on methodologies used, type of cement replacements and their optimum replacement percentages. It also provided information regarding carbonation curing and its optimal parameters to produce an effective sample.

Part 2: Literature Review

2.1. Overview

This chapter initially examines the negative implications of cement production and carbon dioxide (CO_2) sequestration. It then moves on to a discussion regarding the origin of recycled concrete powder (RCP), its characteristics, its use as a supplementary cementitious material (SCM) and its altering properties when subjected to various treatment methods. The optimal water to cement ratio and percentage replacement of RCP as an SCM is also discussed.

2.2. Production of concrete

Concrete is a material composed of water, cement, fine aggregate, coarse aggregate, and sometimes also admixtures or reinforcing fibres (these vary depending on the utilization). Due to its low cost and production simplicity (Miller et al., 2016), it is the world's most sought-after construction material with approximately 30 billion tons of annual production (Meng et al., 2022).

2.3. Portland Cement

Cem 1 (portland cement) is one of the main ingredients required to produce traditional concrete, and its production is increasing proportionally to that of concrete. The production of Cem I includes a calcination process throughout which burning of fossil fuels takes place to heat clay and limestone to approximately 1450 ^{o}C. As a result of this process, one ton of CO_2 is released per 1 ton of Cem I produced, causing the production of Cem I to be the third largest source of CO_2 through anthropogenic activities (Kazemian & Shafei, 2023).

2.4. Construction and Demolition Waste

As explained in the introduction chapter, the last 65 years has seen a rapid growth in population, urbanization, and industrialization. This has resulted in the generation of large quantities of construction and demolition waste (C&DW), having consequential effects on the environment and climate (J. Li et al., 2024).

This significant impact on the environment has prompted research on the possibilities of reusing and repurposing such materials, rather than landfilling waste material or extracting virgin material for new works (Mehdizadeh et al., 2021; Real et al., 2021). Waste from demolished buildings mainly consists of concrete and ceramic residues (Ruth Bola Oliveira et al., 2023), where such material can be repurposed as a type of recycled concrete material (Mao et al., 2023). This aims to reduce greenhouse gas emissions and natural resource consumption (Real et al., 2021).

2.4.1. Recycled Concrete Aggregate (RCA)

The past decades have seen multiple research on producing recycled concrete aggregates from concrete waste to be used as replacements to coarse and/or fine aggregates (Real et al., 2021).

2.4.1.1. Possible Benefits of RCA

RCA has useful benefits within the construction industry. It promotes circular economy through its use as an adequate substitute to natural aggregates. Such applications include employing it within new concrete mixes, backfilling, drainage systems, and pavement layers, which overall result in the reduction of landfilling waste and in the reduction of sourcing new material (Jeon et al., 2024).

In recent years, researchers have explored the possibility of also re-using carbon dioxide by enhancing the properties and microstructure of RCA through carbonation to improve its quality. This strategy also aids in response to climate change concerns (Jeon et al., 2024).

$$Ca(OH)_2\ (s) + HCO_3^-\ (aq) + H^+\ (aq) \rightarrow CaCO_3\ (s) + 2H_2O\ (l)$$

2.4.1.2. Challenges of RCA

A complication that recycled aggregates bring about, is the presence of adhered mortar. The microstructure of this adhered mortar tends to increase the porosity of the sample which has two main problems associated with it:

1. This will result in a sample having a higher water absorption when used within a concrete mix design and may create a product that has high fluidity and deformability (Ilki et al., 2023).
2. Its weak components produce a sample having an overall diminished strength leading to lower mechanical properties when compared to conventional natural aggregates, which is not effective enough to be used as a load-bearing support (Tang et al., 2023).

There are two main methods that are normally used to improve the recycled aggregate's performance. These are either by strengthening or removing the adhered mortar (Tang et al., 2023). Such methods involve carbonation treatment or mechanical grinding, respectively. The latter is currently the most common and simple method used for the removal process of this adhered mortar. However, this procedure tends to yield large amounts of cement paste powder (Mao et al., 2023).

2.4.2. Recycled Concrete Powder (RCP)

In continuation with the previous section, research within recent years has shifted focus on the production of cement replacement from recycled concrete. Hence, the focus of this dissertation will be on the production and activation of RCP to be used as a SCM (Real et al., 2021).

2.4.2.1. Properties and Characteristics of RCP

RCP is the fine recycled aggregate remnants produced during the crushing process of concrete waste to create RCA. Test results have shown that as the particle size of the recycled aggregate becomes finer, the percentage of adhered mortar to the particle surface increased. This means that the finer the particles are, the more their chemical characteristics and composition resemble that of finely ground hardened cement paste, rather than that of finely ground aggregate (Al-Janabi et al., 2024).

Since it has similar properties to that of hardened cement paste, this material has growing interest as its microstructure is rich in calcium and silica which can help promote pozzolanic activity similar to that of fly ash. In more detail it contains compounds and phases such as:

1. Calcium Carbonate
2. Silicon Dioxide
3. Aluminate-Ferrite-Trisulfate Phase
4. Aluminate-Ferrite-Monosulfate Phase
5. Calcium Hydroxide
6. Calcium Silicate Hydrate
7. Unhydrated cement

Hence, it has great potential for cement replacement and CO_2 sequestration (Al-Janabi et al., 2024; Aquino Rocha & Toledo Filho, 2023; J. Li et al., 2024).

2.4.2.2. Challenges of RCP

RCP is obtained from the grinding process of RCA and this creates two main problems:

1. Relatively large mean particle size (D50 > 75µm)
   Larger particles means that the material tends to have high water demand, leading to unreliable performance (Al-Janabi et al., 2024; Aquino Rocha & Toledo Filho, 2023)

2. Low reactivity
   Low reactivity stems from the fact that the resulting material contains varied quantities of unhydrated and hydrated cement phases. Such phases include $Ca(OH)_2$ and C-S-H. The presence of these components can create a positive impact on the performance of the mortar. However, excessive quantities may create a dilution effect since the presence of a lower clinker content results in a strength reduction of the binder phase (Aquino Rocha & Toledo Filho, 2023; Tang et al., 2023).

Essentially, this means that when the cement was mixed with water it underwent hydration reactions to form hydrated cement phases such as C-S-H and $Ca(OH)_2$, which are now present within the RCP attained. These hydration reactions control the cement paste's/concrete's strength development and hardening properties.

Hence, the excess presence of these hydrated phases within the recycled powder reduces the pozzolanic reaction, as once the recycled powder would be used as an SCM and added to water, there would be insufficient cement hydration due to its inert nature. This lack of reactivity is one of the material's main limiting factors and why it is frequently used as an inert filler within construction procedures rather than as a SCM (J. Li et al., 2024; Mehdizadeh et al., 2020).

Several alternative methods have been established and are being tested for the re-activation of RCP to improve their pozzolanic reactivity and be a viable alternative to cement. Some studies include the use of smaller particle sizes, carbonation treatment and thermal treatment, which all have been found to aid in the reactivity of the material (Mehdizadeh et al., 2020).

2.5. Carbon Dioxide Sequestration

CO_2 sequestration relates to the reduction of the carbon footprint generated by concrete production. The term sequestration might imply carbon dioxide removal/capturing, but in reality, its complete meaning refers to the aforesaid and the decrease of CO_2 emissions. Thus, a more precise explanation of the meaning of the term CO_2 sequestration is as follows:

1. Decrease in the production of CO_2 emissions;
2. CO_2 capturing and storing prior to its release, for its utilization throughout the production of concrete (Kazemian & Shafei, 2023).

The former explores options which include: the use of alternative fuels for the manufacturing process, making use of cement production plants that are electrically and thermally more efficient, choosing alternative cementitious materials, and the use of recycled concrete (Kazemian & Shafei, 2023).

The latter aims to use the captured CO_2 throughout the manufacturing process of concrete/mortars to eventually produce a concrete having similar properties to the norm. Main methods include carbonation curing, mineral carbonation, and passive carbonation (Kazemian & Shafei, 2023).

2.6. Carbonation Procedures of Cement-Based Materials

A Portland cement clinker is composed of C_3S, β-C_2S, C_3A and C_4AF. Alite and belite react with CO_2, resulting in an absorption capacity of CO_2 and a denser microstructure (Meng et al., 2022). This makes cement-based materials viable candidates for carbonation sequestration, which helps to compensate for the CO_2 emissions created during Cem I production.

Different approaches can be implemented to achieve CO_2 sequestration within cement-based materials. These include:

- Pre-carbonation during mixing, where CO_2 is introduced during concrete mixing;
- Accelerated carbonation, in which concrete curing occurs under high CO_2 pressures and/or concentrations;
- Weathering carbonation, wherein the concrete is subjected to CO_2 throughout its service life span (Meng et al., 2022).

2.6.1. Pre-carbonation during mixing

This procedure occurs when CO_2 is infused within concrete during the mixing process. This obliges any anhydrous calcium silicates alite and belite present within the mix to react with the introduced CO_2. This brings about the formation $CaCO_3$ and C-S-H gel, as can be seen through the equations below:

$$3CaOSiO_2 + (3\text{-}x)CO_2 + yH_2O \rightarrow xCaO{\cdot}SiO_2{\cdot}yH_2O + (3\text{-}x)CaCO_3$$

$$2CaOSiO_2 + (2\text{-}x)CO_2 + yH_2O \rightarrow xCaO{\cdot}SiO_2{\cdot}yH_2O + (2\text{-}x)CaCO_3$$

These reactions increase the compressive strength of the final sample, as well as improve the initial hydration reactions (Meng et al., 2022).

2.6.1.1. Carbonated Water

A recently developed method of how CO_2 is injected into the concrete mix is through carbonated water. It is a newly developed technology that replaces the normal water used within the concrete mix. In a study done by Meng et al. (2022) different concentrations of CO_2 were used. It was determined that the use of carbonated water improved the overall concrete sample's mechanical properties that were tested within 7 days. There was an increase in the samples compressive strength when compared to the control. This occurred due to the fact that the bubbles originating from the CO_2 increased the porosity within the sample and hence the carbonation depth, which gave rise to a more efficient carbonation reactions (Meng et al., 2022).

2.6.2. Accelerated Carbonation

Accelerated carbonation, also known as **carbonation curing,** involves the process of exposing early-age concrete to specified percentage concentrations of CO_2 (Kazemian & Shafei, 2023). This normally occurs on the same day that the material is cast, or on the following day. During this procedure results have shown that once the initial hydration occurred, any produced $Ca(OH)_2$ reacts with the introduced dissolved CO_2, which produces $CaCO_3$ (Meng et al., 2022).

Another reaction occurs where any C-S-H present is carbonated, resulting in a decalcification process that produces $CaCO_3$ and amorphous silica gel. However, the previous reaction is more readily available since $Ca(OH)_2$ has a higher solubility when compared to the other present calcium compounds (Meng et al., 2022).

Hence, carbon sequestration is made available through the stable minerals that form from the reactions occurring between the varying cement hydration products and cement phases found within the concrete, and the provided CO_2.

Different methods could be used for accelerated carbonation. These include:

- Concentrated carbonation
  Curing of a concrete sample within an enclosed chamber of specified CO_2 concentration, most commonly being that of 20% concentration.

- Pressurised carbonation
  Curing of a concrete sample within an enclosed chamber of specified concentration and pressure. Research has shown increased CO_2 pressure increases the efficiency of carbonation throughout the material by promoting CO_2 diffusivity.

- Flow through curing
  Samples are enclosed within a chamber with CO_2 flowing in and out of the chamber at a specific flow rate. This method is done to replicate the actual exhaust process, where the industrial exhaust created through cement or power plants are used, specifying and adjusting the flow rate.

- Aqueous carbonation
  Concrete samples are carbonated at ambient temperature and pressure within an aqueous solution (alkaline) of preference (for example sodium hydroxide solution). The method involves carbon dioxide to be bubbled at a constant flow into said solution (Meng et al., 2022).

Apart from carbonation curing, **mineral carbonation** is another broad term that falls under accelerated carbonation and can encompass all its subsections. While carbonation curing is a curing method for fresh cement-based products, mineral carbonation is seen to be more as a carbonation sequestration method where minerals rich in calcium and magnesium silicates/oxides present within a material react with CO_2 to form stable inorganic carbonates. Mineral carbonation is often used to treat waste or by-product materials, including: fly ash, steel slag, industrial waste and RCP (Kazemian & Shafei, 2023).

2.6.3. Weathering Carbonation

Weathering carbonation, also known as **passive carbonation**, occurs over the service life of a concrete structure. During this slow process, CO_2 present within the atmosphere reacts with any available cement hydration products found within the structure. Such hydration products include $Ca(OH)_2$ and C-S-H (Meng et al., 2022)

2.7. Treatments for Reactivation of RCP

This dissertation focuses on methods to increase the reactivity of the RCP to be used as a SCM. The main approach to do so is to apply treatments to the powder. The treatment methods that have shown a significant improvement in reactivation properties are as follows:

2.7.1. Thermal Treatment (Calcination)

When subjecting RCP to thermal treatment, results have shown that the material undergoes thermal activation which altered the cement microstructure. Any hydration products present, such as, calcium silicate hydrate, calcium carbonate, portlandite and ettringite – which had formed during the initial curing process – decompose to form calcium silicates such as dicalcium silicate, tricalcium silicate, and calcium oxide. Examples of these decompositions are as shown in the equations below (J. Li et al., 2024; Y. Li et al., 2023).

$$\text{C-S-H} + \text{delta} \rightarrow C_2S + CaO$$

$$Ca(OH)_2 + \text{delta} \rightarrow CaO + H_2O$$

$$CaCO_3 + \text{delta} \rightarrow CaO + CO_2$$

The decomposition reactions above, yield reactive minerals such as calcium oxide and calcium silicate phases, which help improve the properties of recycled powder as they stimulate strength development and hydration (Al-Janabi et al., 2024).

This process therefore reactivates these hydrated products and allows for effective rehydration when subjected to water, as shown in the chemical reaction below (Y. Li et al., 2023; Real et al., 2021). It was also observed that the presence of calcium oxide affected the hydration dynamics and the workability, as it required a higher demand for water (Real et al., 2021).

$$C_3S + H_2O \rightarrow \text{C-S-H} + Ca(OH)_2$$

However, research has shown that the production of calcium silicate phases (C_2S and C_3S) only form when thermal treatment occurred at elevated temperatures. In fact, the quantities of $Ca(OH)_2$ and C-S-H found within the microstructure were seen to decrease as the temperature increased, which signifies their decomposition.

Although what has been stated above is true, results from another research by Al-Janabi et al. (2024) suggests that temperatures exceeding 800 ^oC continued decomposing the microstructure significantly with no production of reactive phases. This means that there is no benefit to the samples' performance, all the while increasing energy use (Al-Janabi et al., 2024). On the other hand, another study by Li et al. (2024) showed that low temperatures such as 400 ^oC result in an incomplete decomposition of the C-S-H gel and $Ca(OH)_2$, therefore, having a decreased effect on the powder's reactivity (J. Li et al., 2024).

Hence, it has been concluded through many studies that the temperature range between 600-800 ^oC gives optimal performance (Al-Janabi et al., 2024; Y. Li et al., 2023; Real et al., 2021).

The main drawback is the high energy consumption and therefore the associated carbon emissions that the thermal treatment activation process requires due to the high temperatures used.

2.7.2. Carbonation Treatment

The previous brief descriptions of the different carbonation procedures seen in section 2.6, suggest that the best method to be adopted in this dissertation is mineral carbonation of RCP. The study will incorporate this through accelerated carbonation in the form of:

- Concentrated Carbonation, which falls under dry carbonation and;
- Aqueous Carbonation.

In this case, since the accelerated carbonation will be applied to the RCP prior to said material being used as a SCM within paste and mortar casts, this procedure is regarded as a pre-treatment rather than a curing method of the cast material.

2.7.2.1. Dry Carbonation- Concentrated

Carbonation treatment done on recycled concrete, be it recycled aggregate or powder, leads to beneficial results. Results have shown that any residual mortar found attached to the RCA is strengthened through carbonation treatment. This occurs due to the added CO_2 reacting with the hydration products found within the residual mortar, to produce calcium carbonate and silica gel (Zhang et al., 2015). The produced limestone fills any capillary pores (voids) within the microstructure densifying the cement matrix, resulting in a more effective bond between the aggregate and cement paste (mortar), due to an increase in strength of the interface transition zone (Jeon et al., 2024; Zhang et al., 2015).

Since a denser product forms with a reduction in voids, this means that there is a reduction in porosity, and hence a reduction in water absorption (Zhang et al., 2015). Thus, such a treatment gives rise to a substance with enhanced mechanical properties (Jeon et al., 2024).

The above relates more to the overall strengthening of the recycled aggregate to be used as aggregate or sand replacement. However, the main aim of this research is to improve the recycled powder to be adequate as a feasible cement replacement.

Even though one is focusing more on recycled powder, the property improvements stated above will still have beneficial effects. However, for the material to achieve a status that can be deemed sufficient to be used as a SCM, one must use carbonation treatment to aid in reactivating the hydration products found within the powder to create a highly reactive material.

The following will focus more on carbonation treatment of the recycled powder. Similar to the properties of carbonated RCA, studies have shown that this treatment is beneficial to the powder's strength development, performance, densification of the mortar mix, and strengthening the interfacial transition zone between the adhered mortar and newly formed mortar (Y. Li et al., 2023). This enhanced mechanical strength owes to the introduced carbon dioxide, which reacts with any available calcium hydroxide, calcium oxide, and any other hydration products to produce calcium carbonate, which fills any available pores, reducing the overall porosity (Mehdizadeh et al., 2020) and increasing the volume density (Al-Janabi et al., 2024). Another study by Li et al. also noted that apart from an increase in production of calcite, there is also the strengthening of the chemical bond between the post hydration products and said calcite (J. Li et al., 2024).

The introduced CO_2 also further reacts with any residual unhydrated calcium silicate phases present, producing amorphous aluminosilicate gel, which reactivates the material, improving pozzolanic and hydration activity, and hence, enhancing the overall cementitious properties (Al-Janabi et al., 2024; Mehdizadeh et al., 2021).

Below are a set of chemical equations representing the main reactions that occur. The main products are calcium carbonate and silica (Zhu et al., 2018):

$$Ca(OH)_2 + CO_2 \rightarrow CaCO_3 + H_2O$$

$$3CaOSiO_2 + (3\text{-}x)CO_2 + yH_2O \rightarrow xCaO{\cdot}SiO_2{\cdot}yH_2O + (3\text{-}x)CaCO_3$$

$$2CaOSiO_2 + (2\text{-}x)CO_2 + yH_2O \rightarrow xCaO{\cdot}SiO_2{\cdot}yH_2O + (2\text{-}x)CaCO_3$$

$$3CaO{\cdot}2SiO_2{\cdot}3H2O + 3CO_2 \rightarrow 3CaCO_3{\cdot}2SiO_2{\cdot}3H_2O$$

2.7.2.1.1. Optimal Dry Carbonation Parameters

Through research it was found that the most common treatment conditions used for dry carbonation were:

- Temperature at 20 ± 2°C
- Relative Humidity at 65 ± 5%
- CO_2 Concentration at 20% (J. Li et al., 2024; Mehdizadeh et al., 2021)

Li et al. (2024) found that the optimal duration for the treatment is 1 day, as it was shown that there were minimal changes to the microstructure of the material after 24 hours, indicating the complete reaction of many of the minerals. It was also seen that with 6 hours of carbonation, there were lower intensities within the spectra absorption peaks when compared to 24 hours, implying an incomplete reaction (J. Li et al., 2024).

2.7.2.2. Aqueous Carbonation

As previously explained in section 2.6.2. aqueous carbonation involves carbonation of the sample in question at a specific temperature and flow rate within an aqueous solution, and if required at a specific pressure (Meng et al., 2022).

When RCP is subjected to aqueous carbonation it goes through a two-step chemical process. Initially, the CO_2 is introduced in the gaseous phase. After, it dissolves into the solution to produce carbonate ions. The second part involves the hydrated clinker and any anhydrous calcium silicate phases found within the RCP to undergo carbonation through their reaction with the already dissolved carbonate ions. The carbonation process involves a set of two reactions as can be seen in the equation below. The main products are calcium carbonate and amorphous alumina-silica gel (Meng et al., 2022).

$$Ca(OH)_2\ (s) + CO_2\ (aq) \rightarrow CaCO_3\ (s) + H_2O\ (l)$$

$$\text{C-A-S-H}\ (s) + CO_2\ (aq) \rightarrow CaCO_3\ (s) + \text{alumina-silica gel}\ (s, gel) + H_2O\ (l) \quad \text{(Zajac et al., 2021)}$$

The initial reaction shows the carbonation of $Ca(OH)_2$. The $CaCO_3$ that forms is mainly produced as calcite crystals, whose morphology consists of a mix of small and large intergrown crystal agglomerates. These crystals tend to form within the pore spaces rather than in the original grains of cement (Zajac et al., 2021), acting as a fine filler and as a result densifying the microstructure. This can lead to improved mortar strength when said material is used as an SCM (Mao et al., 2023).

The second reaction shows that the decomposition and decalcification of the calcium aluminosilicate hydrate, wherein the released calcium ions react with the dissolved carbonate ions to produce both calcite and silica gel. Along with the carbonation of the principal hydrate phase, the partial carbonation of AFt and AFm phases was also seen. Studies involving NMR testing have shown that the produced gel is not pure but is in fact an alumina-silicate structure, which involves aluminium to substitute into the silicate network. Hence, this type of gel has a high specific surface area and is amorphous in nature, meaning it has high pozzolanic reactivity (Zajac et al., 2021).

When compared to dry carbonation treatment, both are seen to produce the same materials. However, various studies have noted improved results when treating using aqueous rather than dry carbonation. Results have shown a higher carbonation efficiency that can occur within fewer hours (Zajac et al., 2021). This occurs since within aqueous treatment, carbonation occurs at a faster rate due to the readily available dissolved carbonate ions, unlike dry carbonation which depends on the diffusion of CO_2 (Meng et al., 2022).

Mao et al. (2023) also found that using aqueous carbonation produces calcium carbonate and silica gel in a uniformly distributed manner. While during dry carbonation they were found to have a distinct layer separating them, meaning a less homogeneous material where performance might be affected (Mao et al., 2023).

2.7.2.2.1. Challenges

Throughout this procedural treatment an alkaline solution is usually the preferred option. An alkali aids in dissolving the present calcium phases within the RCP to produce readily available calcium ions in an accelerated manner, which can react with the dissolved carbonate ions.

However, using an alkali solution was found to have its challenges. Studies have shown that at higher concentrations sulphate ions were found to have dissolved in the solution, which can alter the reactions occurring and hence, the chemical composition of the product (Meng et al., 2022). This can greatly impact the carbonation products' microstructure and size, whereby the produced material would have a decreased reactivity and hence lower strength development and durability.

2.7.2.2.2. Effects of Flow Rates

Mao et al. (2023) found that there are both positive and negative effects to higher and lower flow rates. In this study, the results obtained after using 3 L/min or 5 L/min were analysed. It was observed that an increase in flow rate led to a better rate of CO_2 solubility, hence greater amount of carbonate ions formed, resulting in more rapid carbonation reactions. This promoted higher growth and formation of the $CaCO_3$ crystal nuclei, creating larger crystallite sizes (by 3.0-6.6nm) and more enhanced carbonation products. It is also important to note that a higher CO_2 flow rate was found to transform the pore structure from capillary pores to gel pores, through the incorporation of aluminium into the silica gel. This results in a material having enhanced pozzolanic properties (Mao et al., 2023).

However, it was observed that after some time, the flow rate's effect on the carbonation degree would be redundant, as rapid carbonation reactions resulted in an accumulation of product layer which limited the progression of reactions. It was also noticed that rapid carbonation produced crystals with more defects (Mao et al., 2023).

2.7.2.2.3. Effects of Temperature

A study by Mao et al. (2023) showed that there are both positive and negative implications to increasing the temperature beyond 25 ^{o}C through the treatment process. It was seen that with increasing temperature (not exceeding 80 ^{o}C) there was both crystallization enhancement and a better polymerization degree of the silica gel. These resulted in a better crystallization process, creating larger crystallite sizes together with more vaterite and aragonite formation, as a well as more silica gel formation respectively. These results occur as higher temperatures promote more kinetic energy, increasing reaction rates.

However, on the negative side, higher temperatures were seen to reduce the amount of CO_2 dissolving in the solution, leading to carbonation limitations (Mao et al., 2023).

2.7.2.2.4. Effects of Time

Studies have shown that increased carbonation time produces better carbonation products. Fang et al. (2021) found that 10 minutes of carbonation time produced a lower amount of carbonation products which had small particle sizes. This is further backed up by the study done by Mao et al. (2023) who found that as the carbonation time was increased from 30 to 60 minutes, there was an increase in carbonation products, which resulted in better calcium carbonate crystallinity and more formation of silica gel. This is further proved by another study which found that 2 hours of wet treatment produced a near complete carbonation (Zajac et al., 2021).

2.7.3. Silica Fume

Silica fume is a byproduct of silicon alloys and mainly consists of amorphous (non-crystalline) silica. When silica fume is introduced as a slurry within a mixture in conjunction with recycled concrete, it creates a pozzolanic reaction (Shi et al., 2018).

The addition of pozzolanic materials to recycled concrete introduces additional silicon, leading to the enhancement of calcium silicate formation during the reactivation process, once it reacts with any calcium hydroxide found within the adhered mortar of the recycled concrete. These calcium silicates then react with added water to produce calcium silicate hydrates which are the main binding phases in the production of a cementitious material (Y. Li et al., 2023). Hence, this reaction creates a material of increased density which results in the reduction of porosity, increase in strength, and enhancement of the interface transition zone between the newly created matrix (cement paste) and the recycled concrete. The latter is thanks to the finer particles of nano-silicon dioxide and silica fume (Shi et al., 2018).

When comparing such a reaction, its products and the effects on the final sample, to recycled concrete that has undergone carbonation treatment, results have shown that the addition of silica fume within the mixture still provides a more efficient and beneficial product.

The benefit of carbonation treatment is that it produces calcium carbonate and silica gels, which increase the density of the interfacial transition zone and decrease the porosity of the structure. However, the formation of the calcium silicate hydrate produced by the pozzolanic reaction of the silica fume slurry is far more successful in creating a final product of greater mechanical properties (Shi et al., 2018).

However, it is important to note that the percentage amount of silica fume introduced makes a significant difference to results. Li et al. (2023) found that the introduction of 10% silica fume provided the optimal compressive strength results, whereas the introduction of higher silica fume contents produced lower strength results.

This occurs since the introduction of excessive silica fume led to the formation of low-lime calcium silicates which have a reduced water reactivity and hence insufficient hydration. On the contrary, with just 10% introduction it created the formation of a balanced calcium/silicon ratio which results in a more effective hydration reaction and hence the production of more reactive phases, increasing the overall strength. Such reactive phases include silicate hydrates (Y. Li et al., 2023).

2.7.3.1. The Importance of Ca/Si Ratio

The explanation in section 2.7.3. above, shows how the chemical composition of calcium and silica compounds found within the microstructure of the recycled concrete plays an important role in the performance of strength and the interfacial bond (Tang et al., 2023). This gives an indication that optimal results for the use of recycled concrete powder as an SCM all depends in achieving a balanced Ca/Si ratio. In fact, when researching further, one realizes that it plays a vital role in results of the applied treatments.

As explained in section 2.7.1. the formation of calcium silicate phases (C_2S and C_3S) relies on thermal treatment occurring at elevated temperatures. However, in reality, this is not enough. The elevated temperature has to occur in combination with a balanced Ca/Si ratio. It has been found that with a higher

Ca/Si ratio (lower silica presence), calcination at high temperatures creates calcium silicate minerals that are reactive and have good hydration properties (C_3S, C_2S, CaO). On the other hand, a lower Ca/Si ratio (higher silica presence), creates low-lime calcium silicate phases which are more inert with low reactivity (wollastonite – CS) (Y. Li et al., 2023).

This same can also be said for carbonation treatment. In a study, it was observed that the highest carbonation rate was obtained from a material having a more balanced Ca/Si ratio. However, it was seen that even low-lime calcium silicates still had a certain amount carbonation rate (Ashraf & Olek, 2016).

Understanding the importance of a balanced Ca/Si ratio intrigued the opposite idea of implementing the use of a calcium-based material rather than a silica one. Instead of adding silica fume to improve the Ca/Si ratio as can be seen in section 2.7.3., the implementation of a lime-based material could be an alternative route, such as the use of limewater.

2.7.4. Limewater Soaking Treatment

Through literature, it was seen that most often limewater was implemented as a curing medium for casted paste/mortar samples, rather than using a water bath. This is done with the intention of promoting hydration and preventing calcium leaching during the curing process. Curing in limewater provides a maintained high calcium ion concentration reducing the possibility of portlandite and other calcium phases to dissolve. Hence, this aids the hydration reaction and stabilizes the hydration products, helping in strength development (Y. Li et al., 2023).

However, another study made use of limewater soaking as a pre-treatment method prior to the carbonation treatment for maximum effectiveness. This will be further explained in section 2.7.5.2.

2.7.5. Combination of Treatments

It has been shown that a combination of treatments may have more beneficial results in creating a more reactive material rather than when undergoing a singular treatment.

2.7.5.1. Calcination and Carbonation

When taking into consideration the combination of treatments of calcination and carbonation, a study showed comparisons of strength activity index values. It was found that the original as received RCP had a low strength activity index of 0.6. Upon individual treatment of both calcination and carbonation, this index improved above the 0.75 threshold for useful SCM's, and when subjected to a combination of treatments, the activity index significantly increased close to unity. Within this study three variations were researched, (1) carbonating then calcining at 500^{o}C, (2) calcining at 500^{o}C then carbonating, and (3) carbonating then calcining at 800^{o}C having their activity index at 90.47%, 93.57% and 95.81% respectively. The initial sequence resulted in silica polymerization and the creation of a well-ordered stable calcite after carbonation and structural ordering of the carbonate phases after calcination. The second sequence resulted in the elimination of water and portlandite to produce Calcium Oxide after calcination, and once subjected to carbonation, this CaO is transformed into a mix of reactive aluminosilicate gel and amorphous calcium carbonate (Al-Janabi et al., 2024).

The final treatment variation had the most improved index, indicating that this material may give similar performance to that of Cem I. However, the possibility of calcining at 800°C followed by carbonation was not studied and hence, may show even better results. This is indicated through both variations following a similar sequence while using calcination at 500°C (Al-Janabi et al., 2024).

Another study by Li et al. (2024) focused on one sequence of such a combined treatment, having carbonation followed by calcining at 800°C. Carbonation as the first treatment creates a stable form of $CaCO_3$, such that even after calcining to 800°C this $CaCO_3$ did not decompose. Calcining as the second treatment produced CaO, which is required for the hydration process. Hence, through a combined treatment there is a dual presence of both $CaCO_3$ and CaO, which aids the material in having increased mechanical properties and reactivity respectively (J. Li et al., 2024)

A drawback of calcination as a singular treatment method is that at certain high temperatures any amorphous silica that was present can undergo crystallization and form crystalline silica. This transformation may make the cementitious material less reactive to water, since crystalline silica tends to be less reactive than if it were in an amorphous state (Y. Li et al., 2023). However, this problem may be solved with combination of treatments. Following up with a carbonation treatment means that any calcium silicate phases present will result in calcium carbonate and polymerized silica gel, which most often is found to be in an amorphous state (J. Li et al., 2024; Y. Li et al., 2023).

2.7.5.2. Limewater and Carbonation

In this study by Zhan et al. (2018) limewater soaking was introduced as a pre-treatment method prior to carbonation on already casted mortar samples. Results showed that limewater soaking provided additional foreign calcium ions within the mortar. Once hydrated, the increase in calcium ions produced more calcium hydroxide, which was then reacted with carbon dioxide introduced from the carbonation treatment. This increased the overall production of calcium carbonate and its formation was accelerated. Additionally, this method also optimized the conditions for the carbonation reactions, by creating a more uniform dispersal of moisture within the samples.

The introduction of limewater treatment enhances the carbonation process since carbonation reactions may be limited by an insufficient amount of reactive calcium components. Hence, limewater treatment leads to an increase in carbon dioxide uptake, which results in a sample of increased strength and decreased porosity, when compared to carbonation treatment being done alone (Zhan et al., 2018).

2.8. Cement replacement percentage

2.8.1. Calcination

According to the study by Real et al. (2021) which focused on calcination of recycled cement, the best obtained performance resulted when using up to 15% cement replacement. Higher percentage replacements resulted in free CaO content which caused exothermic reactions, resulting in a reduction in workability. Another reason was that the RCP particles were porous when compared to Cem I. This caused two main problems: the resulting material had decreased stiffness and hardness, and the high surface area meant excessive water absorption (Real et al., 2021)

When compared to carbonation, calcination treatment results in a material of lower optimal percentage replacement since carbonation converted the RCP into two reactive products (silica gel and calcite), while calcination treatment only partly decomposes the hydration products. This means that carbonation treatment resulted in reactive amorphous silica gel and calcite which acts as a filler, making the material less porous, while calcination retains a porous material with comparably lower reactivity due to only partial decomposition occurring (Al-Janabi et al., 2024; Real et al., 2021).

2.8.2. Dry carbonation

Mehdizadel et al. (2021) found that using 5-20% replacement of dry carbonated hydrated cement paste achieved good compressive strength, while samples which used untreated HCP resulted in lower strength. A correlation was also found between the percentage replacement and the water to cement ratio. Improved compressive strength was achieved when using 15% replacement in combination with 0.2 or 0.3 w/c ratio and 20% replacement in combination with 0.4 w/c. Such results are contributed to the fact that higher w/c ratios create improved hydration of the present Cem I, resulting in the production of more hydration products, which upon carbonation, created more calcite.

These replacement percentages can be obtained due to the filler effect of the produced calcite, resulting in a denser and more refined pore microstructure, reducing the overall porosity. This also increases the flowability since lower porosity results in lower water absorption.

Higher replacement percentages are deemed unsuccessful due to the reduction in cement. Even though carbonated powder was successful in achieving filler effects and pozzolanic reactivity, such characteristics where still not effective enough to compensate for the decrease of the main phases found in cement (C_3S and C_2S) (Mehdizadeh et al., 2021).

This was confirmed through another study by Lu et al. (2018), where it was found that 10-20% cement replacement with carbonated HCP increased the cement strength at 90-day testing, while the implementation of 30% replacement decreased it (Lu et al., 2018)

2.8.3. Aqueous Carbonation

Jiang et al. (2022) found that the percentage replacement of cement when using aqueous carbonated HCP correlates to the particle size used. It was seen that 30% replacement was achieved when using fine particles less than 0.15mm. The results showed a strength improvement when compared to the untreated HCP. On the other hand, larger particle size resulted in the optimal replacement percentage to be lower at 20%.

This correlation is due to the fact that the smaller particle sizes obtained the largest resulting percentage of calcite and silica gel created after the carbonation, having 70.7% and 69.5% respectively (Jiang et al., 2022). This occurs since the finer particles have a higher surface area, and hence the dissolution of the calcium bearing phases is more rapid. Once these calcium phases are consumed by the carbonate ions they quickly replenished due to their rapid dissolution, for further reactions. This means longer carbonation reactions can occur.

2.9. Water to Cement Ratio

Research by Lu et al. (2018) investigated the use of 0.4 w/c ratio at 10-30% replacement level of cement using carbonated HCP. The results portrayed this ratio worked best for replacement level between 10-20%, achieving improved strength. It was seen that using such a ratio aided in the occurrence of optimal hydration reactions (Lu et al., 2018)

Another study by Mehdizadeh et al. (2021) made use of 0.3 w/c ratio, where the sample containing 15% replacement achieved improved strength when compared to control samples. A lower ratio was found to work when compared to the previous study due to the finer particle distribution of the material used, resulting in a better packing density, lower porosity and hence, reduced water demand (Mehdizadeh et al., 2021).

2.10. Controlled Curing Conditions

The works of Mehdizadeh et al.(2021), Lu et al. (2018), and Jiang et al. (2022) were found to employ similar curing condition strategies, where the pastes were kept in their respective mould sealed for 24 hours at 20±2^{o}C and 95±5% relative humidity. Once demoulded the samples were immersed in lime saturated water at 20±2^{o}C and 95±5% relative humidity for elongated curing until required for testing day. However, one of the studies employed the use of normal water curing rather than limewater (Jiang et al., 2022; Lu et al., 2018; Mehdizadeh et al., 2021).

2.11. Conclusion

Other than providing information on the treatment methods that exist for reactivation of RCP, this literature review highlights the gaps of knowledge that exist, some of which regard the optimisation of treatment parameters, benefits of combined treatments and the improvement of the cement replacement percentage.

This study tries to address this lack of knowledge or part thereof by exploiting but also adapting and expanding the available information to research new treatment methods as well as optimising existing ones.

All the above confirms the relevance of the study being carried out. Furthermore, this study contributes results which will allow comparison with published literature for further development on the subject matter.

CHAPTER 3 - Methodology

3.1. Overview

The objective of this dissertation was to assess and analyse the characteristic properties of carbonated RCP and its potential as a cement alternative. This research also aimed at achieving more optimal treatment methods and conditions with the hopes of achieving improved mechanical and chemical properties of the SCM.

3.2. Materials

This research focused on recycled concrete (as described in section 3.2.1.) as the primary raw material that was used for the experimental procedure and implemented as a supplementary cementitious material. Other materials used for the research include CEM I 52.5 type cement, and dolomite sand 0/4 as the aggregate.

3.2.1. Collection of Primary Material

The recycled concrete used within this research was of unknown origin and so, has unknown characteristics, composition and mix parameters. Hence, for this reason once the recycled concrete powder was produced using the procedure explained in section 3.2.2., characteristic testing was done on the powder to understand and analyse its composition and nature. Testing included the X-Ray Fluorescence test, through which the chemical composition of the material was determined. These results are shown in the table below:

Table 1 - Chemical Composition of as-received RCP

Oxide	Concentration *(%)*	Oxide	Concentration *(%)*
CaO	62.8	TiO_2	0.209
SiO_2	14.1	MnO	0.064
Na_20	6.76	CuO	0.0217
SO_3	5.48	ZnO	0.0185
Al_2O_3	3.17	CoO	0.0168
Fe_2O_3	2.98	Cr_2O_3	0.0157
MgO	2.29	V_2O_5	0.0108
K_20	1.19	NiO	0.0086
P_2O_5	0.47	Rb_2O	0.0046
Cl	0.244	As_2O_3	0.0038

3.2.2. Material Production – Production of Recycled Concrete Powder

The aim for the recycled concrete fragments obtained for this research was to produce recycled concrete powder that would be fine and efficient enough to be used as cement replacement.
The following are the procedural steps that these recycled concrete fragments went through to be converted into RCP:

1. The course material was rinsed with tap water through a 4mm sieve to remove any contaminants and later any remaining impurities were removed through sedimentation.
2. The material was then left to oven dry at 105 ^{o}C for 24 hours to remove any present moisture.
3. A jaw crusher was used to break down the larger fragments into smaller pieces, which was cleaned prior to its use to eliminate the risk of cross-contamination.
4. A Los Angeles Abrasion machine was used to further breakdown the material into smaller particles, where each batch used 11 steel balls and was run for 1000 revolutions (Ruth Bola Oliveira et al., 2023).
5. The processed material underwent a sieve shaker test for approximately 10 minutes, using a set of standard sieves to determine which sieve size would be best used to filter out from and be used for the fine powder preparation. The below is a representation of the sieve sizes used with their respective retained weight:

Table 2 - Retained Weights from Sieve Shaker Test

Sieve Size	Retained Weight
2mm	711.51g
1mm	852.7g
500	624.64g
250	634.43g
125	483.78g
63	103.03g
45	14.05g
32	1.4g
Bottom Pan	0.48g
Total Original Weight	*3426.02g*

6. Based on the retained weight values achieved, it was determined that material passing from the 1mm sieve should be used for further processing of the material into a finer powder.
7. The sieved/selected material was oven dried for a minimum of 24 hours as part of the conditioning process prior to ball milling, to remove any present moisture.
8. Multiple trial and error testing runs were executed using the ball mill in order to achieve the best resulting fineness of the final powder. The trial runs were performed with the following parameters (Mehdizadeh et al., 2021):

Table 3 - Ball Mill Testing Runs

Trial Run	Material *(g)*	Steel Balls *(No.)*	Steel Beads *(g)*	Speed *(rpm)*	Duration *(Mins)*
1	220	5	180	600	30
2	220	6	180	450	10
3	220	8	250	450	20
4	220	8	250	450	15
Final Run *(Chosen)*	220	8	250	450	10

Through the trial runs it was noted that increase in duration caused agglomeration of the material due to its porous nature. Hence, it was determined that a lower duration of milling decreased the degree of agglomeration while still achieving the required fineness. For this reason, the material build up on the edges of the ball mill container were scraped off every 5 minutes, ensuring that all material was crushed homogeneously.

Figure 1 - Recycled Concrete Material (First), Oven (Second), Jaw Crusher (Third), Los Angeles Machine (Fourth)

Figure 2 – Material after Los Angeles (First), Sieve Shaker (Second), Sieved Material (Third), Oven Drying Material (Fourth)

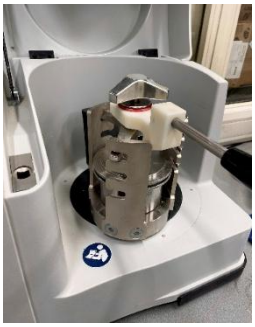

Figure 3 - Planetary Ball Mill PM 100 Machine


Figure 4 – Steel Balls and Beads (Left) and Raw Powder Material (Right)

3.3. Material Preparation

The raw powder produced underwent a series of pre-treatment procedures, giving rise to a series of samples having varied characteristics. The sample codes allocated for each treated material are explained in the table below:

Table 4 - Sample Code Descriptions

Sample Code	Code Description
Cem Con	Cement Control containing **No SCM**
RCP	As-received Recycled Concrete Powder
RCP-Ca	RCP that underwent **Thermal** treatment
RCP-DC	RCP that underwent **Dry Carbonation** treatment
RCP-WC	RCP that underwent **Aqueous Carbonation** treatment
RCP-L	RCP that underwent **Limewater** treatment
RCP-CaWC	RCP that underwent **Calcination** followed by **Aqueous Carbonation** treatment
RCP-CaDC	RCP that underwent **Calcination** followed by **Dry Carbonation** treatment
RCP-LDC	RCP that underwent **Limewater** treatment followed by **Dry Carbonation**

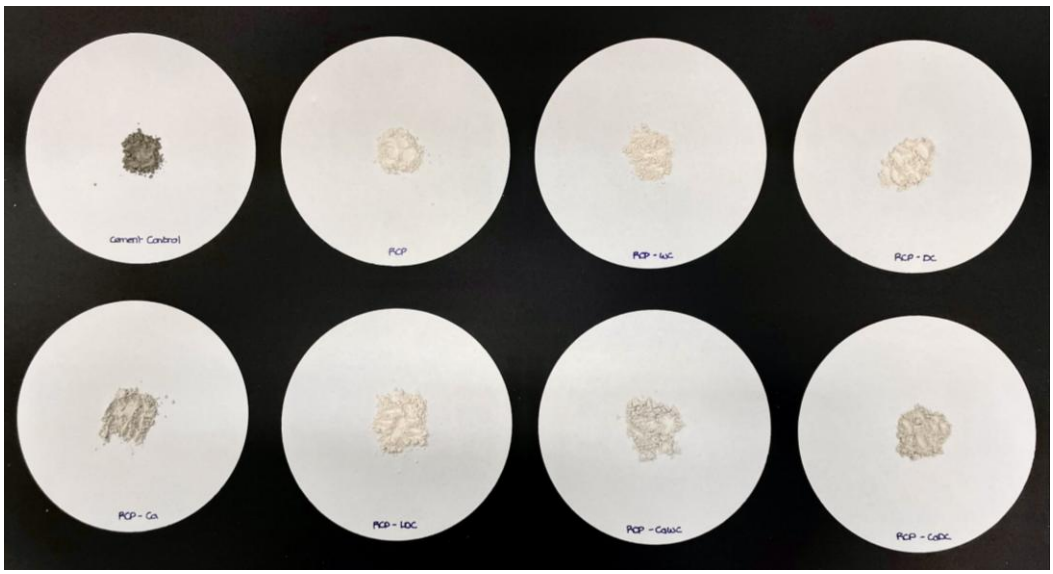

Figure 5 - Samples to be Analysed

These sample codes were also used as the mix design codes, where each represents the mix design that uses that respective treated material as a SCM within the mix.

The conditions of each pre-treatment procedure is shown in a summarized table below and their methods are explained in more depth in sections 3.3.1. to 3.3.5. The parameters used have been obtained from literature, as seen within chapter 2.

Table 5 - Parameters of Pre-Treatment Procedures on RCP

Sample Code	Temperature *(°C)*	RH *(%)*	CO_2 Conc. *(%)*	Flow Rate *(L/min)*	Duration *(hrs)*
RCP-Ca	800	-	-	-	1
RCP-DC	20 ± 1	65 ± 5	20	-	24
RCP-WC	25 ± 1	65 ± 5	99	5	1
RCP-L	20 ± 5	65 ± 5	-	-	24

3.3.1. Calcination

The raw material was placed in silica crucibles with precision in order to not lose or contaminate the material. Heat treatment was done by placing the crucible in a muffle furnace and subjecting the material to a temperature of 800 °C for 1 hour (Al-Janabi et al., 2024). Once turned off the material was left enclosed within the furnace, allowing it to cool down gradually to room temperature until the next day. This ensured no sudden temperature change that may negatively alter the chemical composition of the pre-treated material.

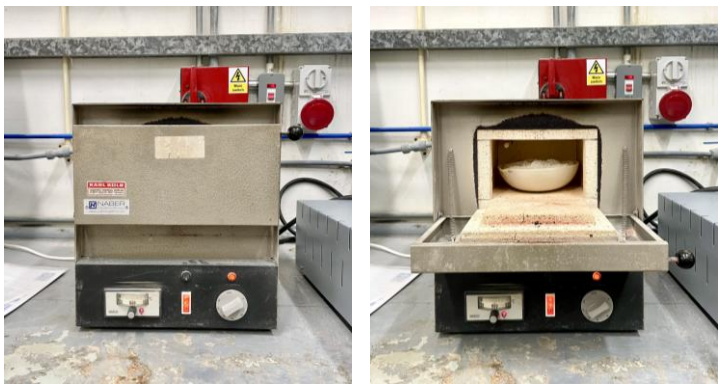

Figure 6 - Muffle Furnace (Left) and Material to be Calcined (Right)

3.3.2. Dry Carbonation

The raw RCP was placed onto and spread into a thin layer across a tray. The tray was placed in a sealed chamber and subjected to 20% CO_2 concentration at 20 ± 1 °C and relative humidity of 65 ± 5% for 24 hours. After 24 hours the carbonated material was oven dried at 105 °C for a minimum of 24 hours.

Figure 7 - Dry Carbonation Set Up Outside Chamber (Left) and Inside Chamber (Right)

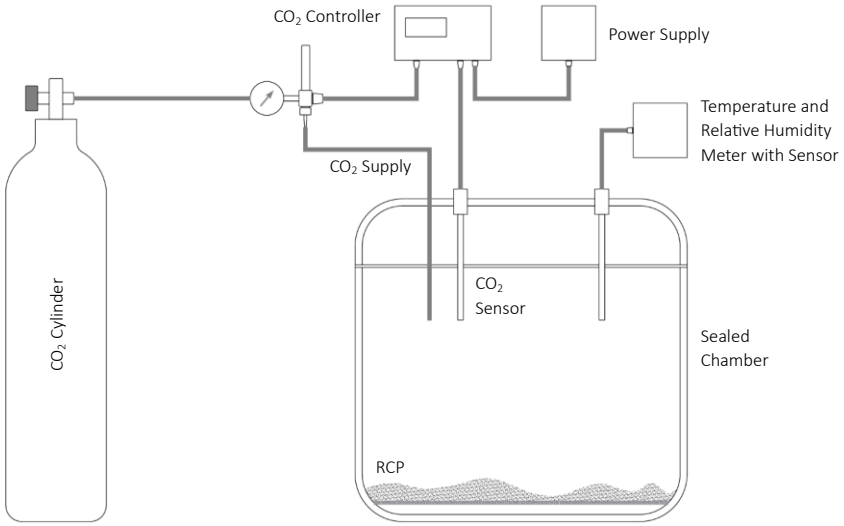

Figure 8 - Diagram of Dry Carbonation Set Up

3.3.3. Aqueous Carbonation

1000 ml of deionized water was heated to 25 °C and once this was reached, 100 g of raw material was added to the same beaker. This carbonation process involved the use of a 1:10 ratio of raw material is to deionised water.

The beaker was placed in a sealed chamber with a controlled temperature of 25 ± 1 °C, where the solution was continuously stirred and pure CO_2 was injected into it at a flow rate of 5L/min for 1 hour. This flow rate was achieved with the use of a flow meter (Mao et al., 2023).

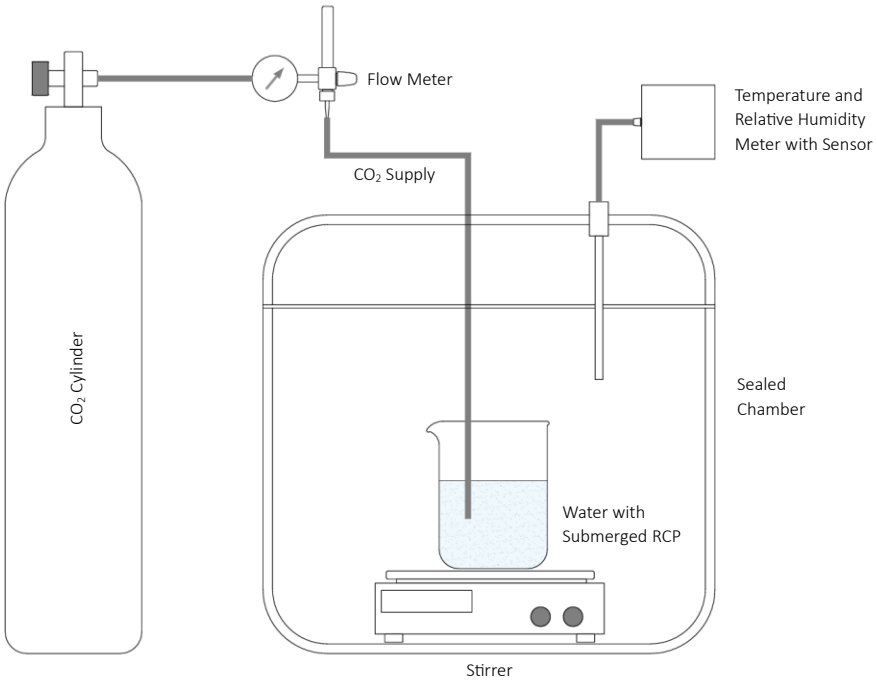

Figure 9 - Diagram of Aqueous Carbonation Set Up

Figure 10 - Flow Meter (Left), Dry Carbonation Set Up Inside Chamber (Middle) and Chamber (Right)

After the hour time mark, the carbonated RCP material was collected from the solution using vacuum pump filtration. The collected material was then oven dried at 105 ^{o}C for a minimum of 24 hours. Every few hours the material was removed from the oven and crushed with a spatula, breaking up any accumulated pieces and re-placed into the oven. This ensured the removal of any trapped moisture.

Once removed from the oven, the material was re-milled to regain its fineness and re-placed into the oven for further drying. Milling was done using 250 g of small beads at 450 rpm for 2 minutes.

Figure 11 - Vacuum Pump Filtration (Left), Retained Material (Middle) and Dried/Crushed Material (Right)

3.3.4. Limewater

The limewater solution was created by dissolving slaked lime ($Ca(OH)_2$) in distilled water and continuously stirring using a magnetic stirrer. This was done until the solution was fully saturated, which was indicated once the particles were seen to settle at the bottom of the beaker, meaning they could no longer dissolve. The solution was then filtered to remove any excess particles.

100 g of raw RCP material was then placed into 1000 ml of limewater solution using a 1:10 ratio of raw material is to limewater solution. The solution was left for 24 hours while being continuously stirred using a magnetic stirrer. After 24 hours, the lime infused RCP was also collected from the solution using the same procedure as explained in section 3.3.3. – Aqueous Carbonation, involving the vacuum pump filtration, oven drying and milling.

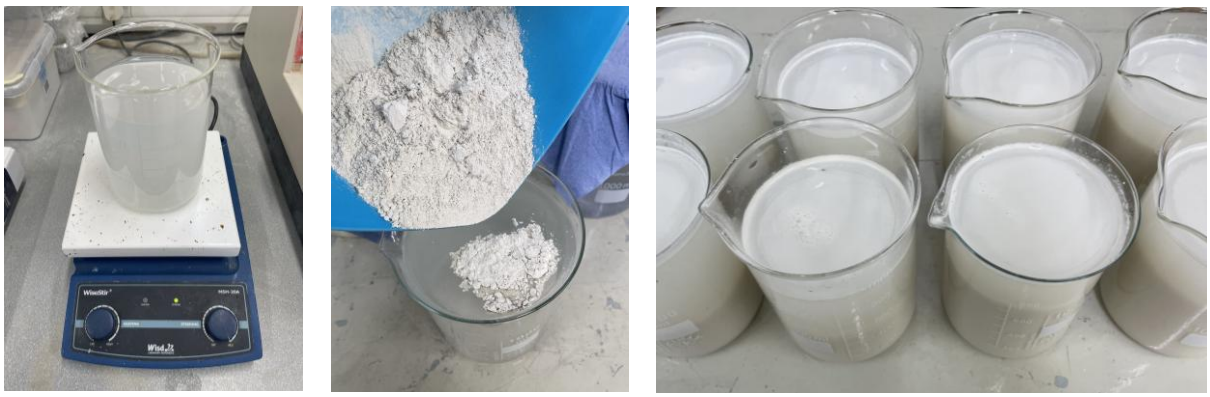

Figure 12 – Slaked Lime being Dissolved (Left), Raw Material Poured into Solution (Middle) and Raw Material within the Limewater Solution

3.3.5. General Treatment Conditions and Precautions

1. Throughout testing involving the use of carbon dioxide, a CO_2 air quality monitor was used for the safety of personnel using the laboratory. This includes both dry and aqueous carbonation.
2. Once all the materials were pretreated, they were placed in sealed containers and mixed thoroughly ensuring a homogeneous product with no moisture entry.

Figure 13 - Carbon Dioxide Air Quality Monitor

3.4. Paste Mix Design

3.4.1. Mix Design and Casting of Samples

The paste samples were done using all material listed within the sample code descriptions. Their mix design proportions were determined through quick trial runs observing the resulting workability and the cast produced after demoulding. The initial mix proportions used were based on the most common proportions found in literature, which had produced best results (Mehdizadeh et al., 2021). However, since the initial raw material used in this study was not precisely the same material as those used in literature, the mix design had to be amended to suit the material used better.

Through this process, it was observed that 300 g of binder would be sufficient to fill two moulds (20 x 20 x 20 mm), producing 18 casts in total for each mix design. Each paste mix was prepared using the mix design proportions found in table 6 below:

Table 6 - Paste Mix Design

Sample Code	Cement *(kg/m^3)*	SCM *(%)*	SCM *(kg/m^3)*	W/B Ratio	Water *(kg/m^3)*	SP *(%)*	SP *(kg/m^3)*
Cem Con	2083.33	0%	0	0.27	562.50	0.6%	12.50
RCP	1666.66	20%	416.67	0.27	562.50	0.6%	12.50
RCP-Ca	1666.66	20%	416.67	0.27	562.50	0.6%	12.50
RCP-DC	1666.66	20%	416.67	0.27	562.50	0.6%	12.50
RCP-WC	1666.66	20%	416.67	0.27	562.50	0.6%	12.50
RCP-CaWC	1666.66	20%	416.67	0.27	562.50	0.6%	12.50
RCP-CaDC	1666.66	20%	416.67	0.27	562.50	0.6%	12.50
RCP-LDC	1666.66	20%	416.67	0.27	562.50	0.6%	12.50

This involved the following procedure:

1. The moulds to be used for casting were washed and cleaned using ethanol to avoid any contaminants.
2. The moulds were also greased using oil to aid in the demoulding process, preventing casts from sticking inside the moulds and potentially cracking.
3. The respective amounts of cement and SCM were mixed in a small bowl.
4. Distilled water and superplasticizer were combined in a separate container.
5. The solution created was poured in segments into the container containing the dry material, while simultaneously mixing.
6. Mixing continued until a homogeneous paste was produced - Hand mixing was found to be a sufficient method for incorporating the material since one was working with small amounts.
7. The pastes were poured into the moulds (20 x 20 x 20 mm) in two sections, after which they were subjected to the vibrating table in order to remove any trapped air bubbles.
8. Each mould was labelled and stored, allowing the curing process to initiate.

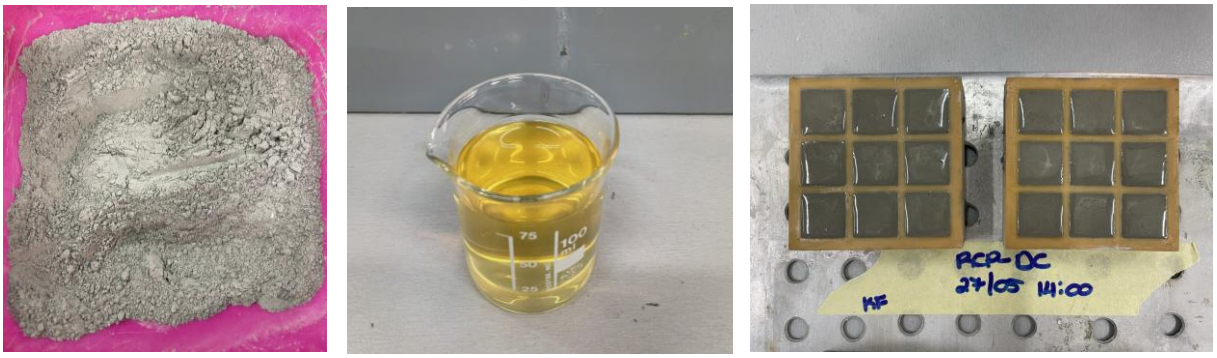

Figure 14 – Mixed Binder (Left), Distilled Water with Superplasticizer (Middle) and Paste Mix placed within Mould (Right)

3.4.2. Curing Parameters

Once each mix was prepared in the moulds, they were allowed to cure at ambient temperature (25 °C) for approximately 12-24 hours. During this period, they were observed until it was determined that the paste samples could be demoulded. Once demoulded they were placed in a water bath at ambient temperature and allowed to cure until testing day.

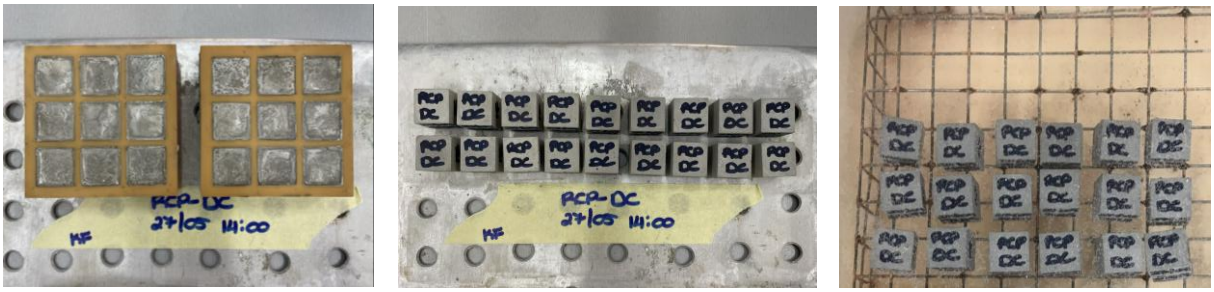

Figure 15 – Curing of Cubes at Ambient Temperature (Left), Demoulding of Cubes (Middle) and Curing within Water Bath (Right)

3.5. Mortar Mix Design

3.5.1. Mix Design and Casting of Samples

The mortar samples were done using a selected number of material from the sample code descriptions list. Similar to that of the paste mix design, the mortar mix design proportions were once again determined through quick trial runs observing the resulting workability and the cast produced after demoulding.

Through this process, it was observed that 500 g of binder would be sufficient to create 6 50x50x50 mm mortar casts for each sample variation. Each mortar mix was prepared using the mix design proportions found in table 7 below:

Table 7 - Mortar Mix Design

Sample Code	Cement *(kg/m³)*	SCM *(%)*	SCM *(kg/m³)*	W/B Ratio	Water *(kg/m³)*
Cem Con	666.67	0%	0	0.4	266.67
RCP-CaWC	533.33	20%	133.33	0.4	266.67
RCP-CaDC	533.33	20%	133.33	0.4	266.67
RCP-LDC	533.33	20%	133.33	0.4	266.67
Sample Code	**B/S Ratio**	**Sand *(kg/m³)***	**SP *(%)***	**SP *(kg/m³)***	
Cem Con	2.75	1833.33	1.5%	10	
RCP-CaWC	2.75	1833.33	1.5%	10	
RCP-CaDC	2.75	1833.33	1.5%	10	
RCP-LDC	2.75	1833.33	1.5%	10	

This involved the same type of procedure as explained in section 3.4.1. for the paste mix and cast creation, with the addition of the following:

1. After the moulds were washed and cleaned, they had to be assembled.
2. The required amount of sand was also included within the binder mix, and they were mixed in a benchtop laboratory concrete mixer.
3. The water and superplasticizer solution created was poured in segments into the mixer containing the dry material and mixed respectively.

Figure 16 – Sand and Binder Mix (First), Distilled Water with Superplasticizer (Second), Mixing of Mortar (Third) and Mortar Mix placed within Mould (Fourth)

3.5.2. Curing Parameters

The same procedure was adopted as can be seen in section 3.4.2.

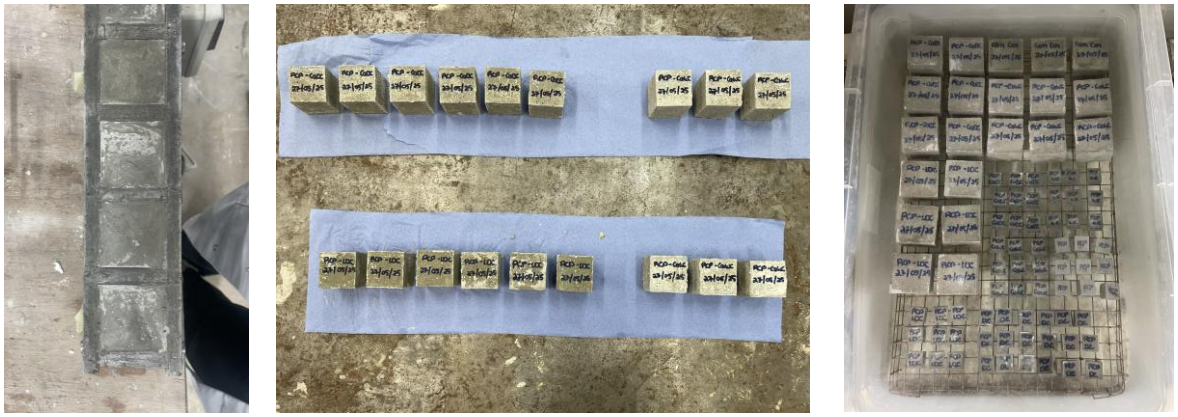

Figure 17 - Curing of Cubes at Ambient Temperature (Left), Demoulding of Cubes (Middle) and Curing within Water Bath (Right)

3.6. Testing Procedures

3.6.1. Characterisation Testing

3.6.1.1. Density Bottle Test

The density bottle test uses an apparatus known as pycnometers to help identify the relative density of cement or powders of similar size and characteristics, through the displacement of a non-reactive liquid. The test procedure was done in accordance with the testing standard EN-196-6:2010, 'Methods of testing cement – Part 6: Determination of fineness – National Annex NC – Method of testing cement for density' (British Standards Institution, 2010)

Procedure 1: This procedure was used to determine the density of the displacement liquid through the following steps:

1. The pycnometer and stopper were weighed empty.
2. The pycnometer was filled with de-aerated distilled water, and the stopper was inserted while making sure that no air bubbles were trapped.
3. The pycnometer was then immersed to the top of its neck, in a water bath of constant temperature (28 °C).
4. After 30 minutes, the apparatus was removed from the water bath, cleaned, allowed to cool, and weighed.
5. The pycnometer was topped up with more de-aerated distilled water, and steps 3 to 4 were repeated for another two times.
6. The mean weight of these three readings was calculated.
7. The mass of the water was then determined.
8. The above procedure was repeated by replacing the de-aerated distilled water with redistilled kerosine as the displacement liquid, to determine its respective mass and density.

Figure 18 – Pycnometers filled with De-aerated Distilled Water (Left) and Pycnometers filled with Redistilled Kerosine (Right)

Procedure 2: The next part of the test focused on finding the relative density of cement. This was done through the following steps:

1. The pycnometer and stopper were weighed empty.
2. Approximately 10 g of cement was weighed and placed in the pycnometer.
3. The pycnometer was half filled with redistilled kerosine.
4. Some beakers were also filled with the redistilled kerosine.
5. Both the pycnometer and the beakers were placed in a vacuum desiccator until no air particles were seen to form.
6. Once removed from the desiccator, the redistilled kerosine from the vacuumed beakers was then used to completely fill the rest of the pycnometer and the stopper was inserted.
7. Steps 3 to 6 from procedure 1 were repeated.
8. Through these steps the relative density was then calculated.

Procedure 3: Finally, the relative density of the fine powders created through treatments were determine using the same steps as explained in procedure 2.

Figure 19 – Pycnometer and Stopper weighed Empty (Left), Cement Placed within Pycnometer (Middle) and Redistilled Kerosine Poured within Pycnometer (Right)

Figure 20 – Pycnometers and Beakers within Desiccator (Left) and Vacuum Desiccator Set Up (Right)

Figure 21 – Pycnometers Completely Filled with Redistilled Kerosine (left), Pycnometers Immersed in Water Bath (Middle) and Pycnometer being Weighed (Right)

3.6.1.2. X-Ray Fluorescence Test

The XRF test is a non-destructive test that was used to determine the sample's chemical and elemental composition. The Bruker S2 Ranger device was used to analyse these oxide compositions. XRF works by bombarding the test material with x-rays, resulting in the atoms found within the tested material to emit secondary fluorescent x-rays. The intensity and energy of these emitted x-rays were measured, indicating which oxides are present as well as their mass percentage.

The test was done on the raw material and on the treated powders explained within section 3.3. prior to casting. The materials were oven dried for a minimum of 24 hours prior to testing.

Figure 22 - Bruker S2 Ranger Device (Left) and Tested Samples within Apparatus (Right)

3.6.1.3. Scanning Electron Microscope Test with EDS Mapping

The SEM-EDS test was used to examine the microstructure of the selected samples. This test involves a high energy electron beam directed on a samples' surface producing secondary electrons and x-rays, which are transformed into various signals and sent to a monitor to create a final 2D image. This was done using Carl Zeiss FESEM with a Gemini II Column (15 kV) and Elect Plus EDS Detector.

This test was done a few selected samples in poste their powder and paste form. The samples selected were those that underwent combined treatments as they were assumed to obtain the most improved results. The sample images captured made use of a magnification of up to 20kx zoom, allowing high-resolution grayscale images to be produced.

The tested samples were first crushed into a powder and oven dried for 24 hours. Carbon tape was applied to the studs used for SEM testing, allowing for the powder of each material to adhere to the studs. Each stud was labelled with their respective sample name and were then stored in a container containing silica gel until test day, ensuring no absorbed moisture.

Prior to the test, the studs were placed in a vacuum chamber for 10 minutes for additional precaution. They were then inserted into the SEM chamber that was then sealed and vacuumed. Sample imaging was produced at magnification levels between 600 x and 14kx.

Figure 23 - Samples Prepared on Carbon Tape

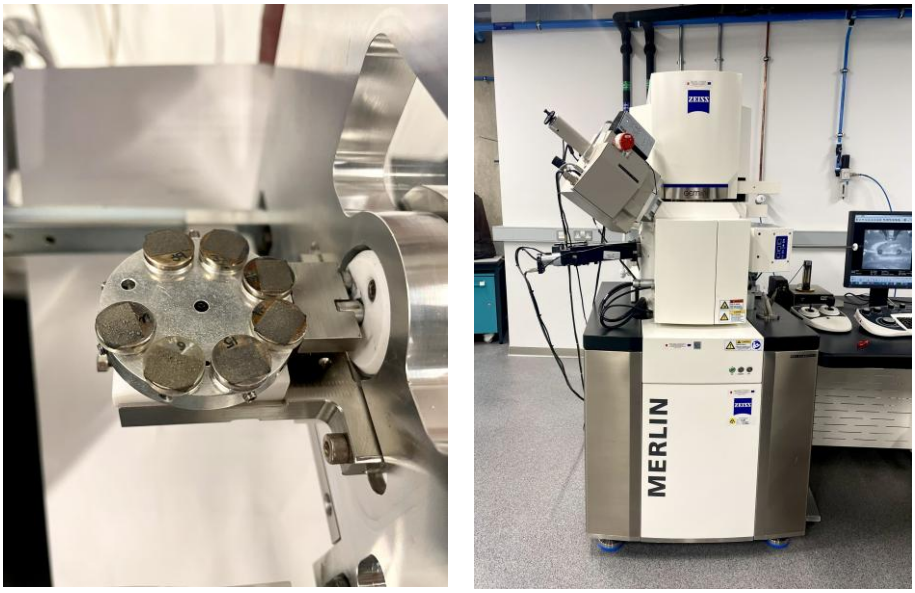

Figure 24 - Samples Prepared for SEM-EDS Testing (Left) and SEM Machine (Right)

3.6.1.4. X-Ray Diffraction Test

The XRD test is a non-destructive test that was used to determine the sample's amorphous and crystalline compositions. XRD works by utilising x-rays that are aimed towards the material, and the intensity and the scattered angles at which the x-rays interact with the material are measured. The XRD machine used for this analysis was a STOE Stadi MP diffractometer equipped with a curved germanium (111) monochromator and a Mythen 1K detector, using Cu $K_{\alpha 1}$ radiation (l = 1.54060 Å).

XRD testing was held on all paste samples at their 7 day age period and their respective original treated powder form. The tested paste samples were first crushed into a powder and then all material was oven dried for 24 hours. The software was adjusted in accordance with the following parameters for such an analysis:

Table 8 - Parameters set for XRD Analysis and Testing

Rotation	2θ
Starting Angle	2°
Ending Angle	90°
Increment	0.015
Scanning Speed	840 sec/step
Tube Voltage	40kV
Current	40mA

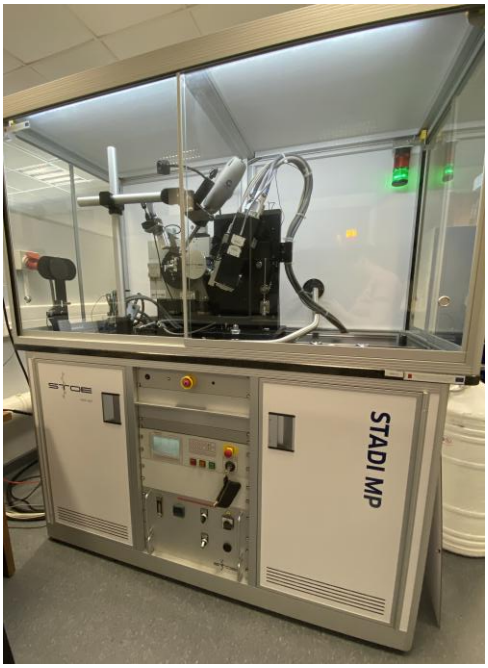

Figure 25 - STOE Stadi MP Diffractometer

3.6.1.5. Fourier-Transform Infrared Spectroscopy Test

The FTIR-KBr test is a test that was used to analyse the sample's molecular composition and chemical bonds. This works by having infrared radiation introduced on the sample, whereby the molecular bonds present absorb specific wavelengths at specific IR frequencies that match their own vibrational energy. A pattern is created through the absorbed frequencies, giving an indication of the material's molecular composition.

The FTIR test was done using a spectrophotometer (IRAffinity-1S) with Shimadzu IR solution 1.50 software, and the FTIR spectra (from 4000 to 500 cm^{-1}) were collected through an average of 20 scans for each sample. This test was performed using KBr as the reference material, having a ratio of 1 mg of sample is to 150 mg of KBr.

FTIR-KBr testing was held on all paste samples at their 7 day age period. The tested paste samples were first crushed into a powder and then all material was oven dried for 24 hours.

Figure 26 – IRAffinity-1S Spectrophotometer

3.6.1.6. Particle Size Distribution Test

The PSD is a test that was used to analyse the sample's proportion and range of particle sizes present, as well as the materials' specific surface area.

This test was done using the Mastersizer 2000's Hydro laser diffraction particle analyser (Malvern Instruments). The testing procedure undertaken was as follows:

1. 0.1 g of the sample being tested was suspended in 100 mL of deionised and underwent 2 minutes of sonication.
2. The instrument was flushed and cleaned twice using water prior to a background scan being done, making sure that it is uncontaminated.
3. The suspended sample was then directly added into the instrument and stirred at 2000 rpm using 50% ultrasound power.
4. To prevent material accumulation and produce improved results, the previous parameters were increased gradually to 3000 rpm and 70% respectively.
5. The sample was measured through an average result created from 5000 measurement snaps of 5 seconds repeated through 30 measurement cycles.

The test was done on the raw material as well as the treated powders explained within section 3.3. prior to casting. The materials were oven dried for a minimum of 24 hours prior to testing.

Figure 27 - Mastersizer 2000's Hydro Laser Diffraction Particle Analyser

3.6.1.7. pH Test

The pH test was done using a phenolphthalein indicator, where a few drops were applied to each treated and untreated material prior to casting. This test was done to help indicate and trace the extent of the carbonation treatment when compared to the other samples that had not undergone such a treatment.

3.6.2. Paste Testing

3.6.2.1. Fresh Property Testing

3.6.2.1.1. Flow Table Test

This test method was used to determine the consistency, that is, the fluidity, of the casted paste. The procedure of the flow table test was done in accordance with the testing standard EN-1015-3:1999, 'Methods of test for mortar for masonry – Part 3: Determination of consistence of fresh mortar (by flow table)' (British Standards Institution, 1999).

This procedure made use of a truncated conical mould which was placed centrally on the plate disc of the flow table. The paste was added into the mould in two subsequent layers, each layer compacted with 10 tampers, and any excess paste was removed from the top. The mould was raised vertically after approximately 15 s, allowing the paste to flow. Subsequently, the flow table disc was jolted 15 times, one per second, allowing the paste to further spread out. The diameters of the paste were measured in two directions at right angles to each other, using vernier callipers.

Figure 28 - Paste Mix Poured into Conical Mould (Left) and Measured Diameter of Spread after Tamping (Right)

3.6.2.1.2. Isothermal Calorimetry

Isothermal calorimetry was used to measure the heat flow created by paste samples throughout their hydration process. This test evaluated the isothermal hydration kinetics of the different samples, helping to understand their early strength development, setting characteristics, effects of compositions, and compatibility of the different materials.

Five paste samples were selected for testing: the mix designs containing the combined treatment materials and both controls. It was made sure that the samples were all prepared under the same mixing conditions for precise comparison, using the same mixture proportions that were specified for the mix design. Also, prior to the sample preparation, the apparatus was calibrated according to the recommendations given by the manufacturer and the baselines were determined.

The prepared sample was placed within an empty vial, its mass was recorded, and the vial was sealed creating a vapour tight setting. The vial was placed in the calorimeter (Calmetrix I-Cal 8000 HPC) and the insertion time was recorded. It was made sure that the specimen ages after the mixing cycle ended and the time they were placed in the calorimeter, were all consistent. Such a test was performed at constant temperature of 23°C (ASTM International, 2014).

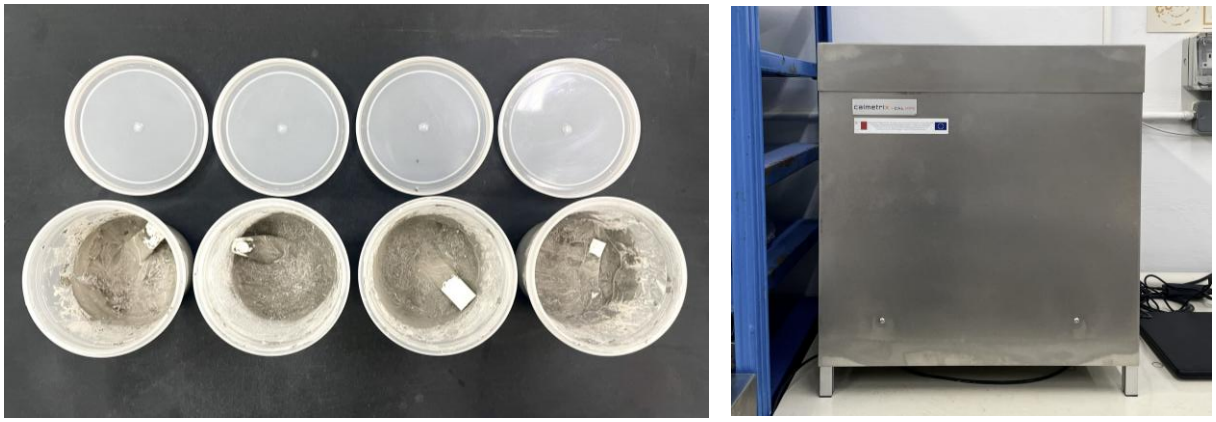

Figure 29 - Prepared Samples within Vials (Left) and Calorimeter Machine (Right)

3.6.2.2. Hardened Property Testing

3.6.2.2.1. Compressive Strength Test

Every variable paste cast underwent a compressive strength test to deduce which of the variables could result in the highest compressive strength prior to failing. This test was imposed on the casted samples at both 7 and 21 age days.

The procedure of the compressive strength test was done in accordance with the testing standard EN-196-1-2005, 'Methods of testing cement – Part 1: Determination of strength' (European Committee for Standardization, 2005). For each variable casted, three samples of each variable were tested having a load rate of 2.4 MPa*s and a sensitivity of 90 kN.

Some precautions taken while the test was being executed to ensure precision and consistency within the results achieved, are as follows:

- The top and bottom plates of the machine that came in contact with the sample were scraped off clean before the sample was placed, ensuring a flat and smooth surface.
- The faces having the smoothest and level surfaces were chosen to come in contact with the machine's compression plates.

Prior to the compressive test, the three samples were weighed, and their dimensions were measured using a digital scale and vernier calliper, respectively. These were taken in order to calculate the density of each sample and also to calculate their final strength in MPa.

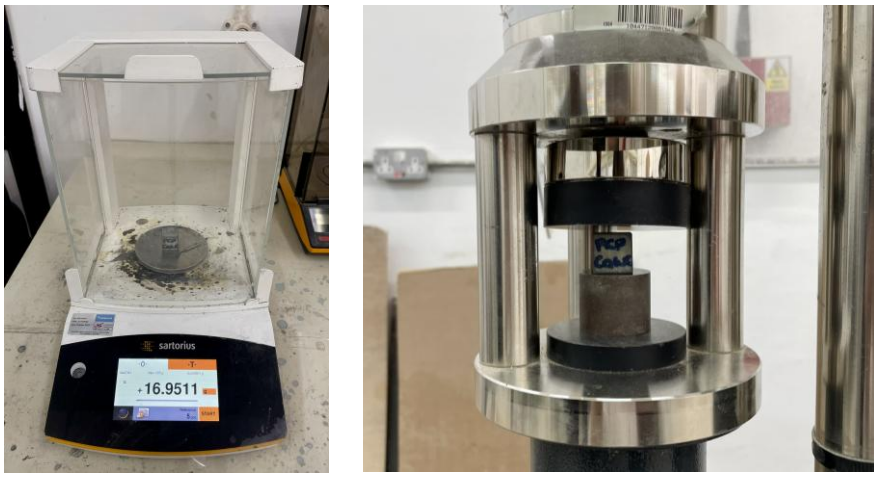

Figure 30 - Weighed Sample (Left) and Sample Loaded in Compression Machine (Right)

Figure 31 - Compression Machine Set Up

3.6.2.2.2. Vacuum Saturation Porosity Test

The scope of this test was to determine the permeable `hardened cement paste samples, which effects their durability, mechanical, and transport properties. Vacuum saturation is an accurate way to determine the accessible pore volume within porous materials such as cement paste, where the pores are small in size or may have entrapped air present, which would prevent complete saturation to occur, especially under standard conditions. Hence, this test involved the application of a vacuum, whereby any entrapped air was removed allowing full saturation of the sample to occur. Such a test was imposed on the casted samples at both 7 and 21 age days.

Prior to the initialisation of the test, the samples underwent conditioning. This involved oven drying at 105 ± 5°C for two days. Once removed from the oven, the samples were left to cool to room temperature, and their oven-dry mass was recorded.

The test set-up is presented in the schematic drawing shown below which mainly consisted of two vacuum desiccators: one contained the samples and the other contained distilled water, which were connected to a vacuum pump and a pressure gauge.

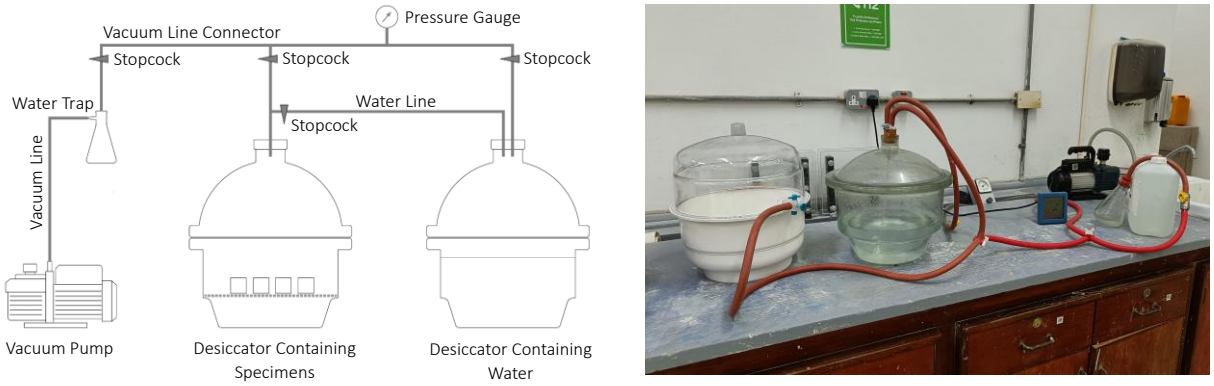

Figure 32 - Diagram of Vacuum Saturation Porosity Set Up (Left) and Vacuum Saturation Porosity Set Up (Right)

Once the samples and the distilled water were placed in their respective desiccators, the vacuum pump was initiated and left to run continuously for 3 hours, making sure that the pressure was below 100 hPa. After 3 hours, the vacuum line that led to the desiccator containing the samples, was closed and the water line connecting the two desiccators was opened. This allowed the deaired water to drain from one desiccator and fill the other containing the specimens. The water line was closed after a sufficient amount of water had entered to cover the samples completely and the vacuum line was reopened. The specimens were then allowed to be covered in water while under vacuum for another hour.

After a total of 4 hours, the vacuum pump was switched off and vacuum line was closed, allowing air to enter the desiccator containing the specimens. The samples were left under water for an additional 20 hours, after which their buoyant mass and saturated surface-dry mass was obtained and tabulated.

Figure 33 - Saturated Surface-dry Mass of Sample (Left) and Buoyant Mass of Sample (Right)

3.6.2.2.3. Sorptivity Test

The scope of this test was to determine the rate of water absorption through the capillary action of unsaturated hardened cement paste samples. This test works by taking note of the mass increase of each specimen as a function of time due to water absorption (ASTM International, 2004). This test was imposed on the casted samples at both 7 and 21 age days.

The specimens underwent consistent sample conditioning prior to the initialisation of the test. This included two steps, where the specimens were dried at 50 ± 2°C for 3 days and after were removed from the oven and stored in a sealed container at 23 ± 2°C. All the surfaces of the samples were sealed using aluminium tape apart from the top face. Said face, which was later subjected to the water absorption, was measured to achieve its surface area.

The test set-up was prepared. This included: a container having specimen supports and enough tap water that its level reached 3 mm above the surface of the specimen subjected to the test. The container was then covered to avoid any moisture loss or evaporation. Once the set-up was completed, a stopwatch was used to measure the mass of each specimen at 0, 1, 5, 10, 20, 30, 60 minutes as well as every hour for the first 6 hours, where each sample face subjected to the water was tapped dry prior to the measurement. These intervals were then followed by a readings every 24 hours which were then recorded and tabulated until a stable weight was achieved.

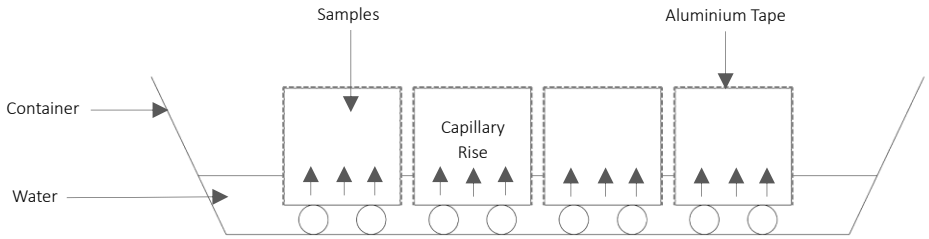

Figure 35 - Diagram of Sorptivity Test Set Up

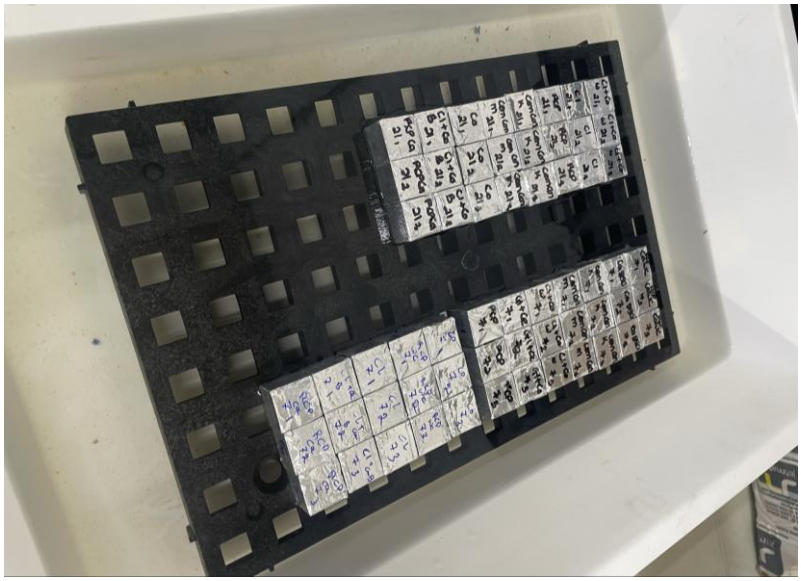

Figure 34 - Samples Placed within Test Set Up

3.6.3. Mortar Testing

3.6.3.1. Fresh Property Testing

3.6.3.1.1. Flow Table Test

The same testing procedure was performed as explained in section 3.6.2.1.1.

Figure 36 - Mortar Mix Poured into Conical Mould (Left) and Measured Diameter of Spread after Tamping (Right)

3.6.3.2. Hardened Property Testing

3.6.3.2.1. Vacuum Saturation Porosity Test

The same testing procedure was performed as explained in section 3.6.2.2.2. This test was imposed on the casted samples at both 7 and 21 age days.

Figure 37 – Samples Placed within Test Set Up (Left), Saturated Surface-dry Mass of Sample (Middle) and Buoyant Mass of Sample (Right)

3.6.3.2.2. Sorptivity Test

The same testing procedure was performed as explained in section 3.6.2.2.3. This test was imposed on the casted samples at both 7 and 21 age days.

Figure 38 - Samples Placed within Test Set Up

3.6.3.2.3. Ultrasonic Pulse Velocity Test

This test is another non-destructive test that is mainly used to evaluate the homogeneity and quality of the sample type under consideration, in this case being mortar. It does so by examining any defects found within the sample such as cracks, voids and cavities, through the determination of pulse velocity. This test was imposed on the casted samples at both 7 and 21 age days (Al Biajawi et al., 2022; Kaliyavaradhan & Ling, 2019).

The test initially involved the determination of the transducer arrangement. It was decided that said arrangement made use of the direct transmission, which involved placing both transducers on opposing faces, at right angles to said faces for maximum energy propagation. Prior to the transducer being placed on the sample surface, a coupling medium (petroleum jelly) was spread across the sample faces to ensure good acoustical contact.

The transit time and the path length were determined by using the ultrasonic test equipment and by measuring the shortest distance between arranged transducers, respectively (British Standards Institution, 2021).

Figure 39 - Petroleum Jelly (Left) and Ultrasonic Pulse Velocity Test Equipment (Right)

3.6.3.2.4. Compressive Strength Test

The same testing procedure was performed as explained in section 3.6.2.2.1., making use of 2400 N/s and 90 kN as the load rate and sensitivity respectively. Such a test was imposed on the casted samples at both 7 and 21 age days.

Figure 40 - Compression Machine Set Up (Left), Sample Loaded in Compression Machine (Middle) and Crushed Sample (Right)

Chapter 4: Results and Discussion

4.1. Overview

This chapter discusses the results obtained from the characteristic; mechanical and durability testing performed on the treated RCP and mix designs of both paste and mortar which have been described in chapter 3.

4.2. Characteristic Tests

4.2.1. X-Ray Fluorescence Test

As explained in section 3.6.1.2., the XRF test was done on the cement control, the raw material and all treated materials, in their original powder form. The resulting mass percentage oxides present within each sample type is shown in table 9 below:

Table 9 - Chemical Composition of Sample Types

Sample Code	Oxide *(%)*									Other Oxides *(%)*
	CaO	SiO_2	Na_20	SO_3	Al_2O_3	Fe_2O_3	MgO	K_20	P_2O_5	
Cem Con	62.80	14.10	6.76	5.48	3.17	2.98	2.29	1.19	0.47	0.76
RCP	75.60	4.05	16.00	1.08	1.54	0.68	-	0.18	0.40	0.47
RCP-Ca	77.40	3.94	10.70	1.26	1.42	0.67	2.73	0.45	0.51	0.92
RCP-DC	70.90	3.56	21.25	0.90	1.36	0.61	-	0.063	0.29	1.07
RCP-WC	69.40	3.86	19.00	0.74	1.36	0.65	3.19	0.48	0.52	0.80
RCP-L	80.60	3.72	10.50	1.00	1.13	0.77	1.50	-	0.32	0.46
RCP-CaDC	63.30	3.12	26.80	0.97	1.10	0.53	3.10	0.25	0.41	0.43
RCP-CaWC	77.20	4.18	10.80	0.92	1.55	0.65	2.96	0.37	0.55	0.81
RCP-LDC	76.40	3.91	13.20	1.03	1.44	0.70	2.46	0.15	0.37	0.35

Other Oxides includes the following:

Cl, TiO_2, MnO, CuO, ZnO, CoO, Cr_2O_3, V_2O_5, NiO, Rb_2O, As_2O_3, Ga_2O_3, SeO_2, Br, SrO, ZrO_2, CdO, Y_2O_3, GeO_2, SnO_2

The below table provides the chemical requirements from various standards that should be met by materials that are intended to be used for cementitious or pozzolanic action. Each material under testing was evaluated against the chemical requirements using their resulting mass percentage oxide composition from the table above.

Table 10 - Chemical Requirements of Sample Types

Standard Requirements		Cem Con		RCP		RCP-Ca		RCP-DC		RCP-WC		RCP-CaDC		RCP-CaWC		RCP-LDC	
Standard Codes	Chemical Requirements	Results *(%)*	Inference	Results *(%)*	Inference	Results *(%)*	Inference	Results *(%)*	Inference	Results *(%)*	Inference	Results *(%)*	Inference	Results *(%)*	Inference	Results *(%)*	Inference
ASTM C618 – 12a	$SiO_2 + Fe_2O_3 + Al_2O_3$, minimum 50-70%	20.25	N.S.	6.27	N.S.	6.03	N.S.	5.53	N.S.	5.87	N.S.	4.75	N.S.	6.38	N.S.	6.05	N.S.
	Loss on ignition, maximum 10%	-	-	-	-	-	-	-	-	-	-	-	-	-	-	-	-
BS EN 450-1:2005	$SiO_2 + Fe_2O_3 + Al_2O_3$, minimum 70%	20.25	N.S.	6.27	N.S.	6.03	N.S.	5.53	N.S.	5.87	N.S.	4.75	N.S.	6.38	N.S.	6.05	N.S.
	Na_2O shall not exceed 5.0%	6.76	N.S.	16.00	N.S.	10.70	N.S.	21.25	N.S.	19.00	N.S.	26.80	N.S.	10.80	N.S.	13.20	N.S.
	MgO shall not be greater than 4.0% by mass	2.29	S	0	S	2.73	S	0	S	3.19	S	3.10	S	2.96	S	2.46	S
BS EN 197-1:2011	SiO_2 shall be not less than 25.0% by mass	14.10	N.S.	4.05	N.S.	3.94	N.S.	3.56	N.S.	3.86	N.S.	3.12	N.S.	4.18	N.S.	3.91	N.S.
	$CaO + SiO_2$, minimum 50% by mass	76.90	S	79.65	S	81.34	S	74.46	S	73.26	S	66.42	S	81.38	S	80.31	S
NBR 12653	$SiO_2 + Fe_2O_3 + Al_2O_3$, minimum 50-70%	20.25	N.S.	6.27	N.S.	6.03	N.S.	5.53	N.S.	5.87	N.S.	4.75	N.S.	6.38	N.S.	6.05	N.S.
	Na_2O, maximum 1.5%	6.76	N.S.	16.00	N.S.	10.70	N.S.	21.25	N.S.	19.00	N.S.	26.80	N.S.	10.80	N.S.	13.20	N.S.

The cement powder also underwent testing to be used as a comparable control to the raw and treated powders. This material only satisfied two clauses, those being a low percentage of MgO and a high percentage of combined CaO and SiO_2. However, it is important to note that the mass percentage oxide values given from the production / distributing facility itself vary slightly, and when these values were compared to the chemical requirements, they actually satisfied four conditions (refer to appendix A).

These 4 included the previous two as well as the low percentage of Na_2O present. This shows that there are some discrepancies in the results due to the XRF testing procedure and should be kept in mind when analysing the other materials, especially the Na_2O presence (largest variation).

In fact, the treated materials all met the same two conditions as the tested cement control powder and did not meet the Na_2O clause. This could be due to the above stated problem or the material itself had a higher value than required. However, this is inconclusive.

Overall, the material with the most idealistic oxide percentages was seen to be the powder that underwent a combination treatment of calcination and aqueous carbonation. However, its SiO_2 percentage was still low when compared to the cement control.

4.2.2. Particle Size Distribution Test

The following test has been conducted on the raw and treated powders as explained in section 3.6.1.6., to understand the effect that the various treatments have on the particle's sizes of RCP. As can be seen from the table below, the cement has the coarsest particle size distribution in comparison to the raw and treated samples, having values of 4.959 µm, 22.257 µm and 79.515 µm corresponding to D(1), D(5) and D(10) respectively. This may indicate that the crushing process used in the production of RCP yielded a finer material than that of commercial cement.

When comparing the individual treatments, aqueous carbonation (RCP-WC) yielded a material with the finest particle size distribution, while the dry carbonation (RCP-DC) produced one with the coarsest. This may indicate that dry carbonation results in particle agglomeration. When comparing the combined treatments, calcination with dry carbonation (RCP-CaDC) yielded a material with a finer particle size than RCP-DC, revealing that the introduction of calcination may have aided the reduction of agglomeration within the proceeding treatment. Overall limewater with dry carbonation treatment (RCP-LDC) produced the coarsest particles from all the treated materials.

Such results are supported through the particle size distribution graph below, which shows the peak volume percentage of cement occurring at particle sizes of approximately 50-80 µm, while all RCP treated samples expect for RCP-LDC occur at approximately 3-5 µm. Also, the RCP samples are seen to have a narrower distribution, while the cement control is seen to have a broader distribution.

The graph shows a double peak known as bimodal distribution for most of the tested materials. This double peak may be an indication of the presence of two distinct populations of particle sizes. This may be due to the fact that the tested powders produced from crushed recycled concrete is made up of two distinct particle elements being cement and aggregate. Another reason for the double peak may be the presence of agglomeration or elongated particles with different end diameters.

Table 11 - Particle Size Distribution for All Samples

Sample Type	D(1) *(µm)*	D(5) *(µm)*	D(10) *(µm)*
Cement	4.959	22.257	79.515
RCP	1.772	5.113	33.314
RCP-Ca	1.721	6.843	40.454
RCP-DC	1.551	7.770	45.883
RCP-WC	1.387	4.728	27.471
RCP-CaDC	2.210	6.879	22.456
RCP-CaWC	1.451	5.888	33.334
RCP-LDC	2.433	13.251	45.989

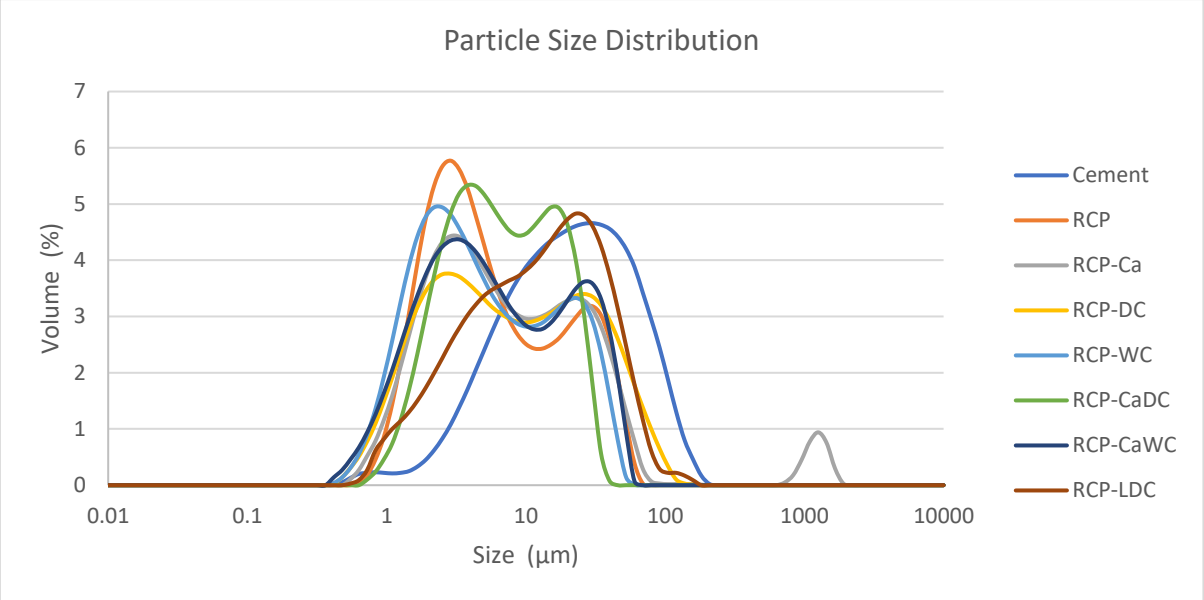

Figure 41 - Particle Size Distribution for All Samples

4.2.3. Density Bottle Test

The following test has been conducted on the raw and treated powders as explained in section 3.6.1.1., to determine the effect that the various treatments have on the relative density of RCP. As can be seen from figure 42 below, the cement control has the highest density at 3117.40 g/cm^3, while the untreated raw material (RCP) has a significantly lower density at 2615.98 g/cm^3. Such a lower density is primarily due to the porous nature of hydrated cement.

4.2.3.1. Effects of Treatments

Calcining showed an increase in density of 3.98% which is likely due to the dehydration of $Ca(OH)_2$ and its transformation into CaO, which is denser and more compact than the original hydrated phases. Such a transformation tends to result in a less porous and crystalline powder.

Carbonation treatment (both dry and aqueous) also increased the density of the powder by 1.25% and 0.70% respectively. Such an increase is due to the reaction of the introduced CO_2 with the $Ca(OH)_2$ to produce $CaCO_3$, which occupy the pores within the microstructure. However, carbonation still yielded a lower density than that shown by calcination.

Combination of treatments yielded the highest density from all treatments at 2727.85 g/cm^3, owing it to calcination with aqueous carbonation. The initial calcination created a material with a denser microstructure, as well as producing more readily available CaO that can react more effectively upon the carbonation treatment. These results show an improvement in the densification of the microstructure.

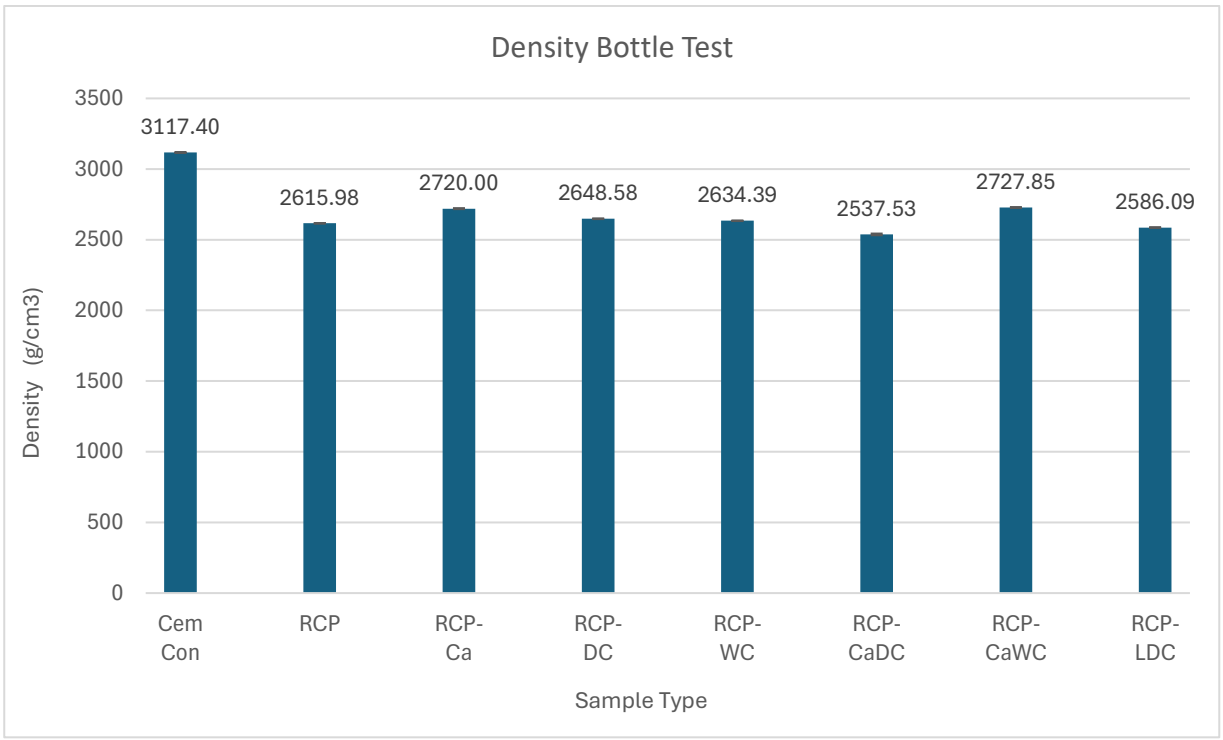

Figure 42 - Density Bottle Test on All Sample Types

4.2.4. pH Test

The following test has been conducted on the raw and treated powders as explained in section 3.6.1.7. This pH test is a small indicatory test that was done to aid in determining whether the treatments had an effect on the subjected powders. It was conducted using phenolphthalein solution that turns pink when subjected to an alkaline solution and remains colourless in an acidic one.

Once subjected to phenolphthalein, both the cement control and the RCP turned pink. This occurs since both powders are considered as alkaline due to the presence of $Ca(OH)_2$ and CaO phases. The darker purple colour of the cement control indicates more alkalinity. This is due to RCP having a higher percentage of $CaCO_3$, which automatically lowers the alkalinity. It is also observed that RCP-Ca turned a slightly darker shade of pink when compared to the original RCP. This indicates that calcination of the original RCP resulted in a lower percentage of $CaCO_3$ and a higher percentage of $Ca(OH)_2$. These two observations correlate with the XRD results.

RCP-DC, RCP-WC, and RCP-LDC all remained colourless, which means that their pH was lowered after carbonation treatment, proving that the treatment occurred. On the other hand, RCP-CaWC and RCP-CaDC did not turn completely colourless, indicating that the prior treatment of calcination inhibited the amount of carbonation reaction that can occur.

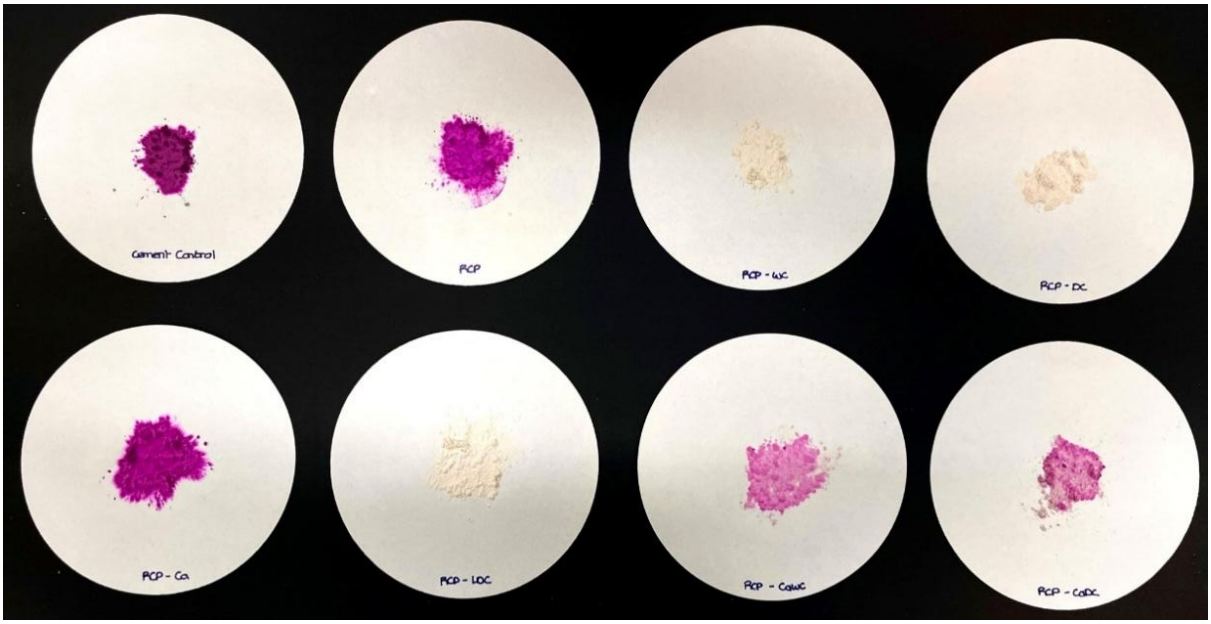

Figure 43 - pH Test on All Sample Types

4.2.5. X-Ray Diffraction Test

XRD testing was done to determine the sample's amorphous and crystalline compositions. Below are the resulting graphs of XRD testing that show the diffraction patterns for all sample paste types at 7 days.

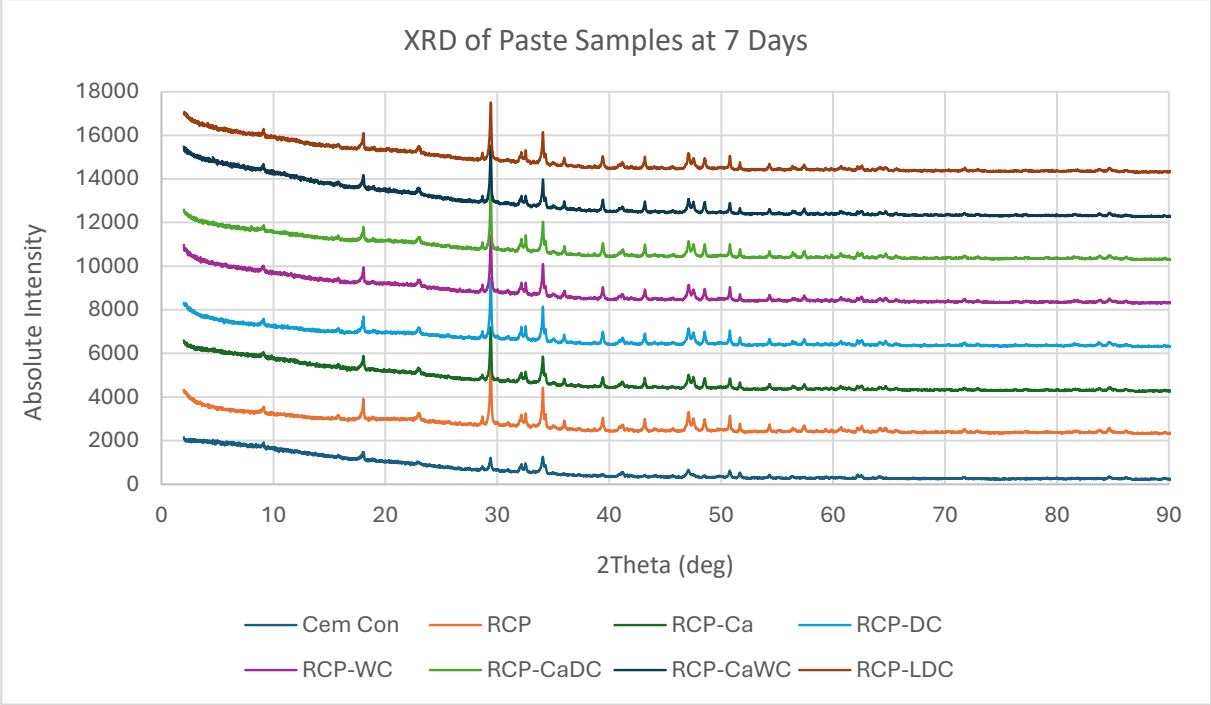

Figure 44 - XRD Patterns of All Paste Samples at 7 Days

From the analysis of the previous graphs, it was determined that the following hydrated phases were present within the 7 day paste samples:

Table 12 - XRD Results_Chemical Phases found within Mix Designs

Sample Code	Calcite *($CaCO_3$)*	Portlandite *($Ca(OH)_2$)*	Tobermorite *(C-S-H)*	Gismondine *(C-A-S-H)*	Belite *(C_2S)*	Alite *(C_3S)*	Alite *(C_3S)*	Total Alite
Cement Control	11.1	21.7	13	4.7	19.2	11.5	19	30.5
RCP	36	16.6	6	2.3	12.2	6.7	20.2	26.9
RCP Ca	31.4	17.4	12	2.1	17.2	6.5	13.1	19.6
RCP DC	33.9	14.9	10.2	0.8	14.8	8.5	16.8	25.3
RCP WC	35.6	15	10.6	1.2	13.6	6.5	17.5	24
RCP CaDC	35.1	15.6	6.3	1.5	13.3	8.9	19.3	28.2
RCP CaWC	35.5	14.1	9	1.5	12.5	6	21	27
RCP LDC	36.8	14.7	6.5	1.8	11.3	6.9	22	28.9

With reference to the above table, it was noted that the cement control paste had the highest percentage of all phases (ref. 2nd – 7th column) at 21.7%, 13%, 4.7%, 19.2% and 30.5% respectively, except for calcite (ref. 1st column) at 11.1%. This percentage of calcite was actually the lowest from all the tested samples.

Through the addition of 20% replacement RCP, the calcite formation increased to 36%, while the percentage of portlandite, tobermorite and gismondine decreased drastically. This indicates that the production of such phases was reduced due to the lack of unhydrated / uncarbonated phases present. This observation also applies to all paste samples making use of treated RCP, where limewater and carbonation treatment showed the highest carbonation percentage.

Therefore, it can be said in general that the addition of carbonated RCP resulted in the precipitation of calcite and the reduction of load bearing phases. However, when analysing the results on a deeper level, each mix design reveals a varying trend regarding the present hydrated phases. The following inferences were made based on the results:

1. Two forms of alite formed within all the mix design pastes. Such a phase controls the early strength development, and upon hydration transforms into a C-S-H phase such as tobermorite, which contributes directly to the compressive strength of the material, as it is a high load bearing phase.

2. Both forms of alite were seen to have an increased percentage within RCP-CaDC, while only one form of alite was seen to increase within the RCP-CaWC sample. This trend was also similar for the same samples with the individual carbonation treatment (RCP-DC and RCP-WC).

3. The percentage of formation of belite was seen to be much less than that of alite when comparing all mix design samples to that of the cement control, when in reality it should be higher since it has barely started reacting within the first 7 days. Such a phase has similar kinetics to alite, however, it possesses a slower reaction rate. Thus, it is responsible for the later term strength (normally 28 days or later), which aids the material in having long term durability and progressive strength gain.

4. The cement control mix was seen to have the highest percentage of belite at 19.2%, followed by RCP-Ca at 17.2% and RCP-DC at 14.8%.

5. RCP-Ca was seen to have the highest percentages of portlandite, tobermorite, gismondine, and belite at 17.4%, 12%, 2.1% and 17.2% respectively, when compared to the other treated samples. This means that calcination produced a material with highest reactivity and a potential for the highest long term strength and durability.

Results are showing that the cement control mix has characteristics of hydrated minerals, which occurs during curing proceeding the reaction process in the presence of water. Limited calcite formation is found since there is only atmospheric carbon dioxide present.

However, the other mix designs, show the occurrence of carbonation alongside the hydration process. This is due to the addition of RCP which supplies additional calcium oxide to the material. This is also seen in those mix designs involving carbonation treatment, as there is an additional introduction of carbon dioxide.

4.2.6. Fourier-Transform Infrared Spectroscopy Test

FTIR testing was done to analyse the sample's molecular composition and bonds. Below are the resulting compilation of FTIR graphs for all sample paste types at 7 days. Refer to table with summarized graph data found in appendix E

This FT-IR analysis reveals the following:

1. Calcination treatment produced a true SCM: Only the thermal treatment successfully converts the RCP into a chemically active material capable of consuming the hydration-released portlandite.
2. Both pastes with the incorporation of carbonated RCP (RCP-DC and RCP-WC) successfully utilize the calcined RCP, as evidenced by the reduced $Ca(OH)_2$ signature.
3. The combination of calcination and dry carbonation treatment (RCP-CaDC) yielded the most optimized C-S-H structure (Si-O frequency), indicating the highest degree of polymerization at 7 days.
4. The application of dry Carbonation Treatment (RCP-CaDC) appears to accelerate C-S-H maturation (peak shift to 964 cm^{-1} more effectively at 7 days, likely due to a localized reaction mechanism).
5. The application of aqueous Carbonation Treatment (RCP-CaWC) promotes the formation of carboaluminates (multiple peaks between 1429 cm^{-1} and 1506 cm^{-1}). These phases are known to contribute significantly to early age strength and densify the paste microstructure by filling pores. The shift in the C-S-H peak is less pronounced than in the CaDC sample.
6. The lime treatment strategy (RCP-LDC) prioritizes physical enhancement over chemical activation. It does not trigger SCM activity (no portlandite consumption) but significantly improves the C-S-H structure via the nucleation effect, similar to the simple RCP inclusion.
7. The resulting values of 873.75 (medium) and 713.66 (weak) is secondary confirmation of calcite.

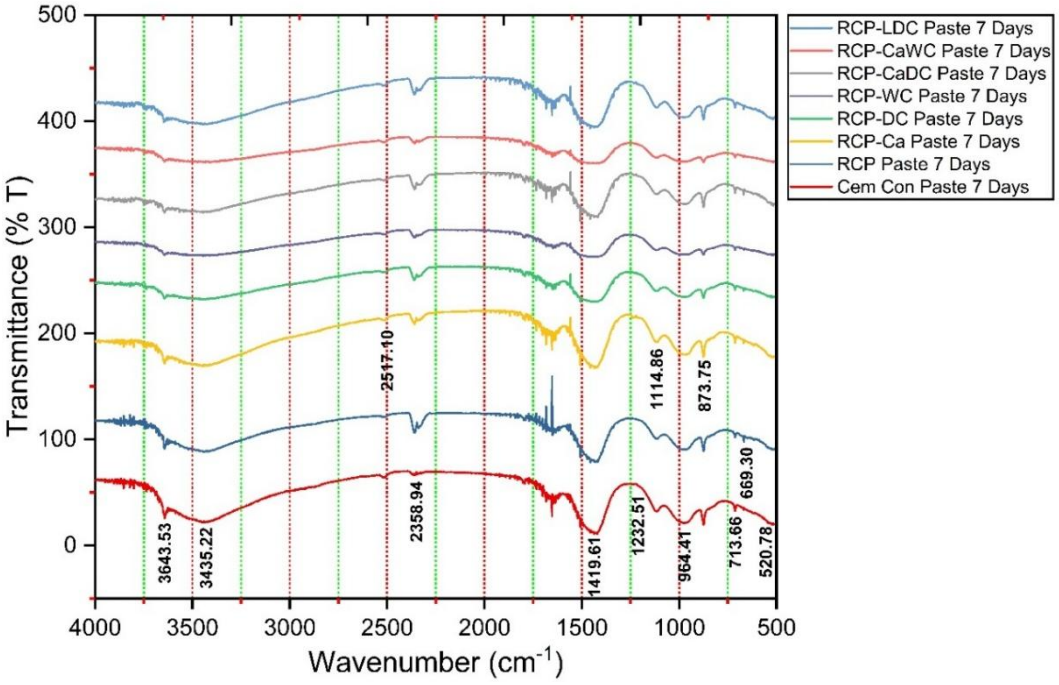

Figure 45 - FTIR Patterns of Mix Designs

4.2.7. Scanning Electron Microscope Test with EDS Mapping

Below are the resulting SEM analysis images done on a selected number of pastes at 7 days that were assumed to have to most improved results when compared to a sample using cement. The paste samples selected are those that make use of RCP that underwent combined treatments.

The images illustrate the cement control sample to have the densest microstructure, as expected. Similarly, RCP-CaDC has a dense microstructure with the exception of some micro-cracks and pores. RCP-CaWC is also seen to have an adequate microstructure. However, an increase in the size of micro-cracks is seen when compared to RCP-CaDC. On the other hand, RCP-LDC is seen to have a highly porous microstructure with diminished characteristics.

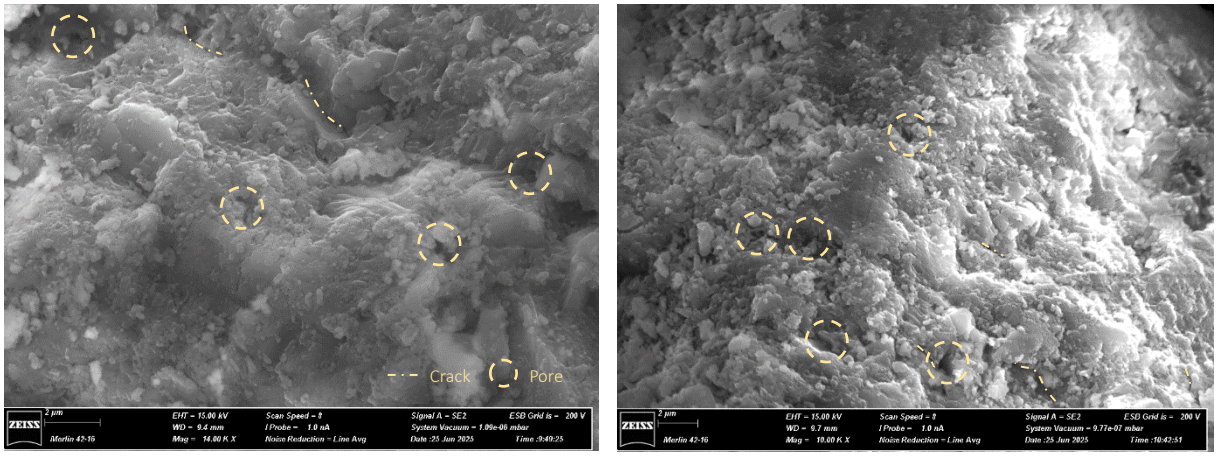

Figure 46 - SEM Images of Cem Con (left) and RCP-CaDC (Right) Pastes at 7 Day Testing

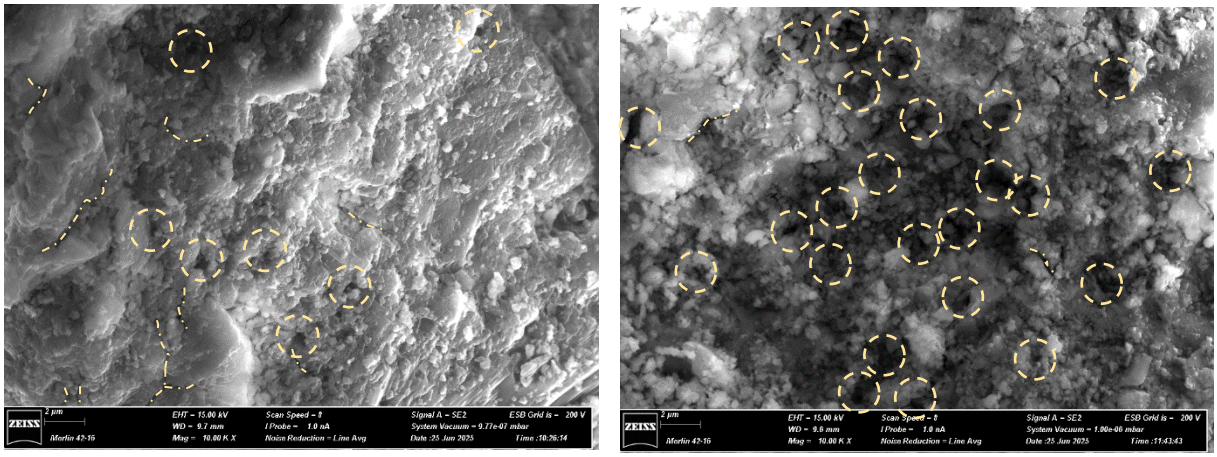

Figure 47 - SEM Images of RCP-CaWC (left) and RCP-LDC (Right) Pastes at 7 Day Testing

4.3. Fresh Property, Mechanical and Durability Tests on Paste and Mortar Samples

4.3.1. Flow Table Test

Overall, most mix designs resulted in a reduced workability when compared to the cement control, expect for RCP-WC and RCP-CaDC. The highest resulting workability is the RCP-WC mix at a 15.46% increase. This could be due to the formation of calcite crystals and other carbonation products, which fill the available pores after carbonation treatment. This means that the structure has a lower internal porosity and hence lower water absorption.

RCP-Ca mix is seen to have a workability found between the cement control mix and the RCP mix. This shows that calcining did have an effect on the RCP and has transformed its physical and chemical structure, making it more similar to that of cement. This occurs since calcination removes bound water found within the hydration products, resulting in the crystal structure collapse of such products (C-S-H, $Ca(OH)_2$). This causes the material to compact on itself at microscopic level, becoming more dense and less porous.

High workability was also seen in RCP-CaDC sample, which is a combination treatment of calcining and dry carbonation. This is due to the combination of both treatments which are explained previously above. This is further seen within the density results. This sample was seen to have the highest density amongst the paste samples containing the treated material, being comparable to that of the cement control. This result proves the densification of the microstructure.

The flowability (water requirement) of the RCP sample was low as expected. This is most probably due to the fact that it is hydrated cement and hence, contains hydrated products which tend to be porous.

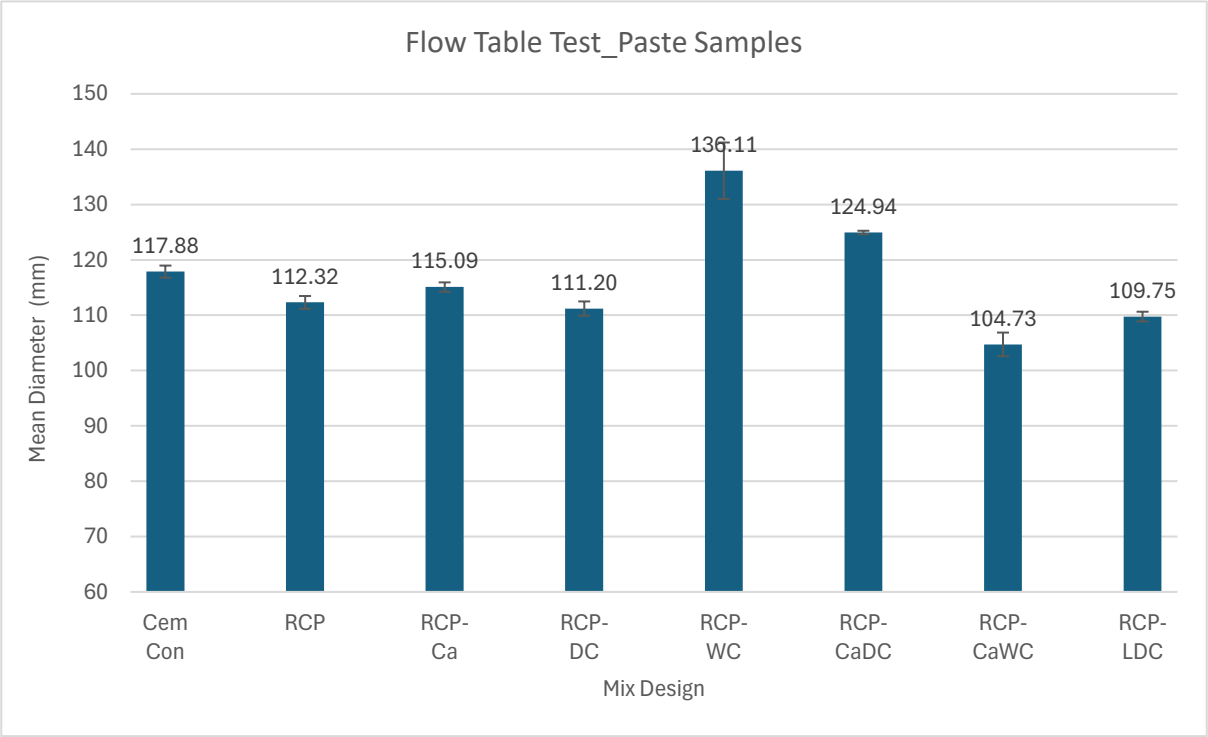

Figure 48 - Flow Table Graph of Paste Mix Designs

4.3.1.1. Flow Table of Mortar Samples

The cement control can be seen to have the lowest flow, while the addition of RCP treated material into the mix design seems to show an increase in fluidity. Similar to the flow results of the paste samples, RCP-CaDC was seen to have an improved flow correlating with a higher density showing the densification of the microstructure.

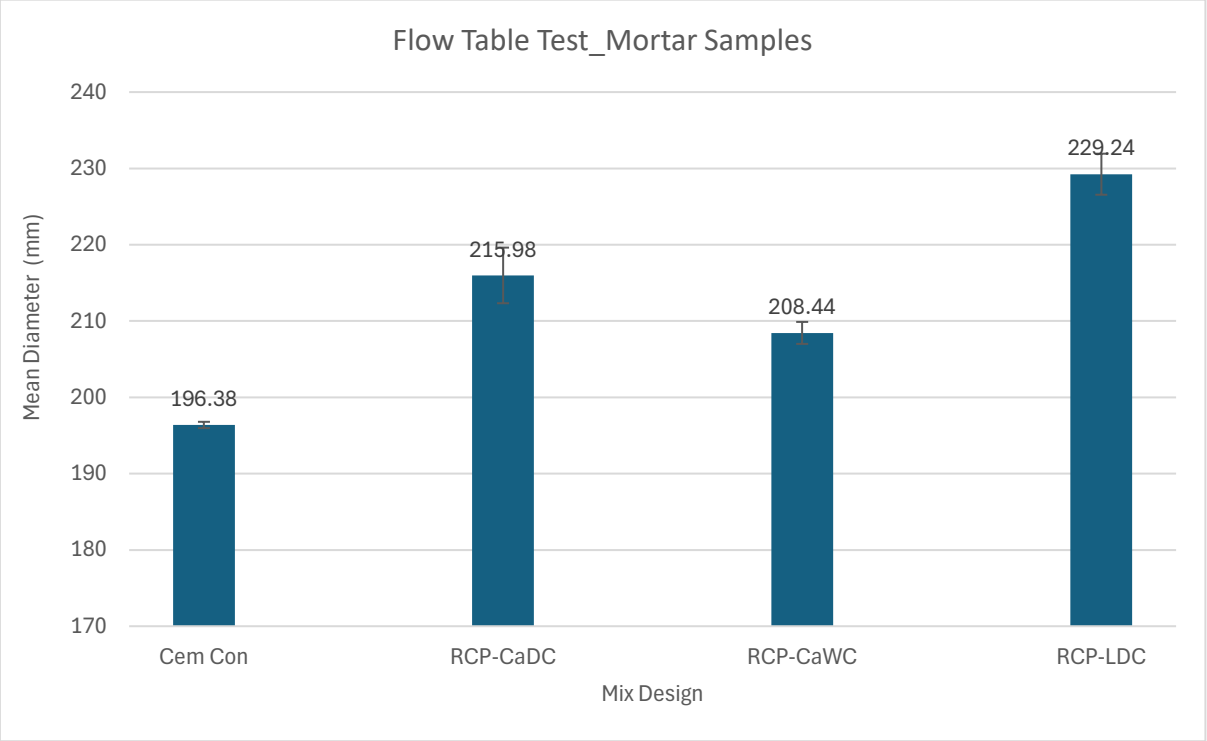

Figure 49 - Flow Table Graph of Mortar Mix Designs

4.3.2. Isothermal Calorimetry Test

The isothermal calorimetry test was performed on cement control and cement pastes that include both raw material (RCP) and RCP that underwent combined treatment. The graph below illustrates the heat flow evolution showing the cement control exhibiting a typical Portland cement hydration profile, characterised by an initial dissolution peak followed by an induction period and a pronounced main hydration peak associated with alite hydration occurring between approximately 12 and 14 h. This mix displayed the highest peak intensity, reflecting unhindered cement hydration.

The RCP mix design showed a reduction in the main hydration peak intensity and a slight delay in peak occurrence relative to the control. This behaviour is attributed primarily to the dilution effect caused by the 20% cement replacement and the limited intrinsic reactivity of the as-received RCP.

The RCP–CaDC mix design exhibited a further reduction in peak intensity and a marginally extended induction period compared to untreated RCP. This suggests that dry carbonation led to partial surface passivation, limiting early-age dissolution and reaction of reactive phases formed during calcination. In contrast, the RCP–CaWC mix design showed an improved hydration kinetics, where the main hydration peak occurred closer in time to that of the cement control and with a higher intensity than both

untreated RCP and RCP–CaDC. This indicates that wet carbonation preserved a higher fraction of reactive phases generated during calcination.

The RCP–LDC mix design exhibited the most favourable hydration behaviour among the RCP mixes. The main hydration peak occurred slightly earlier and reached a higher intensity than other RCP variants, indicating enhanced early-age hydration kinetics.

The cumulative heat release graph illustrated that the cement control consistently exhibited the highest cumulative heat release, reflecting the highest degree of hydration. All RCP-containing mixes showed lower cumulative heat release, consistent with the reduced cement content.

The untreated RCP and RCP–CaDC mixes released the lowest cumulative heat, indicating limited early-age contribution from the SCM. RCP–CaWC demonstrated a higher cumulative heat release than untreated RCP and RCP–CaDC, confirming improved hydration kinetics following combined calcination and aqueous carbonation. The RCP–LDC mix exhibited the highest cumulative heat among the RCP-containing pastes, approaching the trajectory of the cement control, particularly during the acceleration period.

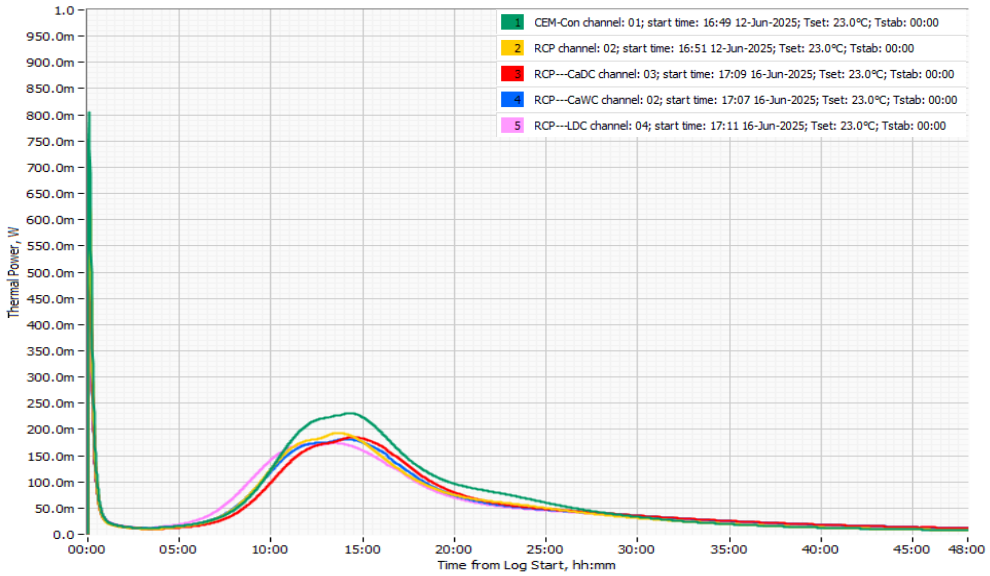

Figure 50 - Heat Flow Evolution Graph on Paste Mix Designs

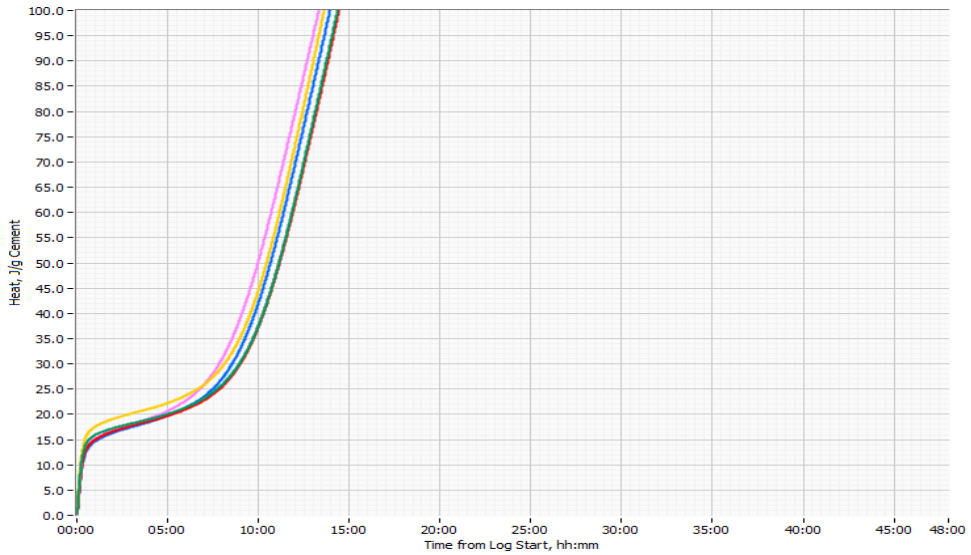

Figure 51 - Cumulative Heat Release Graph on Paste Mix Designs

4.3.3. Compressive Strength Test of Paste Samples

The following test has been conducted on all paste samples as explained in section 3.6.2.2.1. As expected, the results show a trend of increasing compressive strength from 7 day testing to 21 day testing, expect for RCP-LDC, that has a loss of 7 MPa.

Compressive strength of the 7 day paste testing revealed RCP-LDC to have the highest compressive strength at 94.54 MPa, followed by RCP-DC at 86.79 MPa and RCP-CaDC at 83.29 MPa. However, a similar trend was not seen for the compressive strength of 21 day testing. In fact, RCP-CaDC had the highest strength at 114.89 MPa, followed by RCP-DC at 110.3 MPa and RCP-CaWC at 106.63 MPa.

It is also noted that the resulting compressive strength of pastes including aqueous carbonated material (RCP-WC) has an overall lower strength when compared to the paste including the dry carbonated material (RCP-DC). This similar trend was seen with the pastes including the combined treated materials of both dry and aqueous carbonation, where RCP-CaDC overall a higher strength than that of RCP-CaWC.

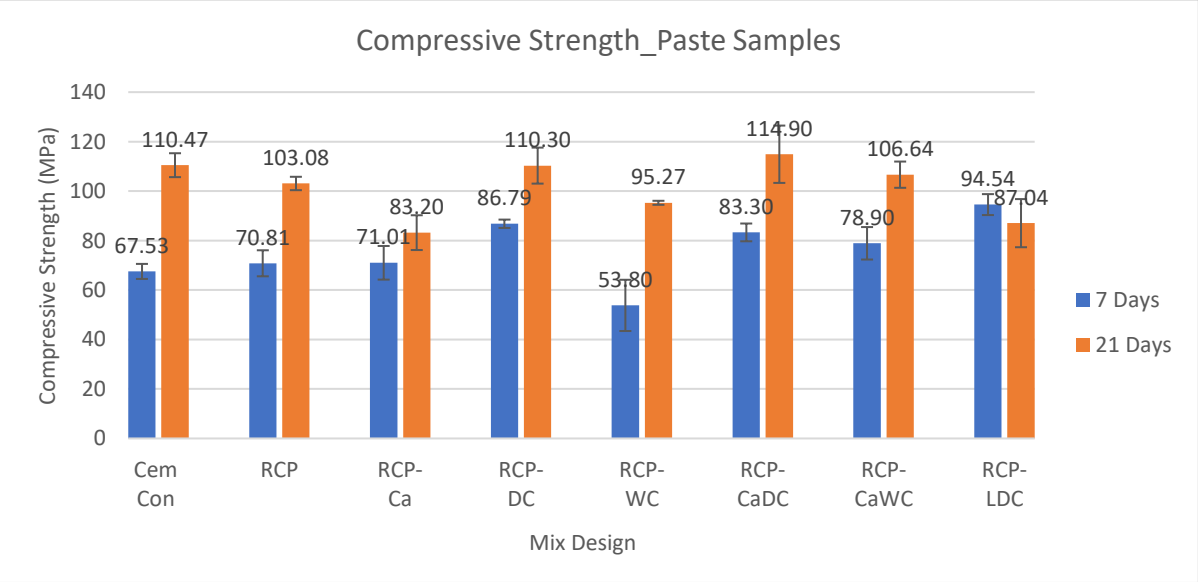

Figure 52 – Compressive Strength Graph of Paste Mix Designs

4.3.3.1. Correlation with XRD Results

RCP-CaDC was seen to have a steady increase in compressive strength from 7 to 21 days, while also having a high alite content of 28.2% at 7 day testing. This means that the early strength phases would have converted into more C-S-H and C-A-S-H phases at 21 days. This observation together with a high percentage calcite formation means that both carbonation and hydration occurred, resulting in a higher compressive strength at 21 day testing, as can be seen.

With regards to RCP-DC at 7 day testing, tobermorite and belite were seen to have a higher percentage and a slightly lower calcite and alite percentage than that of RCP-CaDC. As seen from the compressive results, 7 day strength of RCP-DC was slightly higher than RCP-CaDC, and 21 day strength was slightly lower. This correlates with the XRD results since at 7 days RCP-DC has higher tobermorite and lower alite, meaning that alite was converted in C-S-H earlier on than that of RCP-CaDC, relating to the higher strength. A lower calcite value and higher belite, means that there is a more balanced occurrence between carbonation and hydration, and can mean that later stage compressive testing may result in much better values.

RCP-CaWC was found to have a good percentage of calcite and tobermorite, as well as a considerable amount of belite and alite, which has directly contributed to its strength development of 106.63 MPa at 21 day testing.

Compressive testing of RCP-Ca sample conveyed a lower strength of 71 Mpa and 83.2 MPa at 7 and 21 days respectively. This is reflected in the XRD results that show a lower percentage of calcite and alite when compared to the other treated samples. However as explained in section 4.2.5., it was seen to have the highest percentages of portlandite, tobermorite, gismondine, and belite when compared to the other treated samples, showing potential of improved reactivity and long term strength and durability.

While having the highest compressive strength at 7 days, RCP-LDC is the only sample seen to have a decrease in compressive strength when reaching 21 days. Upon analysis with XRD, such results may be due to the over accumulation of $CaCO_3$ particles, which are soft in nature, providing increased early strength. However, by time such particles may have inhibited the production of the C-S-H structure making it weak.

4.3.3.2. Compressive Strength Test of Mortar Samples

The below graph displays the compressive strength results obtained by the mortar samples. All samples are seen to have an increase in compressive strength from 7 day to 21 day testing. This indicates ongoing hydration reactions. Similar to the paste results found above, the mortar sample containing the replacement material with calcination and dry carbonation treatment obtained the highest compressive strength of 64.67 MPa at 21 days. These results also correlate with the density of each sample, where the cement control has the highest density and the RCP-LDC has the lowest. This is reflected in the compressive strength where the cement control has the highest, and RCP-LDC and RCP-CaWC have the lowest.

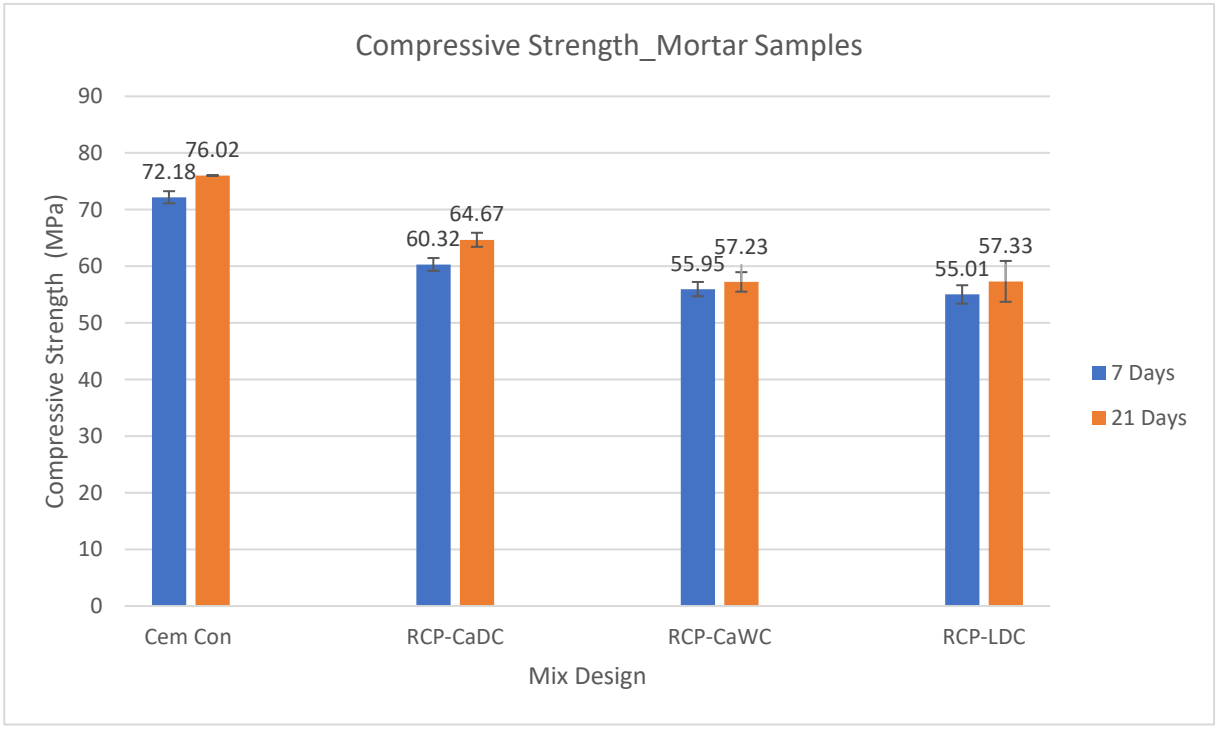

Figure 53 - Compressive Strength Graph of Mortar Mix Design

4.3.4. Vacuum Saturation Porosity of Paste Samples

The following test has been conducted on all paste samples as explained in section 3.6.2.2.2. As expected, all paste samples show a decrease in porosity over time, confirming ongoing hydration. When compared to the cement control mix with porosity of 28.6% at 7 days and 27.5% at 21 days, all design mixes had a higher porosity. The material with the lowest porosity and most comparable to the cement control is the RCP-CaDC sample having a porosity of 29.5% at 7 days and 27.8% at 21 days.

These porosity results correlate with the density of the tested samples, were most samples had an increase in density from 7 to 21 days. It was also seen that RCP-CaDC had the highest density of all the treated samples at 2160.70 kg/m^3 (7 days) and 2182.85 kg/m^3 (21 days). These are comparable to the results of the cement control paste samples, having a density of 2165.50 kg/m^3 (7 days) and 2184.52 kg/m^3 (21 days).

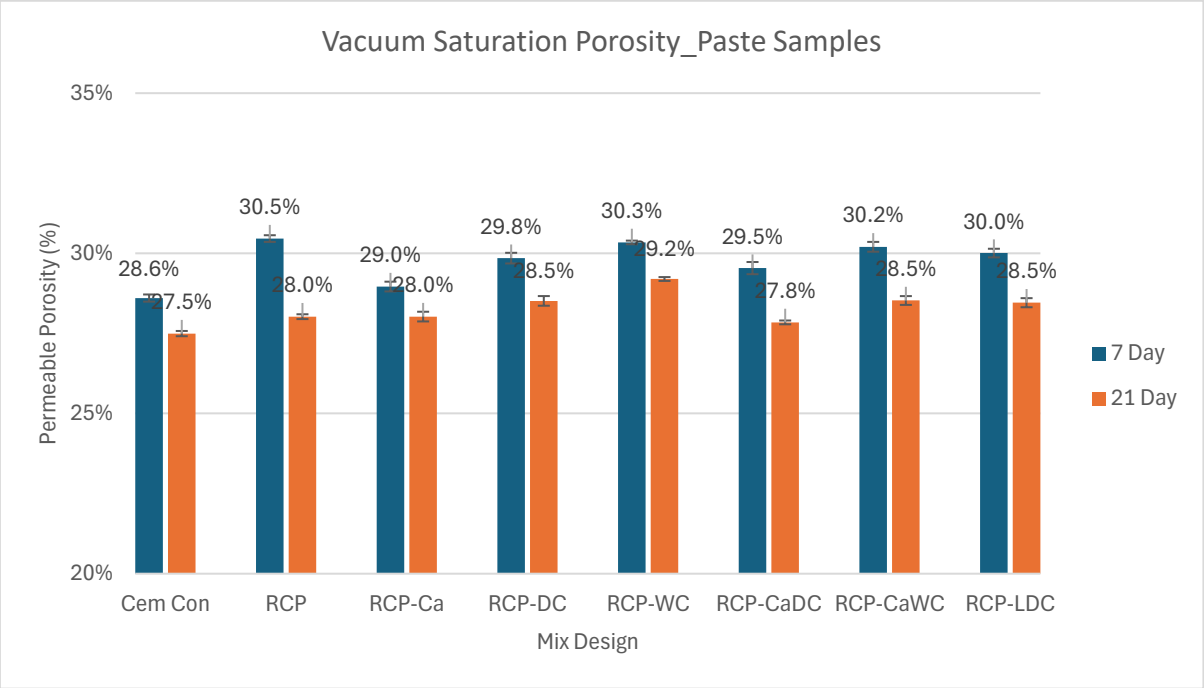

Figure 54 - Vacuum Saturation Porosity Graph of Paste Mix Design

4.3.4.1. Correlation with Compressive Strength Results

When comparing the permeable porosity results with those of compression it can be noticed that a higher porosity of the RCP-DC sample results in a lower compressive strength, while a lower porosity of the RCP-CaDC sample results in a higher compressive strength. This relationship is also seen with the RCP-WC and RCP-CaWC samples, where RCP-WC has high porosity and low compressive strength, while RCP-CaWC has low porosity and a high compressive strength.

4.3.4.2. Vacuum Saturation Porosity of Mortar Samples

The below graph displays the porosity results obtained by the mortar samples. Similar to the porosity results of the paste samples, the majority of samples show a decrease in permeable porosity over time, as well as the cement control having the lowest permeable porosity of 14.9% at 7 days and 14.4% at 21

days. The remaining samples all have an approximate increase to 16.45% at 7 days and 16.4% at 21 days. In fact, these results correlate with the density results showing that all samples have an increase in density from 7 to 21 day testing. Also, all samples including the 20% replacement of treated material yield a lower density than that of the cement control mortar.

These results, show that the introduction of the 20% cement replacement yielded a material with a more porous matrix.

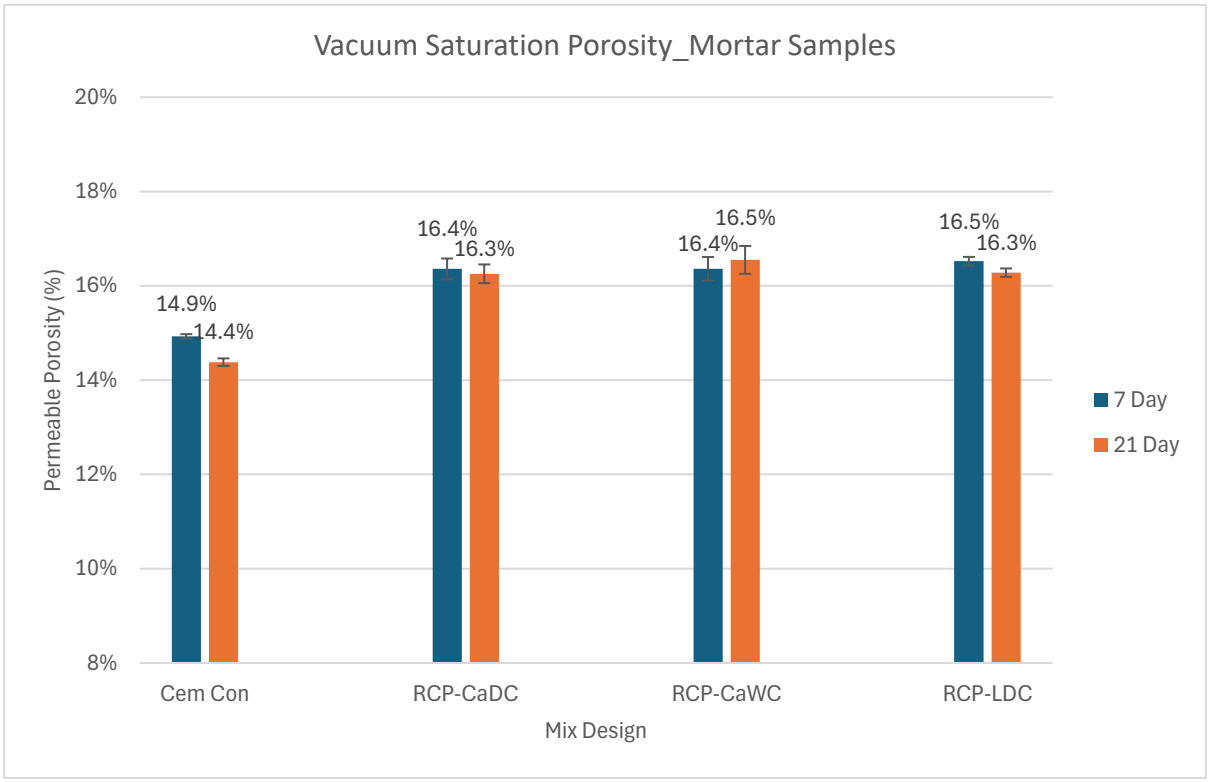

Figure 55 - Vacuum Saturation Porosity Graph of Mortar Mix Design

4.3.5. Sorptivity of Paste Samples

The following test has been conducted on all paste samples as explained in section 3.6.2.2.3. Initial absorption is related to the rapid water uptake within the first 6 hours due to superficial and largely connected pores, while the secondary absorption is related to the slower uptake within the proceeding days due to micro-pores.

As can be seen from the below graphs, both RCP-Ca and RCP-CaDC have the lower initial absorption which correlate with their low porosity. The secondary absorption values are significantly lower than those of the initial, which is to be expected since the larger pores have already been saturated. However, RCP-Ca shows an exception with a spike in absorption at 21 days indicating progressive microcracking. This may lead to durability failure of the mix. It can also be seen that from 7 to 21 days most samples have a reduction in secondary sorptivity. This indicates pore refinement through passing days. Samples with the inclusion of combined treated RCP show an improvement in results when compared to the individual treatments indicating a more complex pore structure.

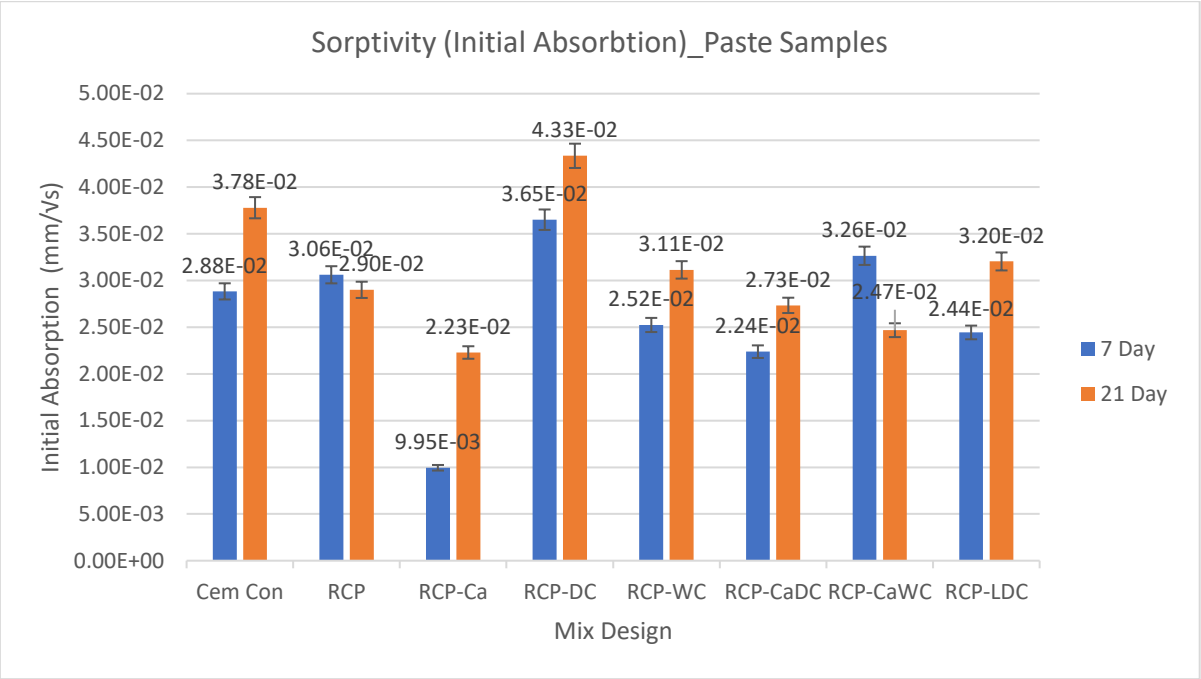

Figure 56 - Initial Absorption of Paste Mix Designs

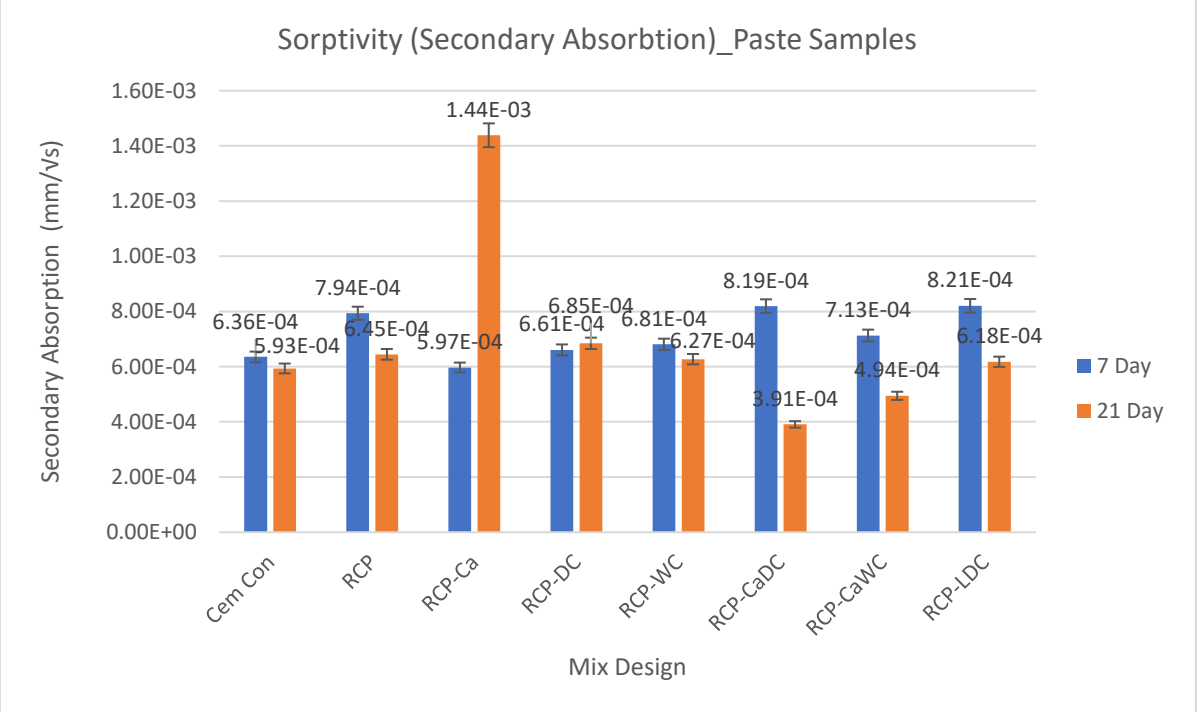

Figure 57 - Secondary Absorption of Paste Mix Designs

4.3.5.1. Sorptivity of Mortar Samples

The below graph displays the sorptivity results obtained by the mortar samples. RCP-CaWC is seen to have the highest initial and secondary absorption. On the other hand, RCP-CaDC yielded results most similar to the cement control, correlating with the highest compressive strength, highest density and

highest UPV achieved. As expected, secondary absorption has an overall significant decrease in values, with the cement control yielding the lowest. A low absorption value of cement correlates with it high density and high strength.

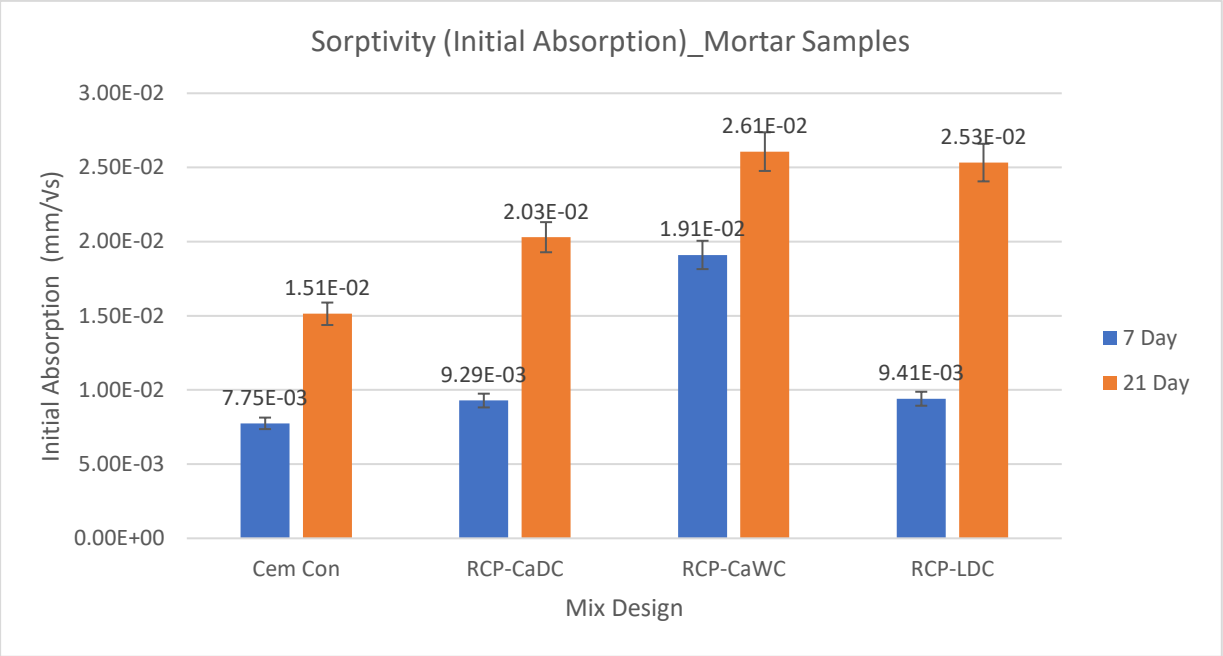

Figure 58 - Initial Absorption of Mortar Mix Designs

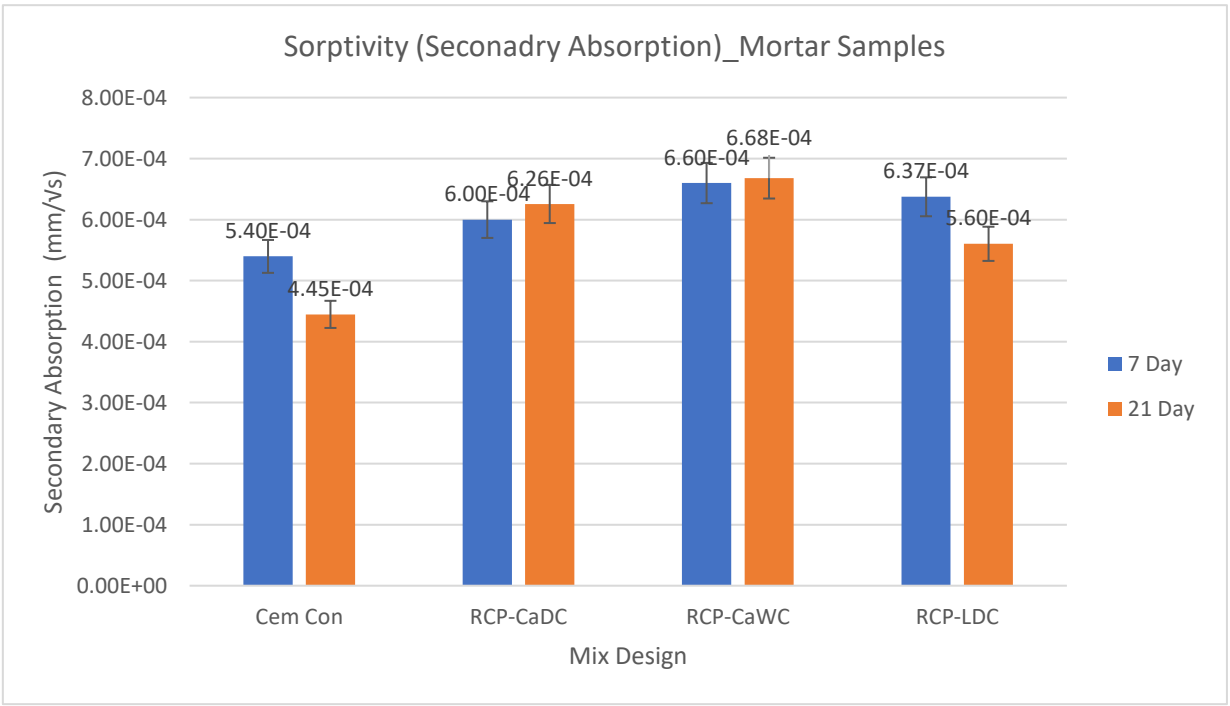

Figure 59 - Secondary Absorption of Mortar Mix Designs

4.3.6. Ultrasonic Pulse Velocity Test

The following test has been conducted on all mortar samples as explained in section 3.6.3.2.3. According to the standard quality classifications, UPV values that lie between 3-3.5k m/s are noted as doubtful, those that lie between 3.5-4.5 km/s are noted as good, and those that exceed 4.5 km/s are excellent (Hassiba et al., 2018). The mortar results in the graph below show an unusual decrease in all the samples when compared to compressive strength and porosity results that increased and decreased respectively. This decrease in velocity may be related to ongoing microstructural changes due to unfinished hydrated dynamics.

The RCP-CaDC sample has the highest velocity of 4.62 km/s (7 days) and 4.26 km/s (21 days) when compared to all samples, including the cement control. This means it has the best UPV performance. Both RCP-CaWC and RCP-LDC have similar performances, lower than that of RCP-CaDC which correlate with the compressive results.

Such results reinforce the data revealing the superior performance of the recycled concrete powder treated through calcination together with dry carbonation.

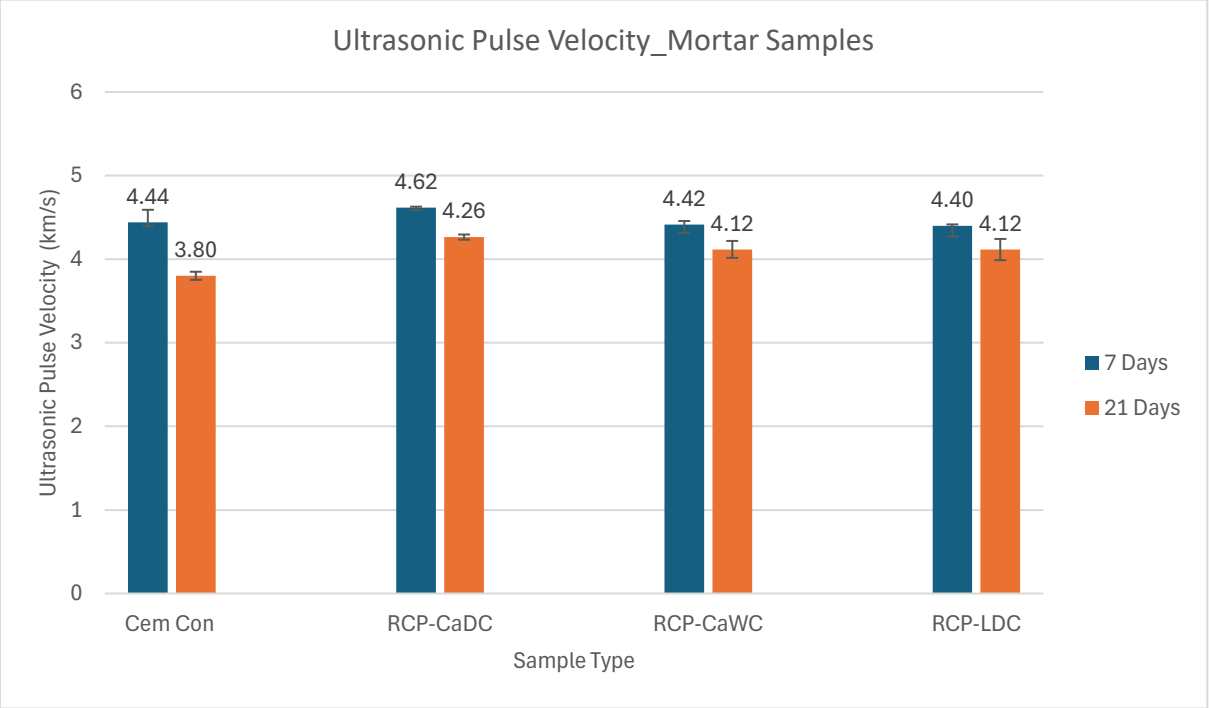

Figure 60 - Ultrasonic Pulse Velocity of Mortar Mix Designs

4.4. Summary of Results

Through XRF testing the RCP powder treated with a combination of calcination and aqueous carbonation was seen to achieve the most idealistic oxide percentages comparable to that of the Cement control. However, its SiO_2 percentage was still low in comparison with the control.

A decrease in particle size was seen from RCP-DC to RCP-CaDC with the introduction of calcination treatment prior to dry carbonation under the analysis of the particle size distribution test. The introduction of calcination aided with the reduction of agglomeration within the material. This produced a material having one of the finest particles sizes, while RCP-LDC was seen to have the coarsest.

Calcination treatment yielded a powder of higher density in comparison to both carbonation treatments, having an increase of 2.97%. This indicates that the transformation of $Ca(OH)_2$ into CaO within calcination is more effective in creating a denser microstructure than the transformation of $Ca(OH)_2$ into $CaCO_3$. However, combination of treatments (RCP-CaWC) was the most effective, as it achieved the overall highest density at 2727.85 g/cm^3.

The calorimetric results demonstrate that the early-age hydration behaviour of cement pastes with 20% replacement RCP (treated or untreated) is strongly dependent on the applied pre-treatment method rather than solely on the replacement level. Untreated RCP primarily acts as an inert filler at early ages, leading to reduced heat evolution due to cement dilution. Calcination introduces reactive phases; however, when followed by dry carbonation, these phases appear partially passivated, reducing their contribution to early hydration.

The RCP-CaWC mix design results in the formation of poorly crystalline carbonate phases and a more reactive surface chemistry, enabling partial recovery of hydration kinetics. Limewater treatment further enhances early-age reactivity by increasing calcium availability and alkalinity, thereby promoting faster alite hydration even in the presence of carbonation. However, RCP-LDC paste mix design also had a decrease in compressive strength of 7 MPa from 7 to 21 day testing, indicating poor long term hydration. This was backed up through SEM and density results which reveal the porous nature of the material.

XRD testing revealed a simultaneous occurrence of carbonation alongside the hydration process occurring within the mix designs with treated RCP. This brings about a competition between carbonation and hydration during the curing process. Whichever of the two has a favourable condition, the reaction kinetics of the material changes in their favour to produce more calcite or belite and alite. In this case, there is clear indication that carbonation treatment has inhibited the hydration reaction. This is seen from the reduction of all the hydration products after the addition of processed RCP.

While the above is true, RCP-CaDC was still seen to have an increased alite percentage of 28.2%, comparable to that of the cement control mix. In fact, RCP-CaDC paste sample had the highest compressive strength followed by RCP-DC, and RCP-CaWC at 21 days. This shows that the early strength phases (alite) converted into more C-S-H and C-A-S-H phases. This is further backed up from the RCP-CaDC mortar sample achieving the highest compressive strength.

In conjunction with the previously stated, RCP-CaDC mix design is seen to also have the highest density, low initial absorption and lowest porosity amongst all pastes using treated RCP. This occurs since initially calcination causes crystal structure collapse of C-S-H and $Ca(OH)_2$ through the removal of the bound water, followed by the formation of calcite crystals through carbonation. This causes the material to compact on itself at microscopic level, followed by calcite formation within available pores, creating a denser and less porous material.

XRD testing also revealed that the RCP-Ca mix design has the highest percentages of the majority of phases after the cement control, meaning it has the highest reactivity. Such results are also backed up through the FTIR testing, which means that this treatment created the possibility of long term strength

and durability. On the other hand, this mix design also resulted in an absorption spike at 21 days, which indicates progressive microcracking.

CHAPTER 5: Conclusion and Recommendations

5.1. Overview

The scope of this research aims at reducing C&DW disposal, by transforming it into RCP which becomes a sufficient and reactive SCM once subjected to carbonation treatment. This aims at reducing cement requirement for concrete production and recycling produced CO_2 through carbonation treatment. This was done by subjecting the produced RCP through a series of treatments for their comparison, observing the effectiveness of carbonation treatment. Such a comparison was done through characteristic, mechanical and durability testing of the treated powders and implementation as 20% cement replacement with paste and mortar samples.

5.2. Conclusions

From this research the following conclusions were determined:

1. The introduction of limewater soaking prior to carbonation produced a material of enhanced early-age hydration kinetics and high compressive strength of 94.54 MPa at 7 day testing. This occurred due to the limewater treatment increasing calcium availability and alkalinity, thereby promoting faster alite hydration even in the presence of carbonation and the presence of an over accumulation of $CaCO_3$ particles. However, through time this mix design resulted in decreased performance as a result of the over accumulation of $CaCO_3$ particles which are soft in nature. This inhibited the production of the C-S-H structure making it a very weak a porous structure. Such results give an indication of an unhealthy concrete mix, and hence such a treatment is not viable.

2. Calcination treatment was found to achieve an SCM with the highest pozzolanic activity. However, low compressive strength was achieved, together with indications of progressive microcracking due to a spike in secondary absorption at 21 days. This may lead to durability failure of the mix with progression of time.

3. RCP-WC mix design had a lower strength than RCP-DC, and similarly, RCP-CaWC had a lower strength than RCP-CaDC. Though both achieving improved and similar results, the use of dry carbonation treatment was superior. This result was unexpected since through literature it was found that dry carbonation produced a material with distinct layer separation of calcite and silica produced, while aqueous carbonation produced a more homogenous material.

4. Following on from the previous point, RCP-DC mix design (singular treatment) resulted in a higher porosity, a lower density and a lower compressive strength in comparison to the RCP-CaDC mix design (combined treatment). Thus, the introduction of calcination as a prior treatment improved its mechanical structure due to the combined reactivity that causes the material to compact on itself at microscopic level, followed by calcite formation within available pores.

5. Both carbonation methods effectively modified the hydration products. Combination of treatments (RCP-CaDC and RCP-CaWC) produced materials with increased formation of alite, contributing to the further production of C-S-H phases, aiding in their early strength development.

   The individual carbonation treatments both yielded materials with an increased formation of tobermorite and belite. The dry carbonation treatment yielded the most optimised C-S-H

structure, as well as accelerating its development, while the aqueous carbonation led to a chemically diverse and beneficial suite of stable carboaluminate phases.

6. Combined treatments involving calcination and either method of carbonation yield good chemical and mechanical results due to the formation of both calcite and hydrated phases, creating a material of increased reactivity and strength.

7. Results from this research have shown that CO2 absorption was successful and led to carbonation treatment which produced potentially suitable SCM, with some of the adopted treatment processes being more effective than others. The RCP material that showed most promise was RCP-CaDC, which achieve the highest compressive strength of 114.90 MPa at 21 days, surpassing that of the cement control.

5.3. Limitations

The X-Ray Fluorescence machine and particle size distribution machine had some limitations. Such limitations may have affected the results.

Maintaining the relative humidity and temperature of the sealed chamber used for both carobnation treatments was a challenge. Such specific and constant parameters are important as they influence the reaction processes that occur. Fluctuations within these set parameters may effect the material resulting in variation of properties, leading to diminished characteristic and mechanical properties.

The muffle furnace used for the thermal treatment process was small in size, which restricted the amount of RCP material that could be conditioned at one time. Hence, to achieve the amount of calcined material required, the furnace was used more than once, leading to more energy consumption than necessary.

5.4. Recommendations

The research conducted within this dissertation revealed promising results. However, further investigations into carbonation of RCP are required to achieve more optimal results for its use as a sufficient SCM.

All cast samples were mechanically and durably tested on 7 day and 21 days due to limited time and hence hydration reactions were still on going and did not show their final potential characteristics. It is therefore recommended that the samples are tested at 90 days to allow for 100% hydration to take place.

Similarly, characteristic testing (including XRD, FTIR and SEM) was done at 7 days. However, it would be beneficial if done at standard testing increments. This would allow for the understanding of the progressive hydration and carbonation reactions occurring within each mix design. Such testing can shed light on calcination yielding a material of increased reactivity while still achieving low density and high water absorption when applied as an SCM within the mix designs.

The introduction of combined treatments improved the performance of RCP as an SCM. However, further analysis is recommended to fine tune the parameters of each treatment when specifically applied as combination treatments for better results. This is more specific to RCP-CaWC, where its singular treatment (aqueous carbonation) also needs optimization. Within this study the flow rate was set to 5L/min. Even though other research showed it to have promising results, it could be that the rapid carbonation reactions resulted in an accumulation of product layer which may have limited the progression of hydrated reactions. Through literature and this dissertation, the use of 1 hour as the treatment duration was positive. However, due to the previously stated, further analysis should be done on the flow rate and time, to find the individual optimal parameters that yield better results together.

For the purpose of this dissertation all mix designs were prepared using a common water to binder ratio of 0.27 across all the samples. This ratio was obtained through trial mixes done on the as received RCP. Research could be done on the water to binder ratios to be specifically created for each individual mix design to be tested. This could potentially optimize the properties of the treated RCP's as an SCM.

The use of CO_2 sequestration (recycling produced CO_2 through carbonation treatment) and the recycling of C&DW to produce RCP to act as an SCM, is considered to be a more sustainable approach than the norm. This is due to the fact that it reduces the amount of CO_2 being emitted through its extraction and use, as well as through the reduction of required cement for concrete production. However, through this research it was found that the combined treatment of calcination followed by dry carbonation produced the best results and most similar to that of the cement control.

The main drawback that the use of calcination brings with it is the high energy consumption and therefore the associated carbon emissions that the thermal treatment activation process requires due to the high temperatures used. Thus, an exhaustive study on energy and life cycle cost assessments, as well as scalability is highly recommended to understand the feasibility of the use of such treatments, mainly calcination, and the use of milling required to transform the recycled concrete into a powder of required fineness which can be used as an SCM. This energy and life cost assessment was not the scope of this study and was not included.

Bibliography

Al Biajawi M.I., Embong R., Muthusamy K.,Ismail N., and Obianyo I.I.,(2022) - 'Recycled coal bottom ash as sustainable materials for cement replacement in cementitious composites: A review', Constr Build Mater, vol. 338.

Al-Janabi, A., Black, L., & Adu-Amankwah, S. (2024). Improvement of Recycled Cement Powder Characteristics from C&D Wastes by Accelerated CO2 Curing and/or Heat Treatment. *RILEM Bookseries*, 274–288.

Alper Ilki, Derya Çavunt, & Yavuz Selim Çavunt. (2023). *Building for the Future: Durable, Sustainable, Resilient*. Springer Nature.

Aquino Rocha J.H. and Toledo Filho R.D.,(2023) - 'The utilization of recycled concrete powder as supplementary cementitious material in cement-based materials: A systematic literature review', *Elsevier Ltd*. doi: 10.1016/j.jobe.2023.107319.

Ashraf, W., & Olek, J. (2016). Carbonation behavior of hydraulic and non-hydraulic calcium silicates: potential of utilizing low-lime calcium silicates in cement-based materials. *Journal of Materials Science*, *51*(13), 6173–6191.

ASTM International, (2004) - *ASTM C1585-04 - Standard test method for measurement of rate of absorption of water by hydraulic-cement concretes*.

ASTM International, (2014)- 'ASTM C1679-14- Standard Practice for Measuring Hydration Kinetics of Hydraulic Cementitious Mixtures Using Isothermal Calorimetry'

British Standards Institution, (1999) - *Method of test for mortar for masonry - Past 3: Determination of consistence of fresh mortar (by flow table) (BS EN 1015-3)*

British Standards Institution, (2021) - *Testing concrete in structures – Part 4: Determination of ultrasonic pulse velocity.(BS EN 12504-4:2021)*

British Standards Institution. (2010). *Methods of testing cement – Part 6: Determination of fineness – National Annex NC – Method of testing cement for density* (BS EN 196-6:2010)

European Committee for Standardization,(2015) - *Methods of testing cement - Part 1: Determination of strength.(EN 196-1:2005)*

Fang, X., Xuan, D., Shen, P., & Poon, C. S. (2021). Fast enhancement of recycled fine aggregates properties by wet carbonation. *Journal of Cleaner Production*, *313*, 127867.

Hassiba B., Mekki M., and Farid R.,(2018) 'The relationship between the compressive strength and ultrasonic pulse velocity concrete with fibers exposed to high temperatures', vol. 3, pp. 2543–3717,[Online].

Jeon, M.-K., Kim, J., Ham, S.-M., Kim, S., Han, A. T., Kim, H., & Kwon, T.-H. (2024). CO2 treatment of recycled concrete aggregates with high mortar contents: From finding optimal treatment condition, quality enhancement, to life cycle assessment. *Construction and Building Materials*, *447*, 137953.

Jiang, Y., Li, L., Lu, J., Shen, P., Ling, T.-C., & Poon, C. S. (2022). Mechanism of carbonating recycled concrete fines in aqueous environment: The particle size effect. *Cement and Concrete Composites*, *133*, 104655.

Kaliyavaradhan S.K. and Ling T.C.,(2019) - 'Performance of concrete with PVC fibres', in *Use of recycled plastics in eco-efficient concrete* , Woodhead Publishing, pp. 369–385.

Kazemian, M., & Shafei, B. (2023). Carbon sequestration and storage in concrete: A state-of-the-art review of compositions, methods, and developments. *Journal of CO2 Utilization*, *70*, 102443.

Li, J., Feng, Y., Zhong, H., Zhang, B., Wang, J., Zhang, B., & Xie, J. (2024). Effect of the Pretreatment on the Properties of Cement-Based Recycled Powder. *Coatings*, *14*(1), 107–107.

Li, Y., Han, D., Wang, H., Lyu, H., Zou, D., & liu, T. (2023). Carbonation curing of mortars produced with reactivated cementitious materials for CO2 sequestration. *Journal of Cleaner Production*, *383*, 135501.

Lu, B., Shi, C., Zhang, J., & Wang, J. (2018). Effects of carbonated hardened cement paste powder on hydration and microstructure of Portland cement. *Construction and Building Materials*, *186*, 699–708.

Mao, Y., He, P., Drissi, S., Zhang, J., Hu, X., & Shi, C. (2023). Effect of conditions on wet carbonation products of recycled cement paste powder. *Cement and Concrete Composites*, *144*, 105307.

Mehdizadeh H., Ling T.-C, Cheng X., and Mo K.H,- 'Effect of particle size and CO2 treatment of waste cement powder on properties of cement paste Effect of particle size and CO 2 treatment of

waste cement powder on properties of cement paste'. [Online]. Available: https://mc06.manuscriptcentral.com/cjce-pubshttps://mc06.manuscriptcentral.com/cjce-pubs

Mehdizadeh, H., Ling, T.-C., Cheng, X., Pan, S.-Y., & Mo, K. H. (2021). CO2 Treatment of Hydrated Cement Powder: Characterization and Application Consideration. *Journal of Materials in Civil Engineering*, *33*(4).

Meng, D., Cise Unluer, Yang, E.-H., & Qian, S. (2022). *Carbon sequestration and utilization in cement-based materials and potential impacts on durability of structural concrete*. *361*, 129610–129610.

Miller, S. A., Horvath, A., & Monteiro, P. J. M. (2016). Readily Implementable Techniques Can Cut Annual CO2 Emissions from the Production of Concrete by over 20%. *Environmental Research Letters*, *11*(7), 074029.

Real, S., Bogas, J. A., Carriço, A., & Hu, S. (2021). Mechanical Characterisation and Shrinkage of Thermoactivated Recycled Cement Concrete. *Applied Sciences*, *11*(6), 2454.

Ruth Bola Oliveira, D., Leite, G., Possan, E., & Marques Filho, J. (2023). Concrete powder waste as a substitution for Portland cement for environment-friendly cement production. *Construction and Building Materials*, *397*, 132382.

Shi, C., Wu, Z., Cao, Z., Ling, T. C., & Zheng, J. (2018). Performance of mortar prepared with recycled concrete aggregate enhanced by CO2 and pozzolan slurry. *Cement and Concrete Composites*, *86*, 130–138.

Tang, Y., Xiao, J., Wang, D., & Zhang, M. (2023). Effect of carbonation treatment on fracture behavior of low-carbon mortar with recycled sand and recycled powder. *Cement & Concrete Composites*, *142*, 105178–105178.

Wu, S., Liu, Q., Li, L., Kang, W., Tiong, M., & Huang, T. (2024). Quantitative characterization of recycled cementitious materials before and after carbonation curing: Carbonation kinetics, phase assemblage, and microstructure. *Construction and Building Materials*, *421*, 135596–135596.

Zajac, M., Skocek, J., Skibsted, J., & Ben Haha, M. (2021). CO2 mineralization of demolished concrete wastes into a supplementary cementitious material – a new CCU approach for the cement industry. *RILEM Technical Letters*, *6*, 53–60.

Zhan, B. J., Xuan, D. X., & Poon, C. S. (2018). Enhancement of recycled aggregate properties by accelerated CO2 curing coupled with limewater soaking process. *Cement and Concrete Composites*, *89*, 230–237.

Zhang, J., Shi, C., Li, Y., Pan, X., Poon, C.-S., & Xie, Z. (2015). Influence of carbonated recycled concrete aggregate on properties of cement mortar. *Construction and Building Materials*, *98*, 1–7.

Zhu, C., Fang, Y., & Wei, H. (2018). Carbonation-cementation of recycled hardened cement paste powder. *Construction and Building Materials*, *192*, 224–232.

APPENDIX A – X-RAY FLUORESENCE TEST

Cem Con			
Standard Codes	Chemical Requirements	Results *(%)*	Inference
ASTM C618 – 12a	$SiO_2 + Fe_2O_3 + Al_2O_3$, minimum 50-70%	26.85	Not Satisfied
	Loss on ignition, maximum 10%	3.20	Satisfied
BS EN 450-1:2005	$SiO_2 + Fe_2O_3 + Al_2O_3$, minimum 70%	26.85	Not Satisfied
	Na_2O shall not exceed 5.0%	0.11	Satisfied
	MgO shall not be greater than 4.0% by mass	1.35	Satisfied
BS EN 197-1:2011	SiO_2 shall be not less than 25.0% by mass	19.50	Not Satisfied
	$CaO + SiO_2$, minimum 50% by mass	83.15	Satisfied
NBR 12653	$SiO_2 + Fe_2O_3 + Al_2O_3$, minimum 50-70%	26.85	Not Satisfied
	Na_2O, maximum 1.5%	0.11	Satisfied

These Cem Con Mass percentage oxide values are those obtained from production / importing / distributing facility, whereas the cem con table found within the XRF test are those obtained through XRF analysis.

The following is a brief description of each standard being used:

ASTM C618 – 12a: is an international specification (based in US) that outlines the properties required for pozzolanic or cementitious action when using coal fly ash and raw or calcined natural pozzolan within concrete production.

BS EN 450-1:2005: is a European standard that specifies physical and chemical properties requirements of siliceous fly ash when being used as a type II addition within the production of concrete.

BS EN 197-1:2011: is the European standard that defines and outlines the specifications, composition and conformity required for common cements.

ABNT NBR 12653: is a Brazilian national standard that provides requirements for pozzolanic materials intended to be used in addition to Portland cement within paste, mortar, and/or concrete production.

Cem Con			
Standard Codes	**Chemical Requirements**	**Results** *(%)*	**Inference**
ASTM C618 – 12a	$SiO_2 + Fe_2O_3 + Al_2O_3$, minimum 50-70%	20.25	Not Satisfied
	Loss on ignition, maximum 10%	-	-
BS EN 450-1:2005	$SiO_2 + Fe_2O_3 + Al_2O_3$, minimum 70%	20.25	Not Satisfied
	Na_2O shall not exceed 5.0%	6.76	Not Satisfied
	MgO shall not be greater than 4.0% by mass	2.29	Satisfied
BS EN 197-1:2011	SiO_2 shall be not less than 25.0% by mass	14.10	Not Satisfied
	$CaO + SiO_2$, minimum 50% by mass	76.90	Satisfied
NBR 12653	$SiO_2 + Fe_2O_3 + Al_2O_3$, minimum 50-70%	20.25	Not Satisfied
	Na_2O, maximum 1.5%	6.76	Not Satisfied

RCP			
Standard Codes	**Chemical Requirements**	**Results** *(%)*	**Inference**
ASTM C618 – 12a	$SiO_2 + Fe_2O_3 + Al_2O_3$, minimum 50-70%	6.27	Not Satisfied
	Loss on ignition, maximum 10%	-	-
BS EN 450-1:2005	$SiO_2 + Fe_2O_3 + Al_2O_3$, minimum 70%	6.27	Not Satisfied
	Na_2O shall not exceed 5.0%	16.00	Not Satisfied
	MgO shall not be greater than 4.0% by mass	0	Satisfied
BS EN 197-1:2011	SiO_2 shall be not less than 25.0% by mass	4.05	Not Satisfied
	$CaO + SiO_2$, minimum 50% by mass	79.65	Satisfied
NBR 12653	$SiO_2 + Fe_2O_3 + Al_2O_3$, minimum 50-70%	6.27	Not Satisfied
	Na_2O, maximum 1.5%	16.00	Not Satisfied

RCP-Ca			
Standard Codes	**Chemical Requirements**	**Results** *(%)*	**Inference**
ASTM C618 – 12a	$SiO_2 + Fe_2O_3 + Al_2O_3$, minimum 50-70%	6.03	Not Satisfied
	Loss on ignition, maximum 10%	-	-
BS EN 450-1:2005	$SiO_2 + Fe_2O_3 + Al_2O_3$, minimum 70%	6.03	Not Satisfied
	Na_2O shall not exceed 5.0%	10.70	Not Satisfied
	MgO shall not be greater than 4.0% by mass	2.73	Satisfied
BS EN 197-1:2011	SiO_2 shall be not less than 25.0% by mass	3.94	Not Satisfied
	$CaO + SiO_2$, minimum 50% by mass	81.34	Satisfied
NBR 12653	$SiO_2 + Fe_2O_3 + Al_2O_3$, minimum 50-70%	6.03	Not Satisfied
	Na_2O, maximum 1.5%	10.70	Not Satisfied

RCP-DC			
Standard Codes	**Chemical Requirements**	**Results** *(%)*	**Inference**
ASTM C618 – 12a	$SiO_2 + Fe_2O_3 + Al_2O_3$, minimum 50-70%	5.53	Not Satisfied
	Loss on ignition, maximum 10%	-	-
BS EN 450-1:2005	$SiO_2 + Fe_2O_3 + Al_2O_3$, minimum 70%	5.53	Not Satisfied
	Na_2O shall not exceed 5.0%	21.25	Not Satisfied
	MgO shall not be greater than 4.0% by mass	0	Satisfied
BS EN 197-1:2011	SiO_2 shall be not less than 25.0% by mass	3.56	Not Satisfied
	$CaO + SiO_2$, minimum 50% by mass	74.46	Satisfied
NBR 12653	$SiO_2 + Fe_2O_3 + Al_2O_3$, minimum 50-70%	5.53	Not Satisfied
	Na_2O, maximum 1.5%	21.25	Not Satisfied

RCP-WC			
Standard Codes	**Chemical Requirements**	**Results** *(%)*	**Inference**
ASTM C618 – 12a	$SiO_2 + Fe_2O_3 + Al_2O_3$, minimum 50-70%	5.87	Not Satisfied
	Loss on ignition, maximum 10%	-	-
BS EN 450-1:2005	$SiO_2 + Fe_2O_3 + Al_2O_3$, minimum 70%	5.87	Not Satisfied
	Na_2O shall not exceed 5.0%	19.00	Not Satisfied
	MgO shall not be greater than 4.0% by mass	3.19	Satisfied
BS EN 197-1:2011	SiO_2 shall be not less than 25.0% by mass	3.86	Not Satisfied
	$CaO + SiO_2$, minimum 50% by mass	73.26	Satisfied
NBR 12653	$SiO_2 + Fe_2O_3 + Al_2O_3$, minimum 50-70%	5.87	Not Satisfied
	Na_2O, maximum 1.5%	19.00	Not Satisfied

RCP-CaDC			
Standard Codes	**Chemical Requirements**	**Results** *(%)*	**Inference**
ASTM C618 – 12a	$SiO_2 + Fe_2O_3 + Al_2O_3$, minimum 50-70%	4.75	Not Satisfied
	Loss on ignition, maximum 10%	-	-
BS EN 450-1:2005	$SiO_2 + Fe_2O_3 + Al_2O_3$, minimum 70%	4.75	Not Satisfied
	Na_2O shall not exceed 5.0%	26.80	Not Satisfied
	MgO shall not be greater than 4.0% by mass	3.10	Satisfied
BS EN 197-1:2011	SiO_2 shall be not less than 25.0% by mass	3.12	Not Satisfied
	$CaO + SiO_2$, minimum 50% by mass	66.42	Satisfied
NBR 12653	$SiO_2 + Fe_2O_3 + Al_2O_3$, minimum 50-70%	4.75	Not Satisfied
	Na_2O, maximum 1.5%	26.80	Not Satisfied

RCP-CaWC			
Standard Codes	**Chemical Requirements**	**Results** *(%)*	**Inference**
ASTM C618 – 12a	$SiO_2 + Fe_2O_3 + Al_2O_3$, minimum 50-70%	6.38	Not Satisfied
	Loss on ignition, maximum 10%	-	-
BS EN 450-1:2005	$SiO_2 + Fe_2O_3 + Al_2O_3$, minimum 70%	6.38	Not Satisfied
	Na_2O shall not exceed 5.0%	10.80	Not Satisfied
	MgO shall not be greater than 4.0% by mass	2.96	Satisfied
BS EN 197-1:2011	SiO_2 shall be not less than 25.0% by mass	4.18	Not Satisfied
	$CaO + SiO_2$, minimum 50% by mass	81.38	Satisfied
NBR 12653	$SiO_2 + Fe_2O_3 + Al_2O_3$, minimum 50-70%	6.38	Not Satisfied
	Na_2O, maximum 1.5%	10.80	Not Satisfied

RCP-LDC			
Standard Codes	**Chemical Requirements**	**Results** *(%)*	**Inference**
ASTM C618 – 12a	$SiO_2 + Fe_2O_3 + Al_2O_3$, minimum 50-70%	6.05	Not Satisfied
	Loss on ignition, maximum 10%	-	-
BS EN 450-1:2005	$SiO_2 + Fe_2O_3 + Al_2O_3$, minimum 70%	6.05	Not Satisfied
	Na_2O shall not exceed 5.0%	13.20	Not Satisfied
	MgO shall not be greater than 4.0% by mass	2.46	Satisfied
BS EN 197-1:2011	SiO_2 shall be not less than 25.0% by mass	3.91	Not Satisfied
	$CaO + SiO_2$, minimum 50% by mass	80.31	Satisfied
NBR 12653	$SiO_2 + Fe_2O_3 + Al_2O_3$, minimum 50-70%	6.05	Not Satisfied
	Na_2O, maximum 1.5%	13.20	Not Satisfied

APPENDIX B – PARTICLE SIZE DISTRIBUTION TEST

Cement Control								
Size *(µm)*	Volume *(%)*		Size *(µm)*	Volume *(%)*		Size *(µm)*	Volume *(%)*
0.01	0		1.096	0.21		120.226	1.3
0.011	0		1.259	0.22		138.038	0.8
0.013	0		1.445	0.25		158.489	0.46
0.015	0		1.66	0.33		181.97	0.17
0.017	0		1.905	0.45		208.93	0.02
0.02	0		2.188	0.62		239.883	0
0.023	0		2.512	0.83		275.423	0
0.026	0		2.884	1.08		316.228	0
0.03	0		3.311	1.38		363.078	0
0.035	0		3.802	1.7		416.869	0
0.04	0		4.365	2.05		478.63	0
0.046	0		5.012	2.4		549.541	0
0.052	0		5.754	2.75		630.957	0
0.06	0		6.607	3.08		724.436	0
0.069	0		7.586	3.39		831.764	0
0.079	0		8.71	3.65		954.993	0
0.091	0		10	3.88		1096.478	0
0.105	0		11.482	4.06		1258.925	0
0.12	0		13.183	4.22		1445.44	0
0.138	0		15.136	4.35		1659.587	0
0.158	0		17.378	4.45		1905.461	0
0.182	0		19.953	4.54		2187.762	0
0.209	0		22.909	4.61		2511.886	0
0.24	0		26.303	4.65		2884.032	0
0.275	0		30.2	4.66		3311.311	0
0.316	0		34.674	4.63		3801.894	0
0.363	0		39.811	4.56		4365.158	0
0.417	0		45.709	4.42		5011.872	0
0.479	0.05		52.481	4.2		5754.399	0
0.55	0.13		60.256	3.88		6606.934	0
0.631	0.2		69.183	3.42		7585.776	0
0.724	0.22		79.433	2.95		8709.636	0
0.832	0.23		91.201	2.45		10000	0
0.955	0.22		104.713	1.88			

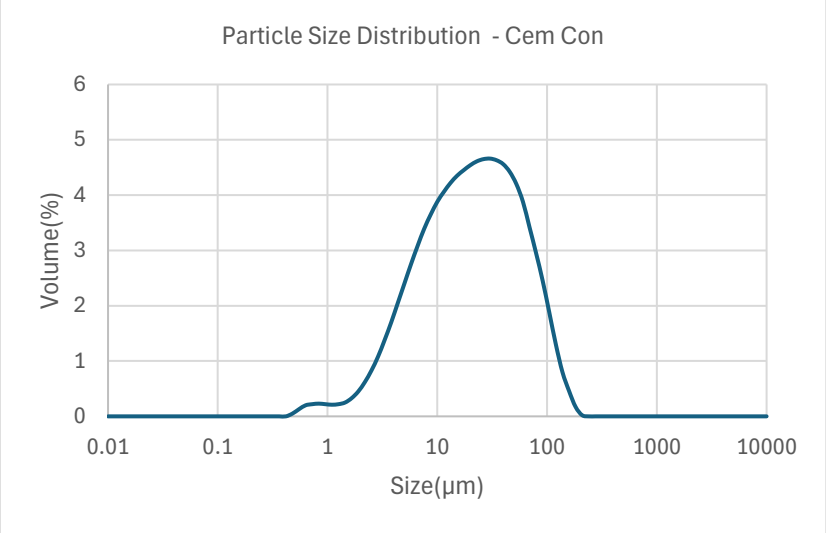

RCP

Size *(μm)*	Volume *(%)*
0.01	0
0.011	0
0.013	0
0.015	0
0.017	0
0.02	0
0.023	0
0.026	0
0.03	0
0.035	0
0.04	0
0.046	0
0.052	0
0.06	0
0.069	0
0.079	0
0.091	0
0.105	0
0.12	0
0.138	0
0.158	0
0.182	0
0.209	0
0.24	0
0.275	0
0.316	0
0.363	0
0.417	0
0.479	0
0.55	0
0.631	0.05
0.724	0.18
0.832	0.46
0.955	0.86

Size *(μm)*	Volume *(%)*
1.096	1.44
1.259	2.19
1.445	3.05
1.66	3.94
1.905	4.73
2.188	5.32
2.512	5.67
2.884	5.77
3.311	5.62
3.802	5.28
4.365	4.79
5.012	4.27
5.754	3.75
6.607	3.3
7.586	2.94
8.71	2.68
10	2.51
11.482	2.43
13.183	2.43
15.136	2.5
17.378	2.62
19.953	2.8
22.909	2.99
26.303	3.15
30.2	3.18
34.674	3.02
39.811	2.6
45.709	1.93
52.481	1.11
60.256	0.39
69.183	0.03
79.433	0
91.201	0
104.713	0

Size *(μm)*	Volume *(%)*
120.226	0
138.038	0
158.489	0
181.97	0
208.93	0
239.883	0
275.423	0
316.228	0
363.078	0
416.869	0
478.63	0
549.541	0
630.957	0
724.436	0
831.764	0
954.993	0
1096.478	0
1258.925	0
1445.44	0
1659.587	0
1905.461	0
2187.762	0
2511.886	0
2884.032	0
3311.311	0
3801.894	0
4365.158	0
5011.872	0
5754.399	0
6606.934	0
7585.776	0
8709.636	0
10000	0

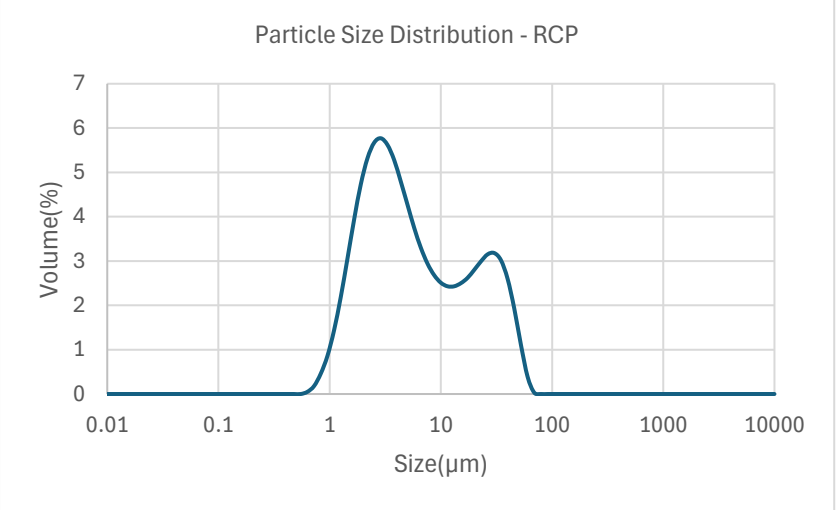

RCP-Ca

Size *(μm)*	Volume *(%)*
0.01	0
0.011	0
0.013	0
0.015	0
0.017	0
0.02	0
0.023	0
0.026	0
0.03	0
0.035	0
0.04	0
0.046	0
0.052	0
0.06	0
0.069	0
0.079	0
0.091	0
0.105	0
0.12	0
0.138	0
0.158	0
0.182	0
0.209	0
0.24	0
0.275	0
0.316	0
0.363	0
0.417	0
0.479	0
0.55	0.11
0.631	0.27
0.724	0.52
0.832	0.79
0.955	1.16

Size *(μm)*	Volume *(%)*
1.096	1.59
1.259	2.11
1.445	2.66
1.66	3.21
1.905	3.69
2.188	4.07
2.512	4.32
2.884	4.43
3.311	4.42
3.802	4.29
4.365	4.08
5.012	3.83
5.754	3.57
6.607	3.34
7.586	3.15
8.71	3.03
10	2.96
11.482	2.96
13.183	3.01
15.136	3.09
17.378	3.2
19.953	3.28
22.909	3.33
26.303	3.28
30.2	3.12
34.674	2.82
39.811	2.39
45.709	1.87
52.481	1.31
60.256	0.78
69.183	0.29
79.433	0.07
91.201	0.03
104.713	0.02

Size *(μm)*	Volume *(%)*
120.226	0.02
138.038	0.02
158.489	0.02
181.97	0.01
208.93	0
239.883	0
275.423	0
316.228	0
363.078	0
416.869	0
478.63	0
549.541	0
630.957	0
724.436	0.05
831.764	0.18
954.993	0.45
1096.478	0.78
1258.925	0.94
1445.44	0.75
1659.587	0.3
1905.461	0.03
2187.762	0
2511.886	0
2884.032	0
3311.311	0
3801.894	0
4365.158	0
5011.872	0
5754.399	0
6606.934	0
7585.776	0
8709.636	0
10000	0

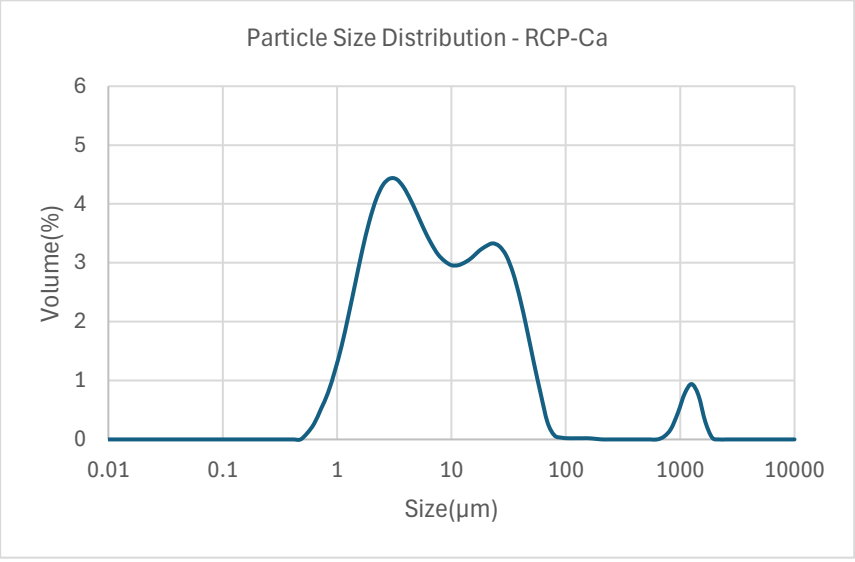

RCP-DC

Size *(μm)*	Volume *(%)*
0.01	0
0.011	0
0.013	0
0.015	0
0.017	0
0.02	0
0.023	0
0.026	0
0.03	0
0.035	0
0.04	0
0.046	0
0.052	0
0.06	0
0.069	0
0.079	0
0.091	0
0.105	0
0.12	0
0.138	0
0.158	0
0.182	0
0.209	0
0.24	0
0.275	0
0.316	0
0.363	0
0.417	0.03
0.479	0.14
0.55	0.31
0.631	0.51
0.724	0.78
0.832	1.1
0.955	1.49

Size (*μm)*	Volume *(%)*
1.096	1.91
1.259	2.36
1.445	2.79
1.66	3.16
1.905	3.45
2.188	3.65
2.512	3.75
2.884	3.76
3.311	3.71
3.802	3.6
4.365	3.46
5.012	3.31
5.754	3.16
6.607	3.05
7.586	2.96
8.71	2.91
10	2.89
11.482	2.92
13.183	2.98
15.136	3.06
17.378	3.17
19.953	3.28
22.909	3.37
26.303	3.4
30.2	3.35
34.674	3.2
39.811	2.94
45.709	2.6
52.481	2.2
60.256	1.78
69.183	1.38
79.433	1
91.201	0.65
104.713	0.34

Size *(μm)*	Volume *(%)*
120.226	0.1
138.038	0.03
158.489	0.01
181.97	0
208.93	0
239.883	0
275.423	0
316.228	0
363.078	0
416.869	0
478.63	0
549.541	0
630.957	0
724.436	0
831.764	0
954.993	0
1096.478	0
1258.925	0
1445.44	0
1659.587	0
1905.461	0
2187.762	0
2511.886	0
2884.032	0
3311.311	0
3801.894	0
4365.158	0
5011.872	0
5754.399	0
6606.934	0
7585.776	0
8709.636	0
10000	0

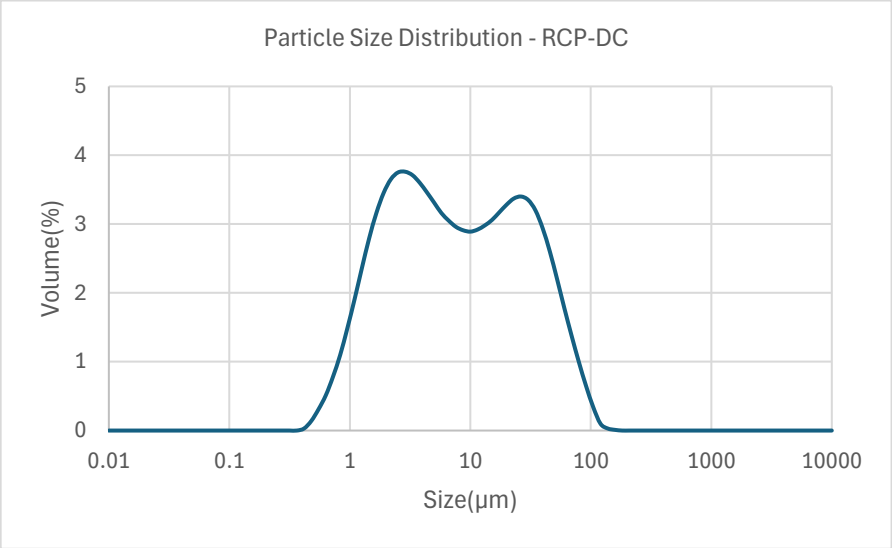

RCP--WC	

Size (μm)	Volume (%)
0.01	0
0.011	0
0.013	0
0.015	0
0.017	0
0.02	0
0.023	0
0.026	0
0.03	0
0.035	0
0.04	0
0.046	0
0.052	0
0.06	0
0.069	0
0.079	0
0.091	0
0.105	0
0.12	0
0.138	0
0.158	0
0.182	0
0.209	0
0.24	0
0.275	0
0.316	0
0.363	0
0.417	0.04
0.479	0.14
0.55	0.31
0.631	0.55
0.724	0.9
0.832	1.36
0.955	1.93

Size (μm)	Volume (%)
1.096	2.57
1.259	3.26
1.445	3.9
1.66	4.42
1.905	4.77
2.188	4.94
2.512	4.94
2.884	4.81
3.311	4.57
3.802	4.28
4.365	3.96
5.012	3.65
5.754	3.37
6.607	3.15
7.586	2.98
8.71	2.87
10	2.82
11.482	2.83
13.183	2.89
15.136	3.01
17.378	3.15
19.953	3.28
22.909	3.33
26.303	3.23
30.2	2.91
34.674	2.35
39.811	1.6
45.709	0.8
52.481	0.14
60.256	0.01
69.183	0
79.433	0
91.201	0
104.713	0

Size (μm)	Volume (%)
120.226	0
138.038	0
158.489	0
181.97	0
208.93	0
239.883	0
275.423	0
316.228	0
363.078	0
416.869	0
478.63	0
549.541	0
630.957	0
724.436	0
831.764	0
954.993	0
1096.478	0
1258.925	0
1445.44	0
1659.587	0
1905.461	0
2187.762	0
2511.886	0
2884.032	0
3311.311	0
3801.894	0
4365.158	0
5011.872	0
5754.399	0
6606.934	0
7585.776	0
8709.636	0
10000	0

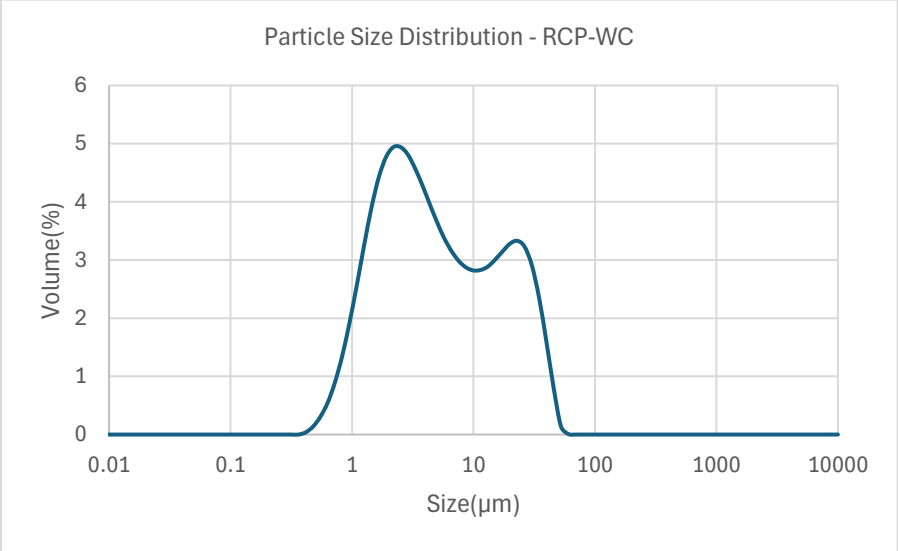

RCP-CaDC	

Size *(μm)*	Volume *(%)*
0.01	0
0.011	0
0.013	0
0.015	0
0.017	0
0.02	0
0.023	0
0.026	0
0.03	0
0.035	0
0.04	0
0.046	0
0.052	0
0.06	0
0.069	0
0.079	0
0.091	0
0.105	0
0.12	0
0.138	0
0.158	0
0.182	0
0.209	0
0.24	0
0.275	0
0.316	0
0.363	0
0.417	0
0.479	0
0.55	0
0.631	0
0.724	0.1
0.832	0.24
0.955	0.46

Size *(μm)*	Volume *(%)*
1.096	0.74
1.259	1.16
1.445	1.69
1.66	2.33
1.905	3.03
2.188	3.72
2.512	4.34
2.884	4.84
3.311	5.18
3.802	5.33
4.365	5.32
5.012	5.17
5.754	4.95
6.607	4.72
7.586	4.53
8.71	4.44
10	4.47
11.482	4.61
13.183	4.79
15.136	4.94
17.378	4.92
19.953	4.62
22.909	3.98
26.303	2.99
30.2	1.76
34.674	0.56
39.811	0.08
45.709	0
52.481	0
60.256	0
69.183	0
79.433	0
91.201	0
104.713	0

Size *(μm)*	Volume *(%)*
120.226	0
138.038	0
158.489	0
181.97	0
208.93	0
239.883	0
275.423	0
316.228	0
363.078	0
416.869	0
478.63	0
549.541	0
630.957	0
724.436	0
831.764	0
954.993	0
1096.478	0
1258.925	0
1445.44	0
1659.587	0
1905.461	0
2187.762	0
2511.886	0
2884.032	0
3311.311	0
3801.894	0
4365.158	0
5011.872	0
5754.399	0
6606.934	0
7585.776	0
8709.636	0
10000	0

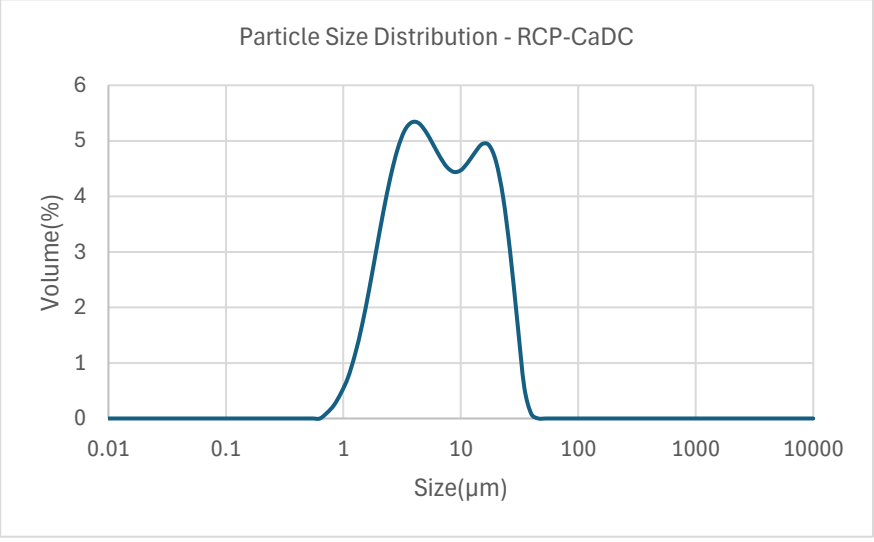

RCP-CaWC

Size (μm)	Volume (%)
0.01	0
0.011	0
0.013	0
0.015	0
0.017	0
0.02	0
0.023	0
0.026	0
0.03	0
0.035	0
0.04	0
0.046	0
0.052	0
0.06	0
0.069	0
0.079	0
0.091	0
0.105	0
0.12	0
0.138	0
0.158	0
0.182	0
0.209	0
0.24	0
0.275	0
0.316	0
0.363	0
0.417	0.14
0.479	0.27
0.55	0.46
0.631	0.67
0.724	0.94
0.832	1.26
0.955	1.64

Size (μm)	Volume (%)
1.096	2.05
1.259	2.5
1.445	2.95
1.66	3.37
1.905	3.74
2.188	4.04
2.512	4.24
2.884	4.35
3.311	4.37
3.802	4.3
4.365	4.15
5.012	3.94
5.754	3.69
6.607	3.44
7.586	3.19
8.71	2.99
10	2.84
11.482	2.77
13.183	2.78
15.136	2.89
17.378	3.07
19.953	3.29
22.909	3.5
26.303	3.62
30.2	3.58
34.674	3.31
39.811	2.75
45.709	1.93
52.481	0.93
60.256	0.07
69.183	0
79.433	0
91.201	0
104.713	0

Size (μm)	Volume (%)
120.226	0
138.038	0
158.489	0
181.97	0
208.93	0
239.883	0
275.423	0
316.228	0
363.078	0
416.869	0
478.63	0
549.541	0
630.957	0
724.436	0
831.764	0
954.993	0
1096.478	0
1258.925	0
1445.44	0
1659.587	0
1905.461	0
2187.762	0
2511.886	0
2884.032	0
3311.311	0
3801.894	0
4365.158	0
5011.872	0
5754.399	0
6606.934	0
7585.776	0
8709.636	0
10000	0

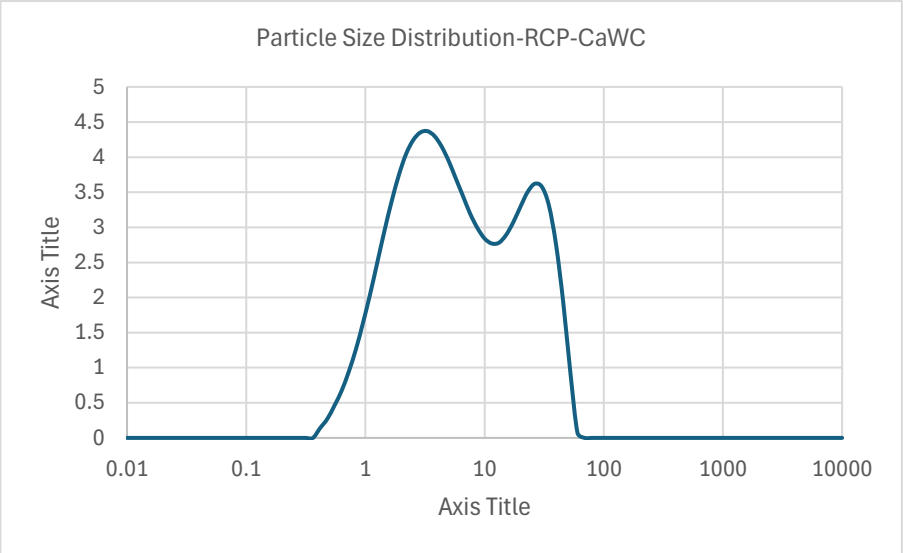

RCP-LDC

Size *(μm)*	Volume *(%)*	Size *(μm)*	Volume *(%)*	Size *(μm)*	Volume *(%)*
0.01	0	1.096	1	120.226	0.22
0.011	0	1.259	1.14	138.038	0.17
0.013	0	1.445	1.3	158.489	0.09
0.015	0	1.66	1.5	181.97	0
0.017	0	1.905	1.73	208.93	0
0.02	0	2.188	1.99	239.883	0
0.023	0	2.512	2.26	275.423	0
0.026	0	2.884	2.54	316.228	0
0.03	0	3.311	2.79	363.078	0
0.035	0	3.802	3.02	416.869	0
0.04	0	4.365	3.21	478.63	0
0.046	0	5.012	3.37	549.541	0
0.052	0	5.754	3.48	630.957	0
0.06	0	6.607	3.56	724.436	0
0.069	0	7.586	3.64	831.764	0
0.079	0	8.71	3.71	954.993	0
0.091	0	10	3.82	1096.478	0
0.105	0	11.482	3.96	1258.925	0
0.12	0	13.183	4.14	1445.44	0
0.138	0	15.136	4.35	1659.587	0
0.158	0	17.378	4.56	1905.461	0
0.182	0	19.953	4.73	2187.762	0
0.209	0	22.909	4.83	2511.886	0
0.24	0	26.303	4.79	2884.032	0
0.275	0	30.2	4.6	3311.311	0
0.316	0	34.674	4.25	3801.894	0
0.363	0	39.811	3.75	4365.158	0
0.417	0	45.709	3.14	5011.872	0
0.479	0	52.481	2.47	5754.399	0
0.55	0.03	60.256	1.79	6606.934	0
0.631	0.09	69.183	1.16	7585.776	0
0.724	0.27	79.433	0.61	8709.636	0
0.832	0.62	91.201	0.29	10000	0
0.955	0.82	104.713	0.22		

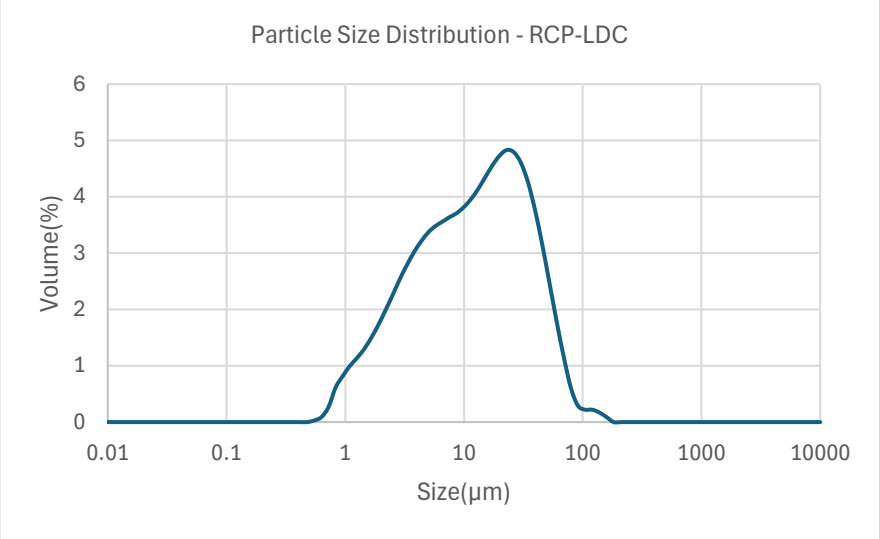

APPENDIX C – DENSITY BOTTLE TEST

Density Bottle – Kerosine Type 1

1) Mass of Water					
Container No.	1	2	3	4	5
Weight of Empty Container	26.3292	38.3917	38.8893	35.2052	37.7839
Weight of Container Full of Water (M1)	74.6002	88.5744	88.9950	84.9126	88.1414
Weight of Container Full of Water (M2)	74.6071	88.5189	88.9254	84.8825	88.0766
Weight of Container Full of Water (M3)	74.5440	88.4810	88.8935	84.8994	88.0365
Mean of M1, M2, M3	74.5838	88.5248	88.9380	84.8982	88.0848
Weight of Water (W1)	48.2546	50.1331	50.0487	49.6930	50.3009

2) Mass of Kerosine (Displacement Liquid)					
Container No.	1	2	3	4	5
Weight of Empty Container	26.3291	38.3911	38.8891	35.2049	37.7838
Weight of Container Full of Kerosine (M1)	64.8319	78.4378	78.8658	74.7651	78.0172
Weight of Container Full of Kerosine (M2)	64.7978	78.4048	78.8549	74.7449	77.9994
Weight of Container Full of Kerosine (M3)	64.8187	78.4272	78.8566	74.7625	77.9985
Mean of M1, M2, M3 (W3)	64.8161	78.4233	78.8591	74.7575	78.0050
Weight of Kerosine (W2)	38.4870	40.0322	39.9700	39.5526	40.2212

Density of Redistilled Kerosine (Pl)					
Pw = Density of pure water at the selected operating temperature (water bath) Operating Temperature (Water Bath) = 28					
Ie. Pw =	0.9963	0.9963	0.9963	0.9963	0.9963
Pl = (W2/W1) x Pw	0.7946	0.7956	0.7957	0.7930	0.7967

3) Mass of Cement (W5)					
Container No.	1	2	3	4	5
Weight of Empty Container	26.3286	38.3913	38.8890	35.2045	37.7836
Weight of Container with Cement	36.0980	46.9932	48.6221	45.1500	47.6359
Weight of Cement (W4)	9.7694	8.6019	9.7331	9.9455	9.8523
Weight of Container Full of Cement + Kerosine (M1)	72.0814	85.6866	86.1142	82.1660	85.2972
Weight of Container Full of Cement + Kerosine (M2)	72.1230	85.6795	86.1308	82.1439	85.3471
Weight of Container Full of Cement + Kerosine (M3)	72.0801	85.6337	86.0803	82.1413	85.3195
Mean of M1, M2, M3 (W5)	72.0948	85.6666	86.1084	82.1504	85.3213

Density of Cement (P)					
P = (W4 x Pl) / (W3 + W4- W5)					
P (*g/cm3*) =	3.1168	5.0372	3.1180	3.0897	3.0949
Density of Cement kg/m^3	3116.8264	5037.1907	3117.9716	3089.6843	3094.8987

4a) Density of Recycled Concrete Powder (RCP)					
Container No.	1	2	3	4	5
Weight of Empty Container	26.3286	38.3913	38.889	35.2045	37.7836
Weight of Container with Powder	36.1947	48.227	48.7814	45.1509	47.6976
Weight of Powder (W4)	9.8661	9.8357	9.8924	9.9464	9.914
Weight of Container Full of Powder + Kerosine (M1)	71.6754	85.2272	85.7292	81.7018	84.8871
Weight of Container Full of Powder + Kerosine (M2)	71.6828	85.2542	85.7451	81.7368	84.8916
Weight of Container Full of Powder + Kerosine (M3)	71.7051	85.2773	85.7575	81.7843	84.9097
Mean of M1, M2, M3 (W5)	71.6878	85.2529	85.7439	81.7410	84.8961

RCP = (W4 x Pl) / (W3 + W4- W5)	2.6181	2.6030	2.6170	2.6620	2.6127
Density of Recycled Concrete Powder (RCP) g/cm^3	2618.1358	2603.04467	2617.0871	2662.0382	2612.7304

4b) Density of Recycled Concrete Powder- Calcined (RCP-Ca)					
Container No.	1	2	3	4	5
Weight of Empty Container	26.3286	38.3913	38.889	35.2045	37.7836
Weight of Container with Powder	36.3205	48.3866	48.8605	45.2018	47.7705
Weight of Powder (W4)	9.9919	9.9953	9.9715	9.9973	9.9869
Weight of Container Full of Powder + Kerosine (M1)	71.9185	85.5145	85.9134	81.8882	85.0684
Weight of Container Full of Powder + Kerosine (M2)	71.8993	85.4749	85.8884	81.7747	85.0466
Weight of Container Full of Powder + Kerosine (M3)	71.9193	85.5164	85.922	81.7735	85.0823
Mean of M1, M2, M3 (W5)	71.9123	85.5019	85.9079	81.8121	85.0657

RCP-Ca = (W4 x Pl)/(W3 + W4- W5)	2.7419	2.7263	2.7146	2.6940	2.7189
Density of Recycled Concrete Powder- Calcined (RCP-Ca) g/cm^3	2741.9886	2726.3961	2714.6446	2694.0888	2718.9493

4c) Density of Recycled Concrete Powder- Wet Carbonation (RCP-WC)					
Container No.	1	2	3	4	5
Weight of Empty Container	26.3286	38.3913	38.889	35.2045	37.7836
Weight of Container with Powder	36.3188	48.3901	48.8778	45.1989	47.7742
Weight of Powder (W4)	9.9902	9.9988	9.9888	9.9944	9.9906
Weight of Container Full of Powder + Kerosine (M1)	71.8041	85.4122	85.8386	81.793	84.976
Weight of Container Full of Powder + Kerosine (M2)	71.8281	85.4323	85.8611	81.7871	84.9939
Weight of Container Full of Powder + Kerosine (M3)	71.761	85.3549	85.7868	81.7455	84.9019
Mean of M1, M2, M3 (W5)	71.7977	85.3998	85.8288	81.7752	84.9572

RCP-WC = (W4 x Pl)/(W3 + W4-W5)	2.6386	2.6320	2.6325	2.6625	2.6195
Density of Recycled Concrete Powder- Wet Carbonation (RCP-WC) g/cm^3	2638.6140	2632.0252	2632.5243	2662.5140	2619.5148

Density Bottle – Kerosine Type 2

1) Mass of Water					
Container No.	1	2	3	4	5
Weight of Empty Container	26.3292	38.3917	38.8893	35.2052	37.7839
Weight of Container Full of Water (M1)	74.6002	88.5744	88.9950	84.9126	88.1414
Weight of Container Full of Water (M2)	74.6071	88.5189	88.9254	84.8825	88.0766
Weight of Container Full of Water (M3)	74.5440	88.4810	88.8935	84.8994	88.0365
Mean of M1, M2, M3	74.5838	88.5248	88.9380	84.8982	88.0848
Weight of Water (W1)	48.2546	50.1331	50.0487	49.6930	50.3009

2) Mass of Kerosine (Displacement Liquid)					
Container No.	1	2	3	4	5
Weight of Empty Container	26.3279	38.3911	38.8884	35.2051	37.7831
Weight of Container Full of Kerosine (M1)	64.5334	78.1066	78.5776	74.4312	77.6609
Weight of Container Full of Kerosine (M2)	64.5599	78.1394	78.5700	74.4167	77.6911
Weight of Container Full of Kerosine (M3)	64.5034	78.0933	78.5185	74.4168	77.6660
Mean of M1, M2, M3 (W3)	64.5322	78.1131	78.5554	74.4216	77.6727
Weight of Kerosine (W2)	38.2043	39.7220	39.6670	39.2165	39.8896

Density of Redistilled Kerosine (Pl)					
Pw = Density of pure water at the selected operating temperature (water bath) Operating Temperature (Water Bath) = 28					
Ie. Pw =	0.9963	0.9963	0.9963	0.9963	0.9963
Pl = (W2/W1) x Pw	0.7888	0.7894	0.7896	0.7863	0.7901

4d) Density of Calcined & Wet Carbonation (RCP-CaWC)					
Container No.	1	2	3	4	5
Weight of Empty Container	26.3286	38.3913	38.8890	35.2045	37.7836
Weight of Container with Powder	36.3170	48.3770	48.8724	45.1920	47.7636
Weight of Powder (W4)	9.9884	9.9857	9.9834	9.9875	9.9800
Weight of Container Full of Powder + Kerosine (M1)	71.6387	85.2126	85.6725	81.5399	84.7971
Weight of Container Full of Powder + Kerosine (M2)	71.5667	85.1553	85.6156	81.5323	84.7448
Weight of Container Full of Powder + Kerosine (M3)	71.6732	85.2611	85.7092	81.5354	84.8494
Mean of M1, M2, M3 (W5)	71.6262	85.2097	85.6658	81.5359	84.7971

RCP-CaWC = (W4 x Pl) / (W3 + W4- W5)	2.7221	2.7284	2.7439	2.7331	2.7613
Density of Calcined & Wet Carbonation (RCP-CaWC) *g/cm^3*	2722.0538	2728.3991	2743.9074	2733.0942	2761.2876

4e) Density of Dry Carbonation (RCP-DC)					
Container No.	1	2	3	4	5
Weight of Empty Container	26.3286	38.3913	38.8890	35.2045	37.7836
Weight of Container with Powder	36.3016	48.3619	48.8671	45.1786	47.7609
Weight of Powder (W4)	9.9730	9.9706	9.9781	9.9741	9.9773
Weght of Container Full of Powder + Kerosine (M1)	71.5733	85.1436	85.5891	81.5064	84.7332
Weght of Container Full of Powder + Kerosine (M2)	71.5144	85.0874	85.5335	81.4676	84.6696
Weght of Container Full of Powder + Kerosine (M3)	71.5225	85.1161	85.5372	81.4625	84.6803
Mean of M1, M2, M3 (W5)	71.5367	85.1157	85.5533	81.4788	84.6944

RCP-DC = (W4 x Pl) / (W3 + W4- W5)	2.6500	2.6519	2.6438	2.6886	2.6671
Density of Dry Carbonation (RCP-DC) *g/cm^3*	2650.0441	2651.8830	2643.8028	2688.5974	2667.1091

4f) Density of Calcined & Dry Carbonation (RCP-CaDC)					
Container No.	1	2	3	4	5
Weight of Empty Container	26.3286	38.3913	38.8890	35.2045	37.7836
Weight of Container with Powder	36.3254	48.3855	48.8827	45.1882	47.7651
Weight of Powder (W4)	9.9968	9.9942	9.9937	9.9837	9.9815
Weight of Container Full of Powder + Kerosine (M1)	71.4724	85.0287	85.5402	81.3275	84.5580
Weight of Container Full of Powder + Kerosine (M2)	71.3940	84.9650	85.4702	81.2784	84.5070
Weight of Container Full of Powder + Kerosine (M3)	71.4461	85.0273	85.5237	81.2801	84.5487
Mean of M1, M2, M3 (W5)	71.4375	85.0070	85.5114	81.2953	84.5379

RCP-CaDC = (W4 x Pl) / (W3 + W4-W5)	2.5507	2.5447	2.5978	2.5241	2.5307
Density of Calcined & Dry Carbonation (RCP-CaDC) *g/cm^3*	2550.653	2544.727	2597.813	2524.0858	2530.6647

4g) Density of Limewater & Dry Carbonation (RCP-LDC)					
Container No.	1	2	3	4	5
Weight of Empty Container	26.3286	38.3913	38.8890	35.2045	37.7836
Weight of Container with Powder	36.3116	48.3711	48.8626	45.1806	47.7636
Weight of Powder (W4)	9.9830	9.9798	9.9736	9.9761	9.9800
Weght of Container Full of Powder + Kerosine (M1)	71.4259	84.9956	85.4303	81.3722	84.5702
Weght of Container Full of Powder + Kerosine (M2)	71.4647	85.0481	85.4581	81.3658	85.5818
Weght of Container Full of Powder + Kerosine (M3)	71.5144	85.0931	85.5230	81.3645	84.6371
Mean of M1, M2, M3 (W5)	71.4683	85.0456	85.4705	81.3675	84.9297

RCP-LDC = (W4 x Pl) / (W3 + W4-W5)	2.5844	2.5853	2.5750	2.5886	2.8958
Density of Limewater & Dry Carbonation (RCP-LDC) *g/cm^3*	2584.4445	2585.2562	2574.9575	2588.5583	2895.7537

APPENDIX D – X-RAY DIFFRACTION TEST

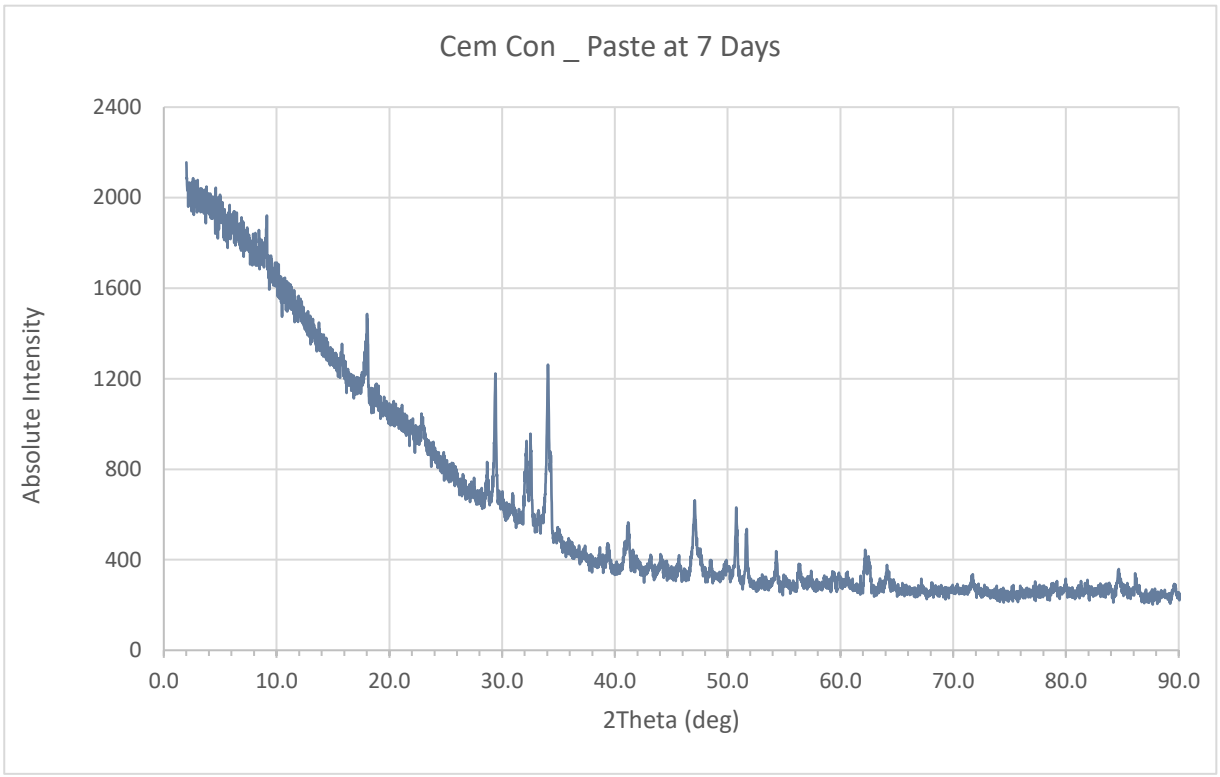
Cem Con _ Paste at 7 Days
Absolute Intensity
2400
2000
1600
1200
800
400
0
0.0
10.0
20.0
30.0
40.0
50.0
60.0
70.0
80.0
90.0
2Theta (deg)

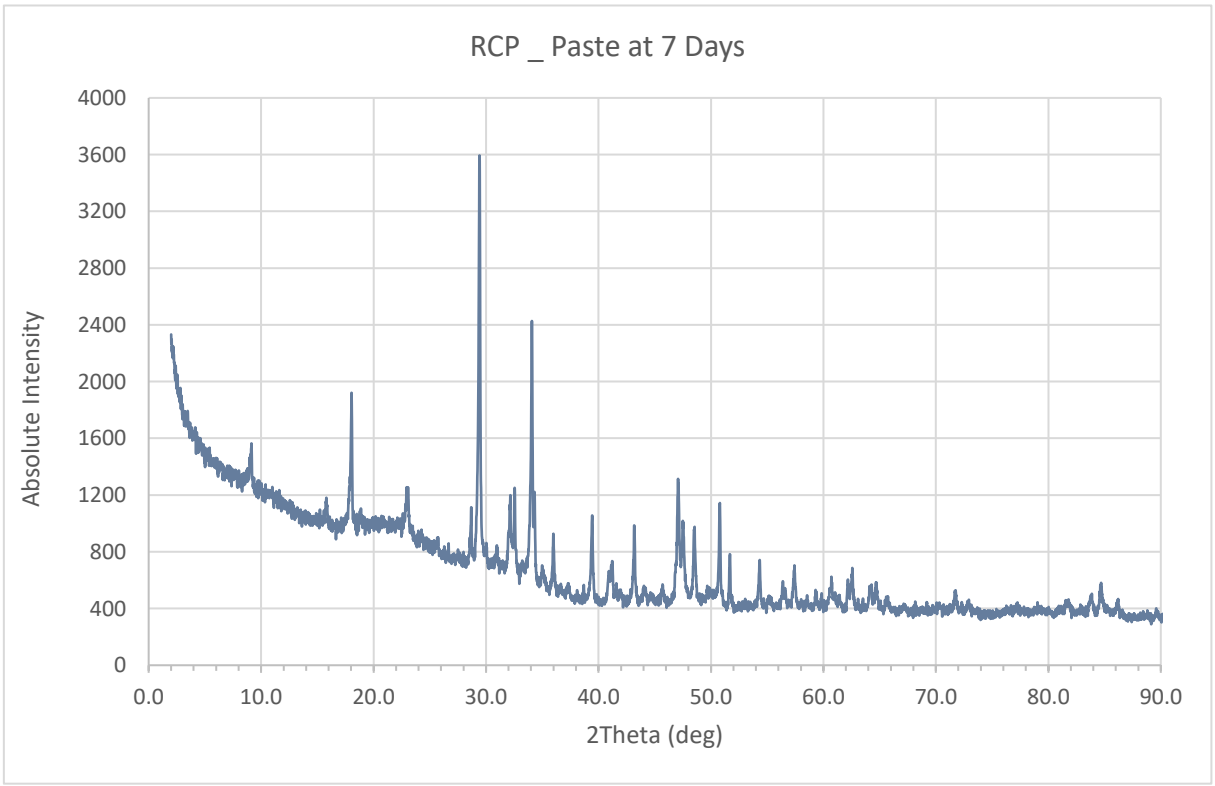
RCP _ Paste at 7 Days
Absolute Intensity
4000
3600
3200
2800
2400
2000
1600
1200
800
400
0
0.0
10.0
20.0
30.0
40.0
50.0
60.0
70.0
80.0
90.0
2Theta (deg)

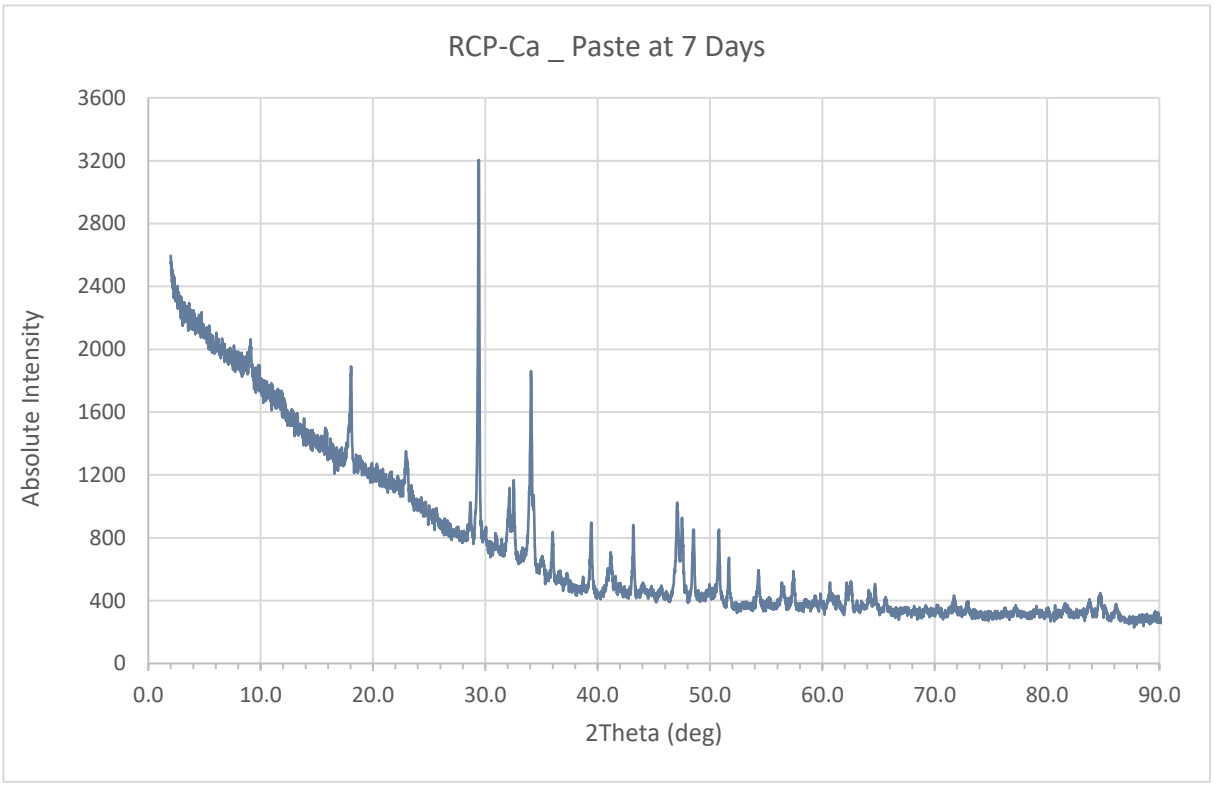
RCP-Ca _ Paste at 7 Days
Absolute Intensity
3600
3200
2800
2400
2000
1600
1200
800
400
0
0.0
10.0
20.0
30.0
40.0
50.0
60.0
70.0
80.0
90.0
2Theta (deg)

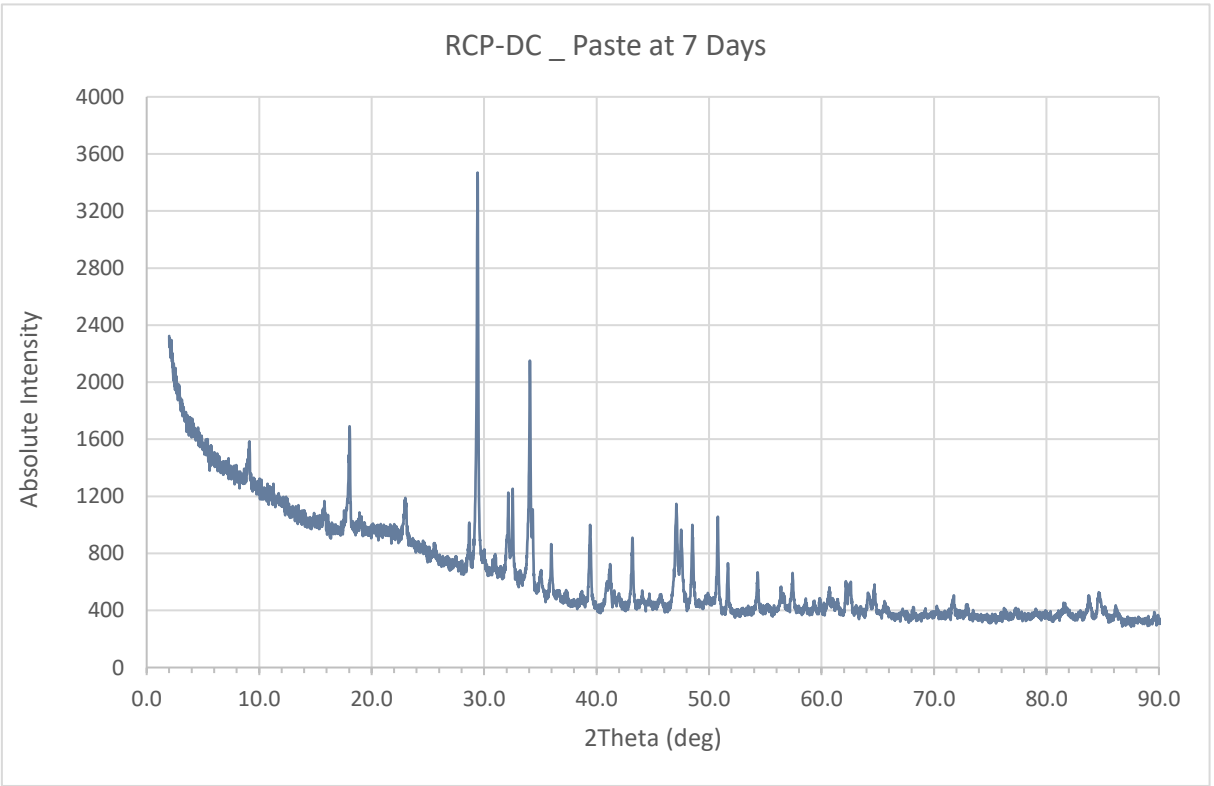
RCP-DC _ Paste at 7 Days
Absolute Intensity
4000
3600
3200
2800
2400
2000
1600
1200
800
400
0
0.0
10.0
20.0
30.0
40.0
50.0
60.0
70.0
80.0
90.0
2Theta (deg)

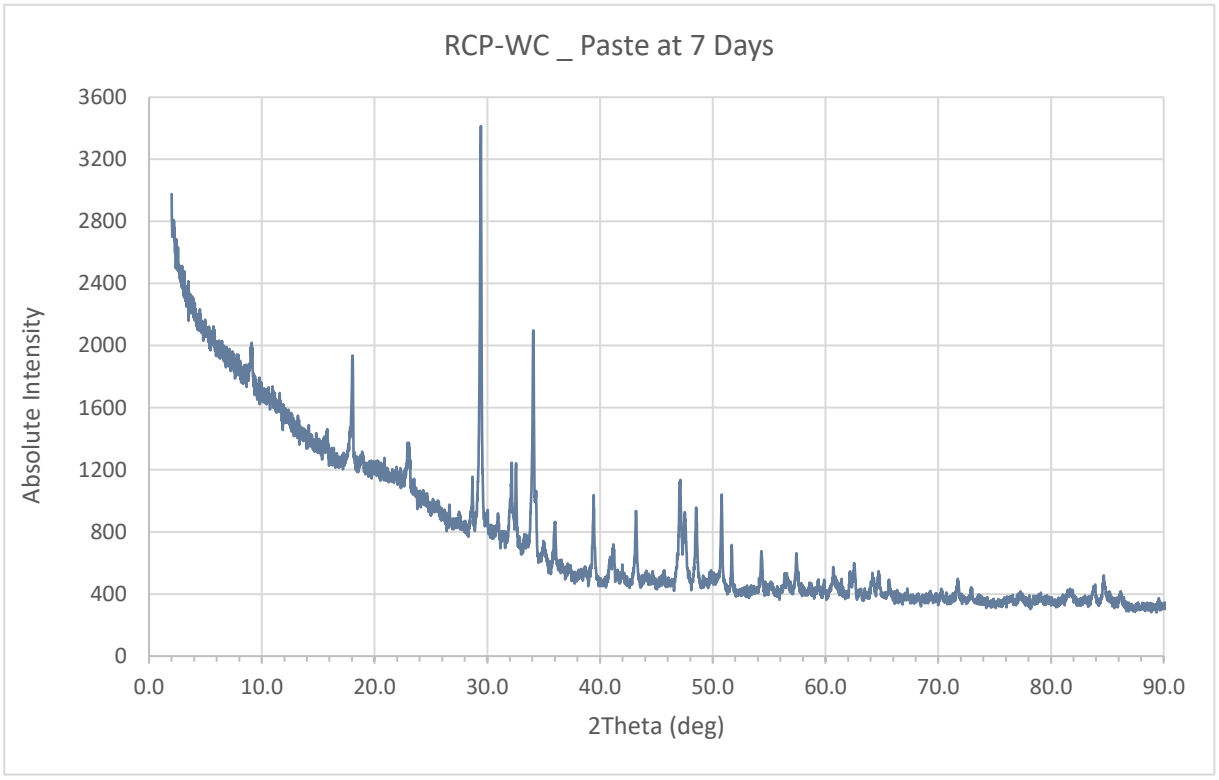
RCP-WC _ Paste at 7 Days
Absolute Intensity
3600
3200
2800
2400
2000
1600
1200
800
400
0
0.0
10.0
20.0
30.0
40.0
50.0
60.0
70.0
80.0
90.0
2Theta (deg)

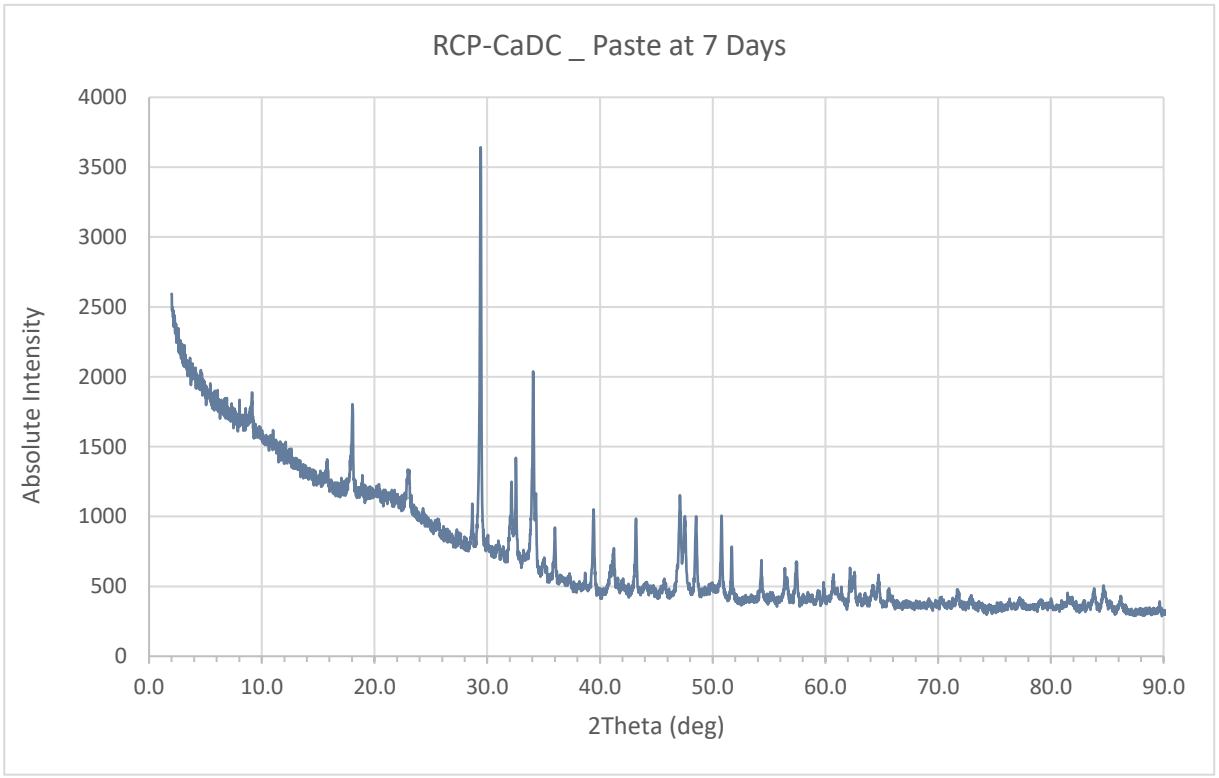
RCP-CaDC _ Paste at 7 Days
Absolute Intensity
4000
3500
3000
2500
2000
1500
1000
500
0
0.0
10.0
20.0
30.0
40.0
50.0
60.0
70.0
80.0
90.0
2Theta (deg)

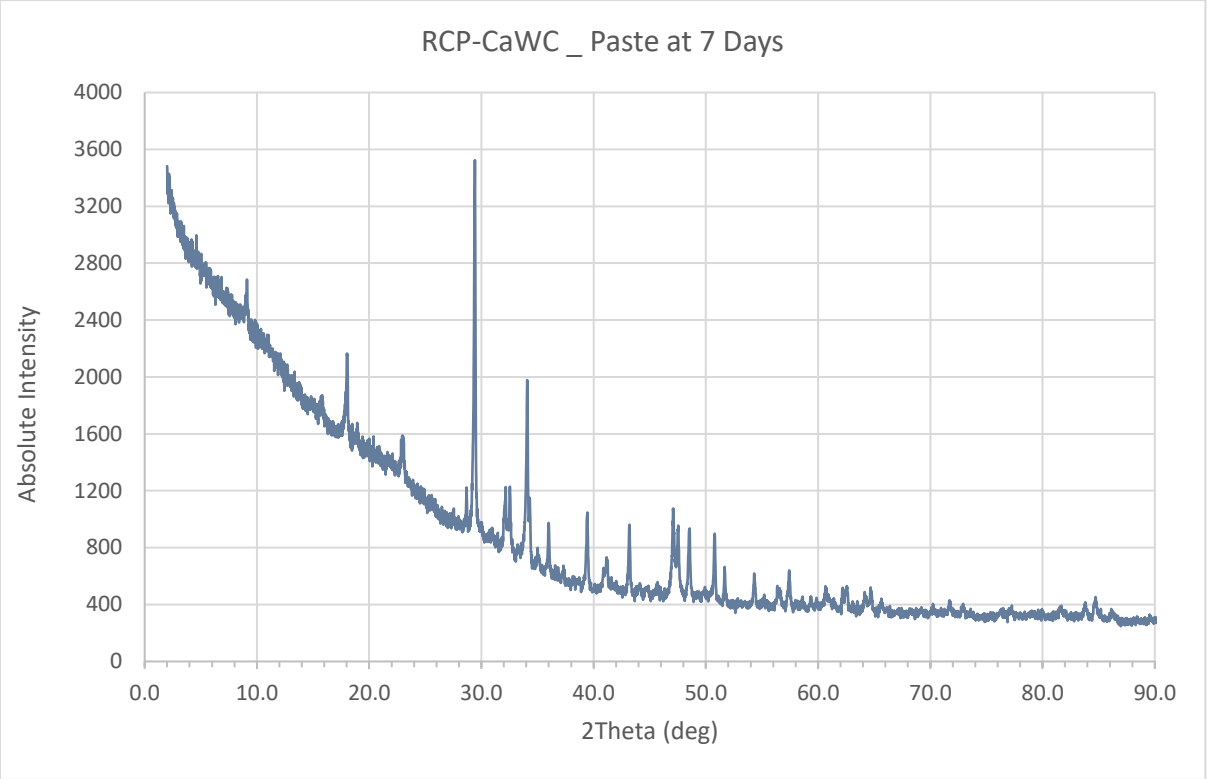
RCP-CaWC _ Paste at 7 Days
Absolute Intensity
4000
3600
3200
2800
2400
2000
1600
1200
800
400
0
0.0
10.0
20.0
30.0
40.0
50.0
60.0
70.0
80.0
90.0
2Theta (deg)

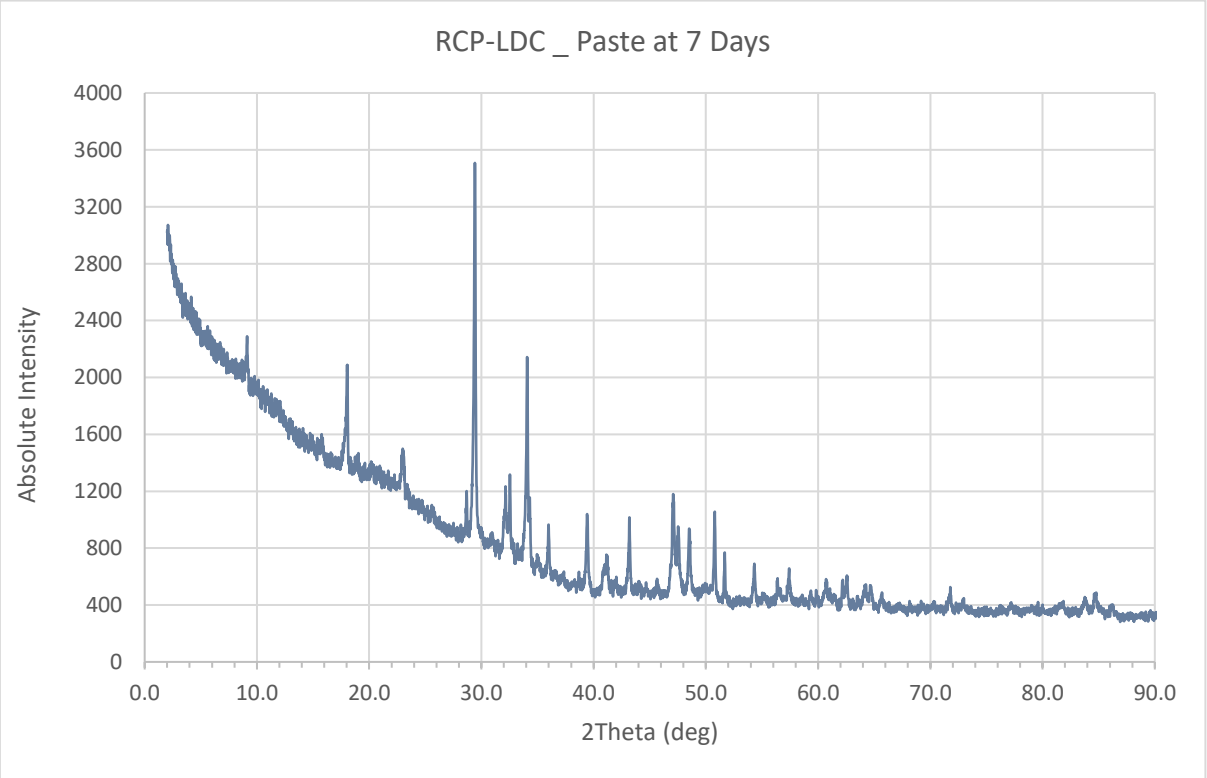
RCP-LDC _ Paste at 7 Days
Absolute Intensity
4000
3600
3200
2800
2400
2000
1600
1200
800
400
0
0.0
10.0
20.0
30.0
40.0
50.0
60.0
70.0
80.0
90.0
2Theta (deg)

APPENDIX E – FOURIER-TRANSFORM INFRARED SPECTROSCOPY TEST

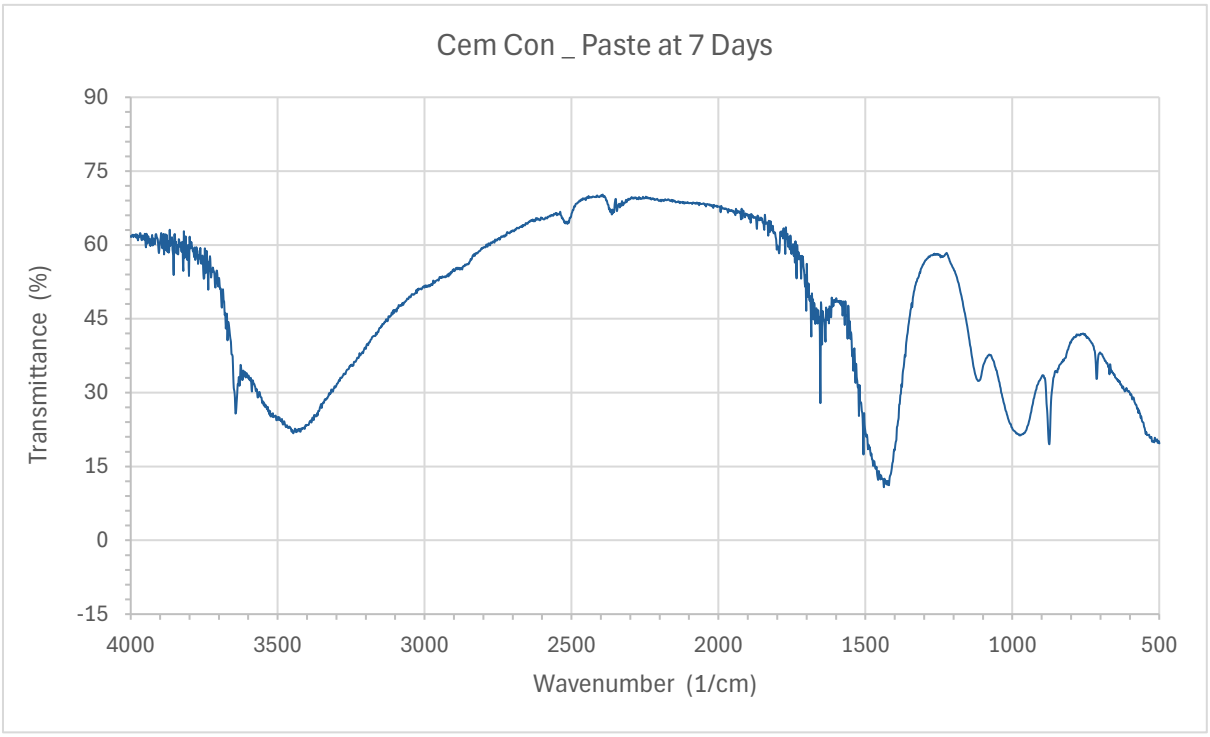
Cem Con _ Paste at 7 Days
Transmittance (%)
90
75
60
45
30
15
0
-15
4000
3500
3000
2500
2000
1500
1000
500
Wavenumber (1/cm)

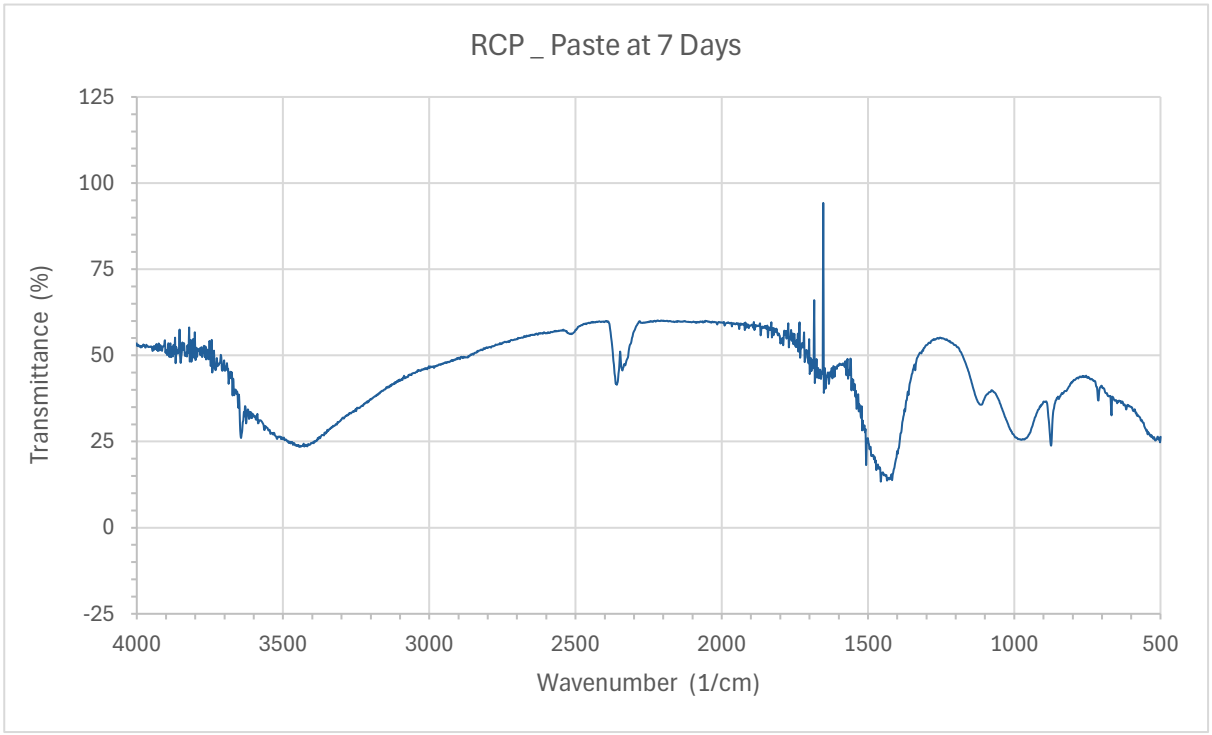
RCP _ Paste at 7 Days
Transmittance (%)
125
100
75
50
25
0
-25
4000
3500
3000
2500
2000
1500
1000
500
Wavenumber (1/cm)

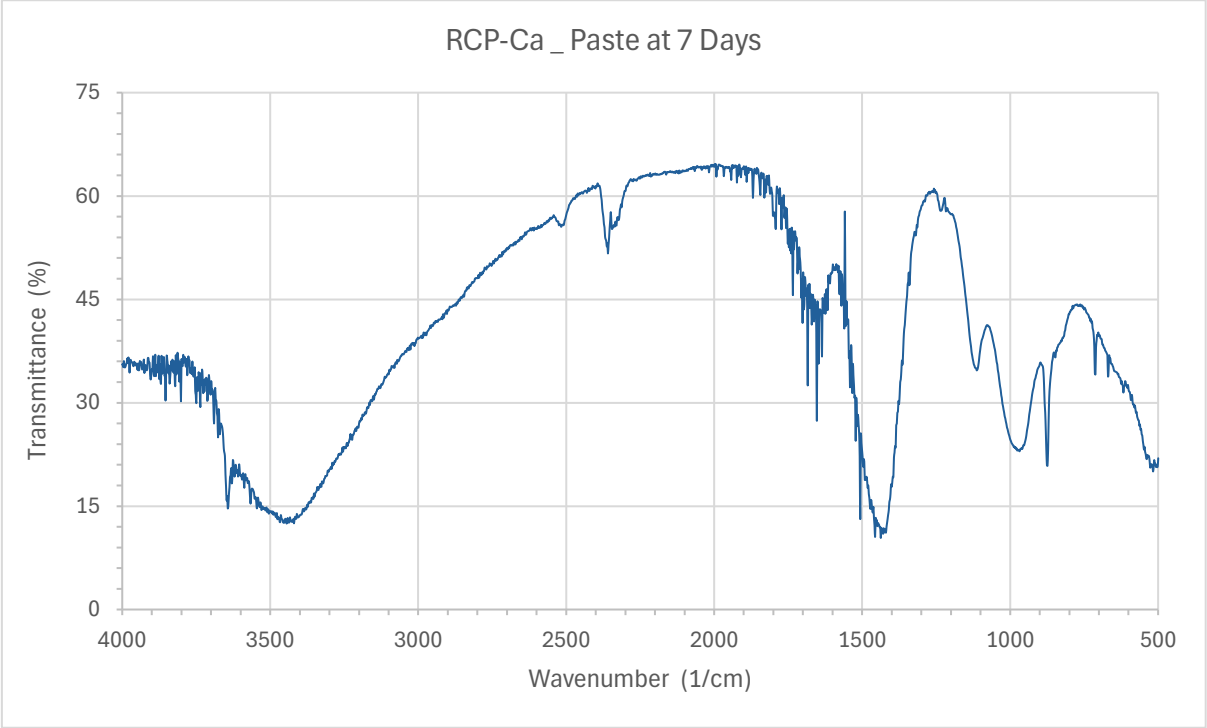
RCP-Ca _ Paste at 7 Days
Transmittance (%)
75
60
45
30
15
0
4000
3500
3000
2500
2000
1500
1000
500
Wavenumber (1/cm)

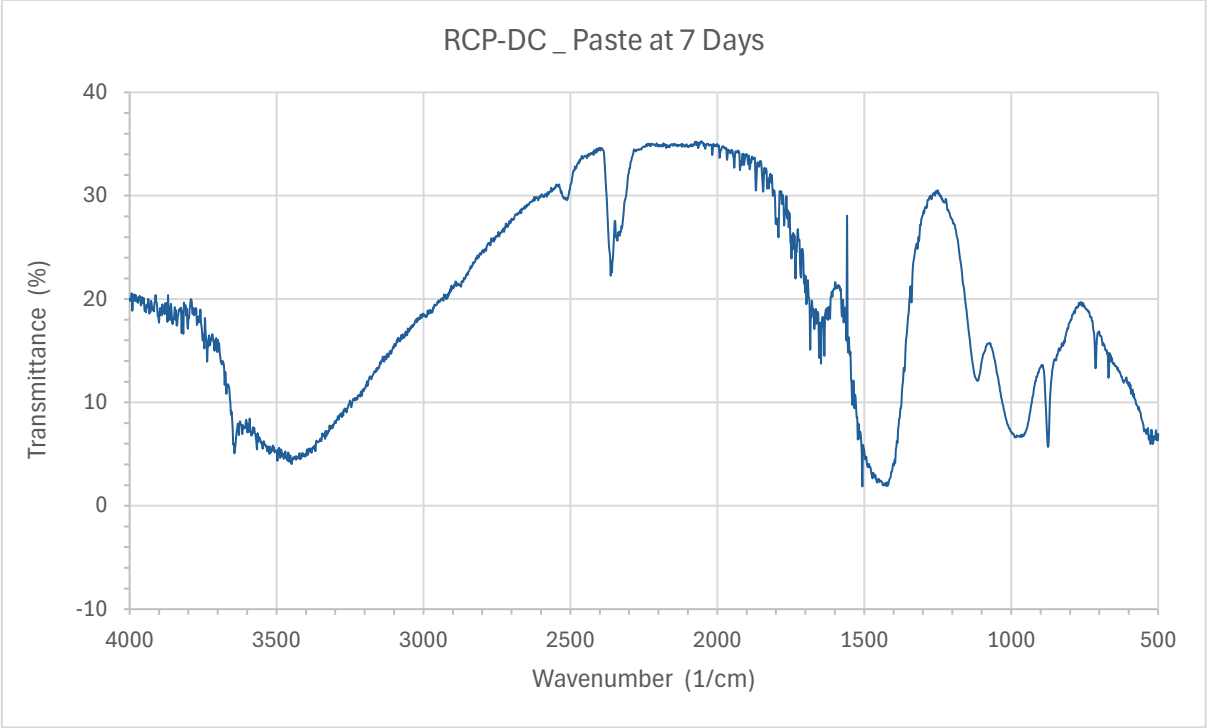
RCP-DC _ Paste at 7 Days
Transmittance (%)
40
30
20
10
0
-10
4000
3500
3000
2500
2000
1500
1000
500
Wavenumber (1/cm)

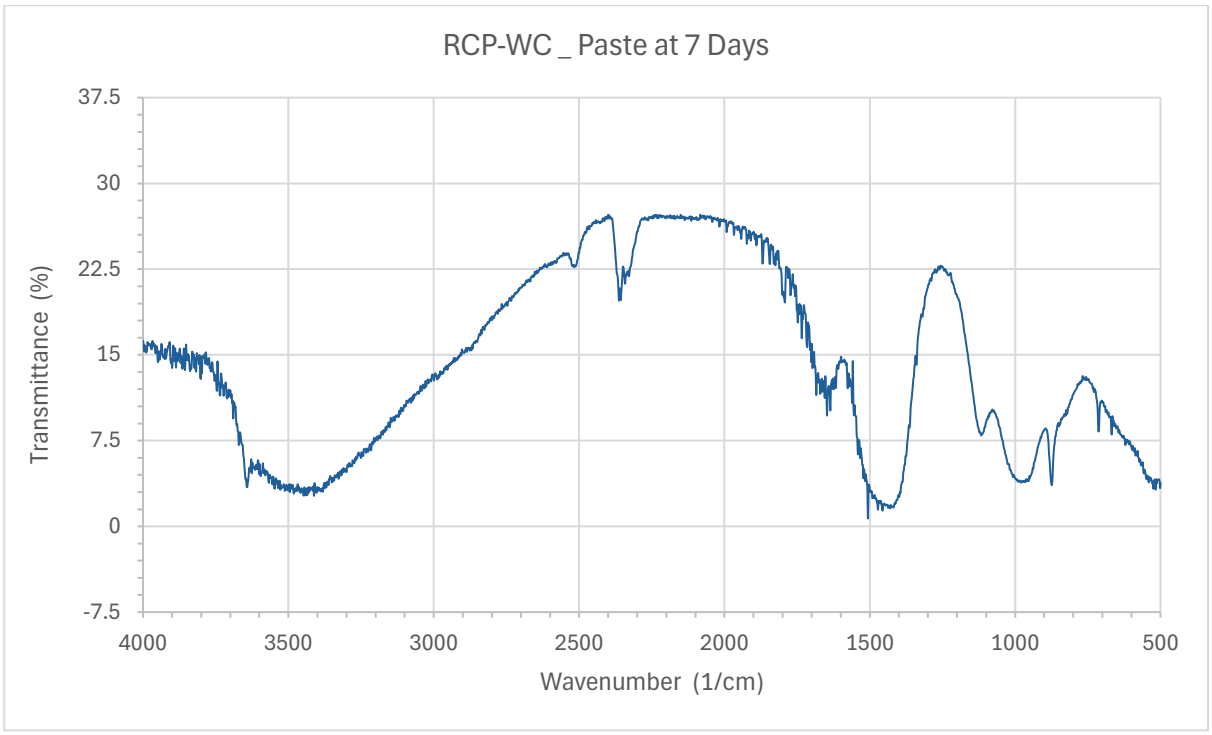
RCP-WC _ Paste at 7 Days
Transmittance (%)
37.5
30
22.5
15
7.5
0
-7.5
4000
3500
3000
2500
2000
1500
1000
500
Wavenumber (1/cm)

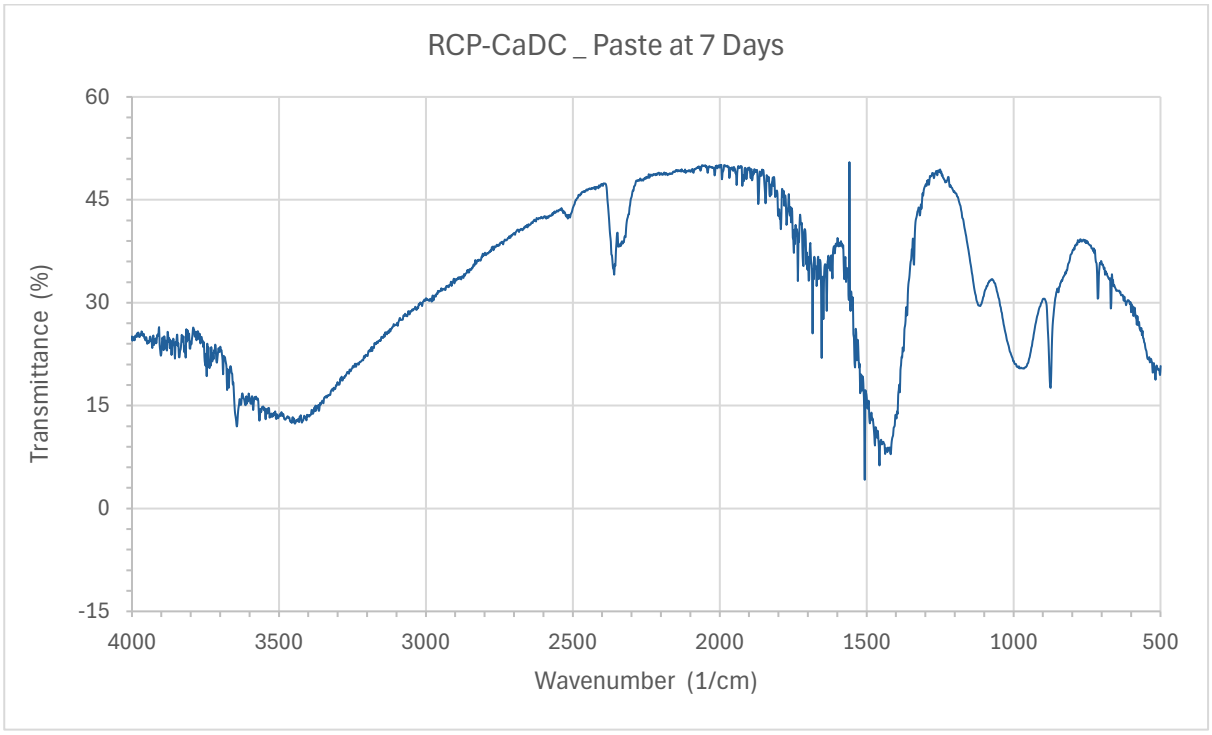
RCP-CaDC _ Paste at 7 Days
Transmittance (%)
60
45
30
15
0
-15
4000
3500
3000
2500
2000
1500
1000
500
Wavenumber (1/cm)

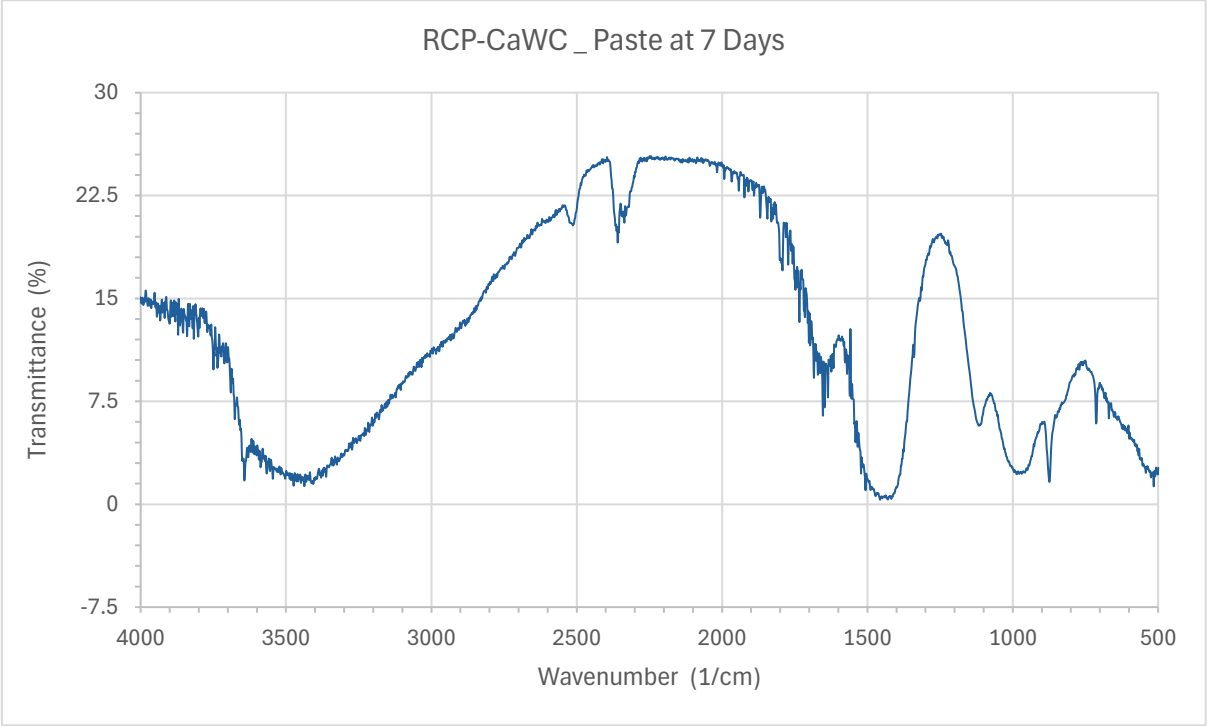
RCP-CaWC _ Paste at 7 Days
Transmittance (%)
30
22.5
15
7.5
0
-7.5
4000
3500
3000
2500
2000
1500
1000
500
Wavenumber (1/cm)

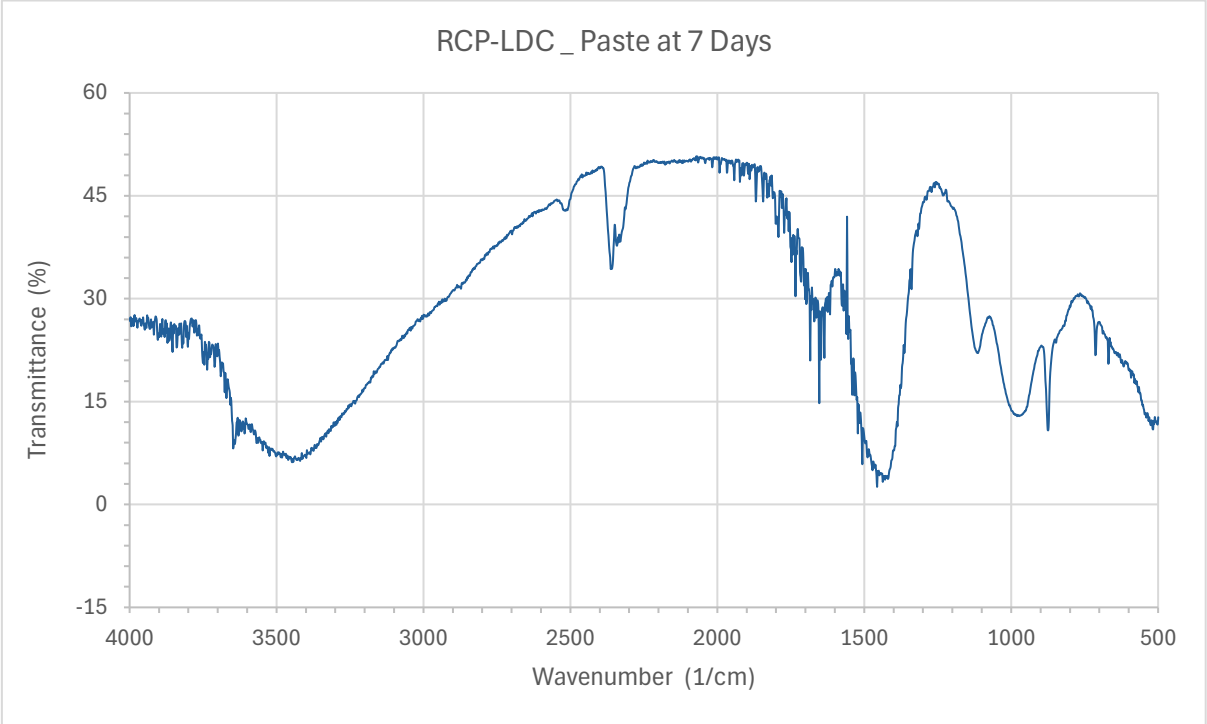
RCP-LDC _ Paste at 7 Days
Transmittance (%)
60
45
30
15
0
-15
4000
3500
3000
2500
2000
1500
1000
500
Wavenumber (1/cm)

FTIR Graph Analysis

Wavenumber *(cm^{-1})*	Functional Group / Compound	Control	RCP	RCP-Ca	RCP-DC	RCP-WC	RCP-CaDC	RCP-CaWC	RCP-LDC	Key Comparative Analysis
3643.53	Portlandite *$Ca(OH)_2$* O-H Stretch	Sharp, Strong	Sharp, Strong	Sharp, Medium	Sharp, Strong	Sharp, Medium	Sharp, Medium	Sharp, Medium	Sharp, Strong 3647.39	This sharp band is the unambiguous signature of crystalline $Ca(OH)_2$, confirming the progress of cement hydration. Calcination is seen as the sole SCM activator. The RCP-LDC paste shows a strong $Ca(OH)_2$ signal, identical to the non-calcined samples (Control, RCP, RCP-DC). The lime treatment provided $Ca(OH)_2$ but did not initiate the pozzolanic consumption seen in the Calcined samples.
1791.87	Carbonate *CO_3^{2-}* Overtone/ Combination	Not Present	Not Present	Not Present	Not Present	Not Present	Not Present	Sharp, Weak 1791.87	Not Present	Confirms that aqueous carbonation treatment (RCP-CaWC) was seen to create the most distinct and robust $CaCO_3$ phases.
1506- 1417	Carbonate *CO_3^{2-}* Asymmetric Stretch v3	1419.61	1417.68	1419.61 and 1400.32	Multiple peaks: 1400-1460	Multiple peaks: 1400-1460	1417.68	Multiple peaks: 1430-1506	1419.61	This intense peak is due to the formation of calcite. Lower carbonate formation. Despite the dry carbonation treatment, RCP-LDC only shows the main calcite peak, similar to the Control. This is in sharp contrast to the plain RCP-DC sample which showed complex carbonate formation. This suggests the lime soaking may have passivated the aggregate surface or reduced its reactivity towards CO_2 gas during the treatment.
1112- 1116	Sulfate Containing Phases *SO_4^{2-}* Asymmetric Stretch	1116.78	1112.93	1112.93	1112.93	1116.78	1112.93	1116.78	1112.93	Indicates the presence of phases like **Ettringite (AFt)** or **Monosulfate (AFm).** All modified pastes show the presence of sulfate phases.
977- 958	Calcium Silicate Hydrate Gel *C-S-H* Asymmetric Stretch (Si-O)	975.98 and 958.62	966.34	968.27	987.55	948.98 and 966.34	964.41	977.91	(Strong, Broad) 968.27	These are the most critical bands, which confirm the formation of the primary binding phase, C-S-H. Excellent C-S-H polymerization is seen. The RCP-LDC sample exhibits a clear red shift 968.27, similar to the plain RCP and RCP-Ca samples. This suggests the combined physical effects of the aggregate and the presence of additional $Ca(OH)_2$ create optimal nucleation sites, enhancing the maturity of the C-S-H structure at 7 days.

APPENDIX F – SCANNING ELECTRON MICROSCOPE TEST WITH EDS MAPPING

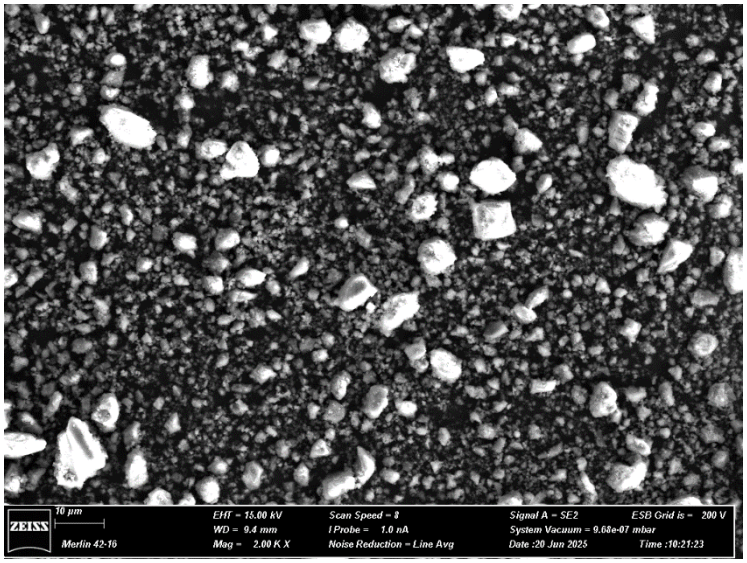
10 µm
EHT = 15.00 kV
WD = 9.4 mm
Mag = 2.00 K X
Scan Speed = 8
I Probe = 1.0 nA
Noise Reduction = Line Avg
Signal A = SE2
System Vacuum = 9.68e-07 mbar
ESB Grid is = 200 V
Date :20 Jun 2025
Time :10:21:23
ZEISS
Merlin 42-16

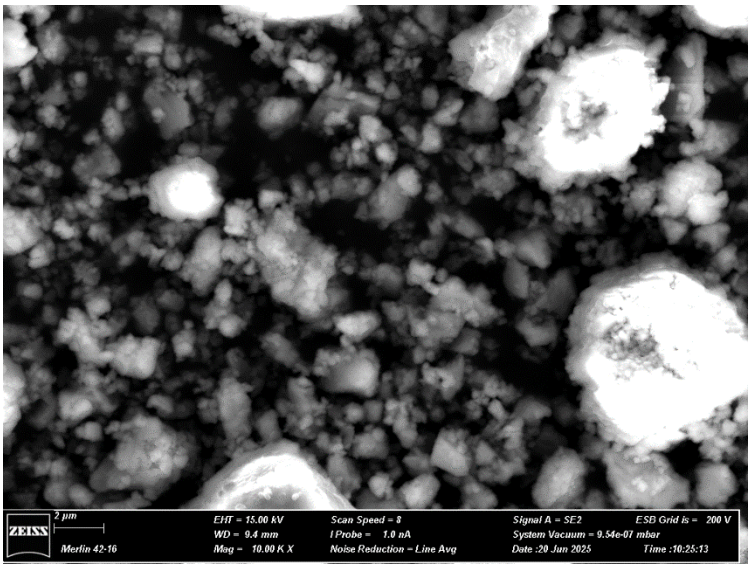
2 µm
EHT = 15.00 kV
WD = 9.4 mm
Mag = 10.00 K X
Scan Speed = 8
I Probe = 1.0 nA
Noise Reduction = Line Avg
Signal A = SE2
System Vacuum = 9.54e-07 mbar
ESB Grid is = 200 V
Date :20 Jun 2025
Time :10:25:13
ZEISS
Merlin 42-16

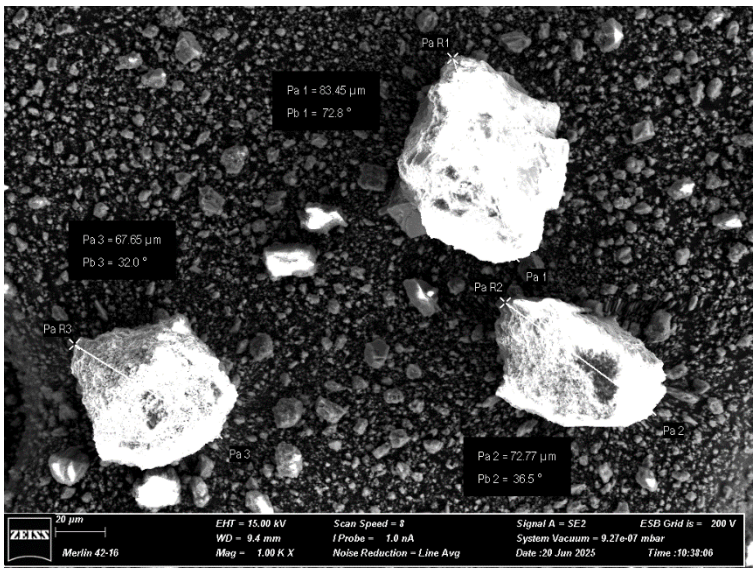
Pa R1
Pa 1 = 83.45 µm
Pb 1 = 72.8 °
Pa 3 = 67.65 µm
Pb 3 = 32.0 °
Pa R2
Pa 1
Pa R3
Pa 2
Pa 3
Pa 2 = 72.77 µm
Pb 2 = 36.5 °
20 µm
EHT = 15.00 kV
WD = 9.4 mm
Mag = 1.00 K X
Scan Speed = 8
I Probe = 1.0 nA
Noise Reduction = Line Avg
Signal A = SE2
System Vacuum = 9.27e-07 mbar
ESB Grid is = 200 V
Date :20 Jun 2025
Time :10:38:06
ZEISS
Merlin 42-16

RCP-CaDC POWDER – SEM IMAGES

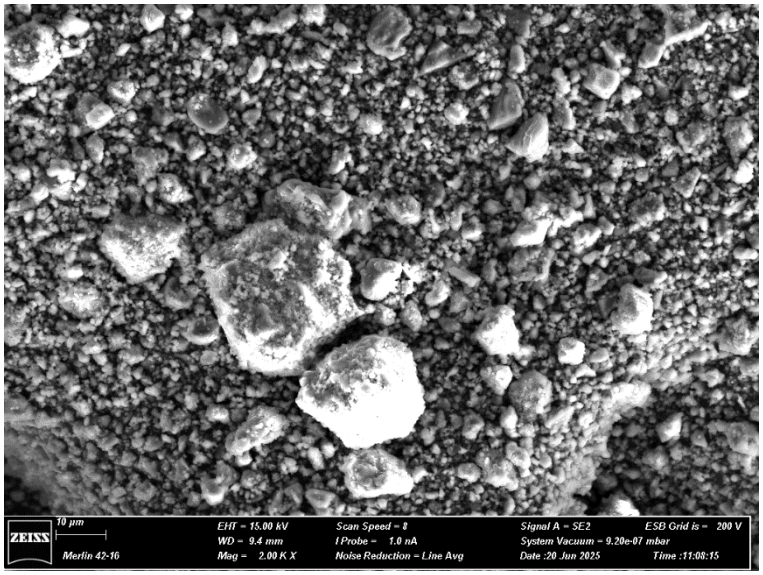

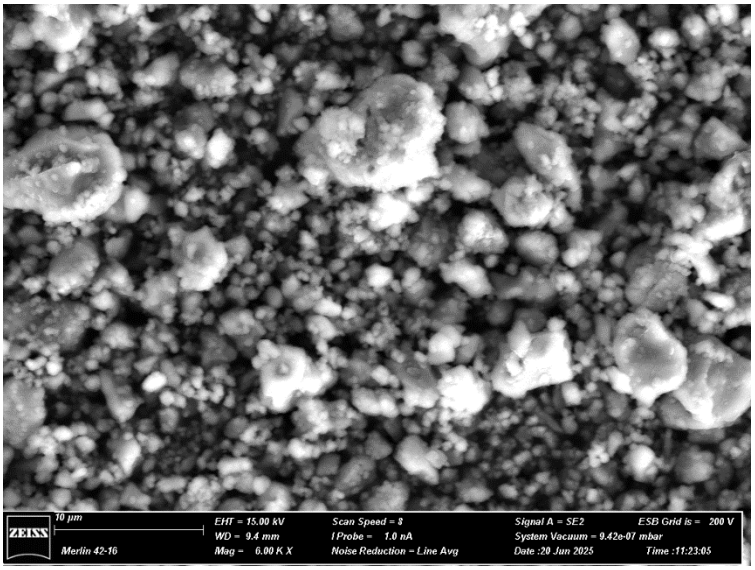

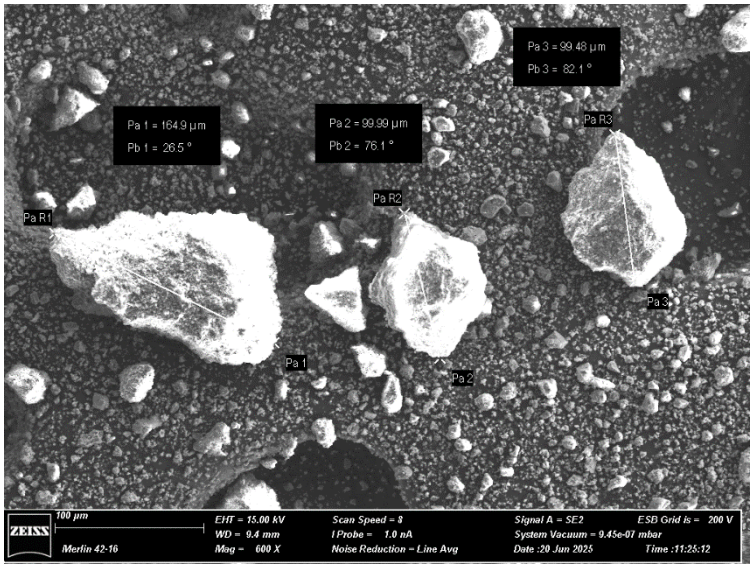

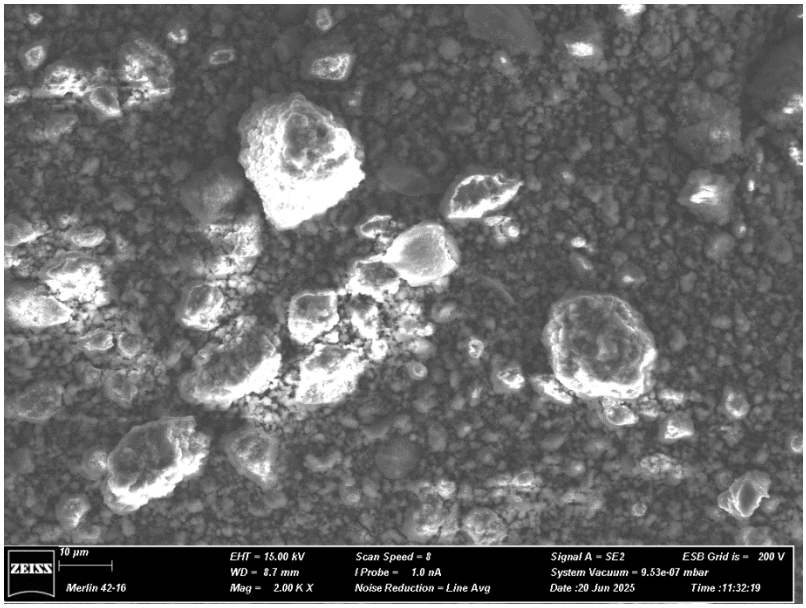
10 µm
ZEISS
Merlin 42-16
EHT = 15.00 kV
WD = 8.7 mm
Mag = 2.00 K X
Scan Speed = 8
I Probe = 1.0 nA
Noise Reduction = Line Avg
Signal A = SE2
System Vacuum = 9.53e-07 mbar
Date :20 Jun 2025
ESB Grid is = 200 V
Time :11:32:19

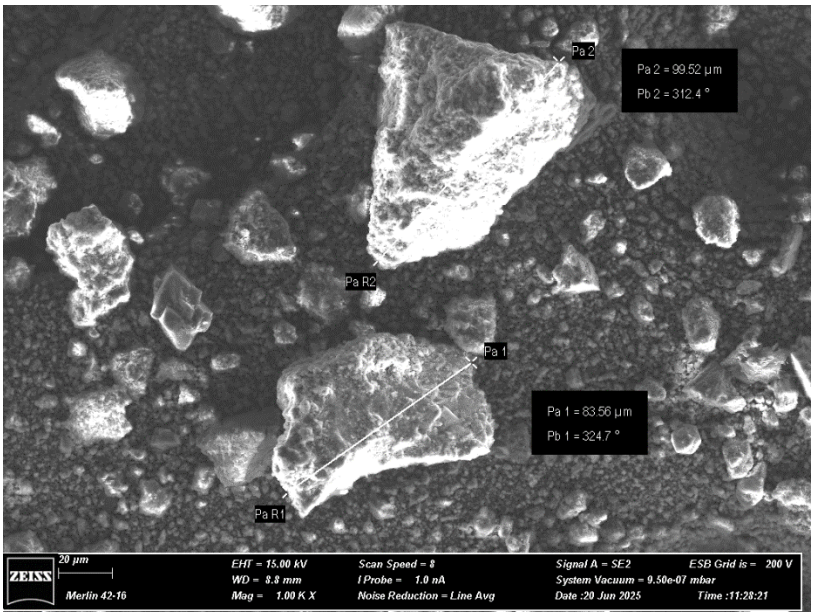
Pa 2
Pa 2 = 99.52 µm
Pb 2 = 312.4 °
Pa R2
Pa 1
Pa 1 = 83.56 µm
Pb 1 = 324.7 °
Pa R1
20 µm
ZEISS
Merlin 42-16
EHT = 15.00 kV
WD = 8.8 mm
Mag = 1.00 K X
Scan Speed = 8
I Probe = 1.0 nA
Noise Reduction = Line Avg
Signal A = SE2
System Vacuum = 9.50e-07 mbar
Date :20 Jun 2025
ESB Grid is = 200 V
Time :11:28:21

RCP-LDC POWDER – SEM IMAGES

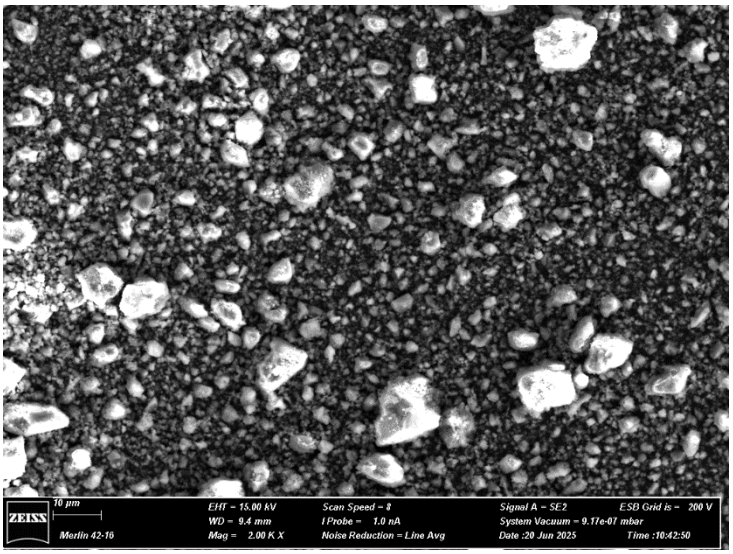

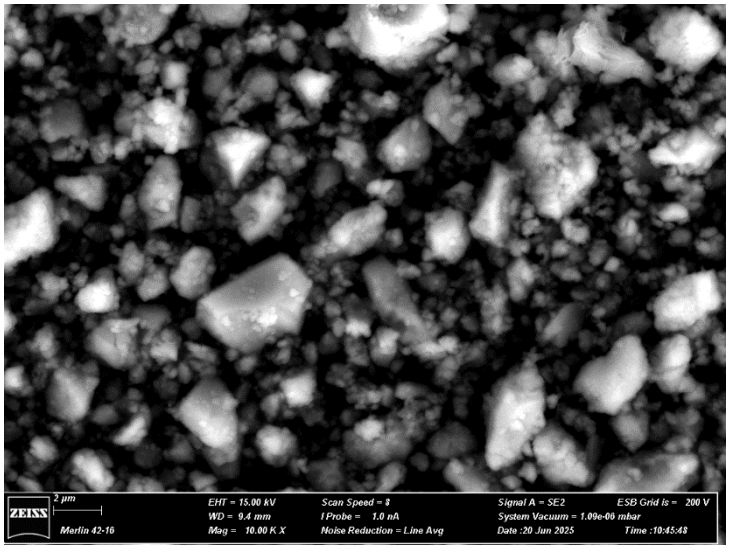

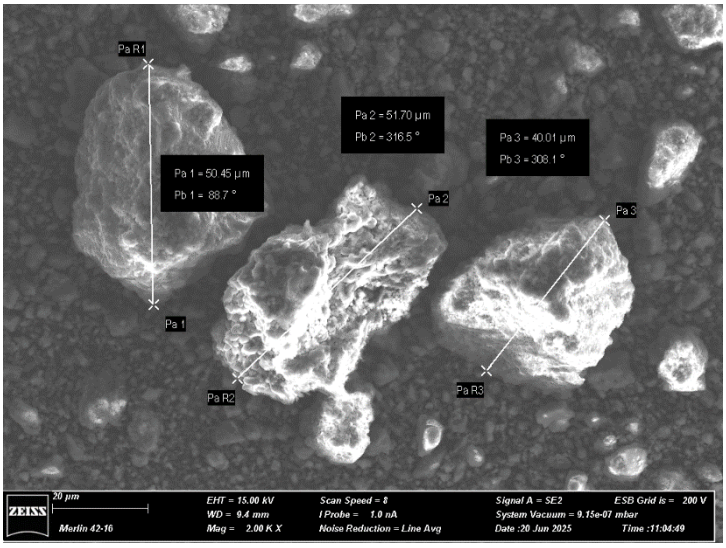

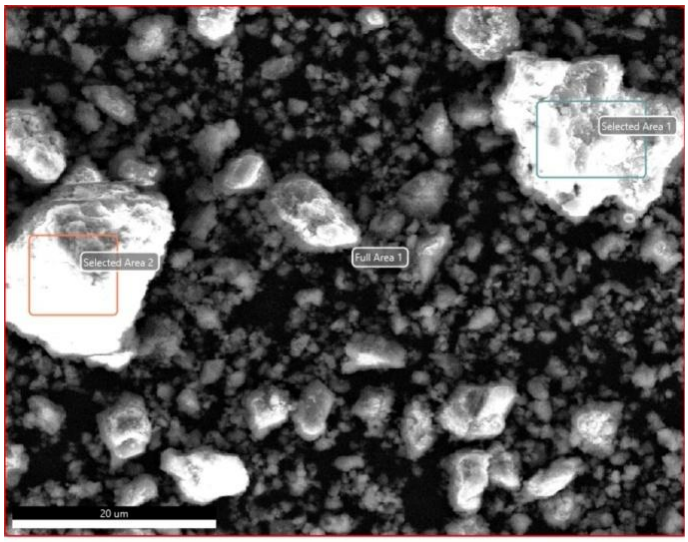

Element	Weight %	MDL	Atomic %	Error %
RCP | Area 2 | Full Area 1				
C K	34.08	0.08	50.90	5.71
O K	28.61	0.10	32.07	7.92
Mg K	0.15	0.08	0.11	20.38
Al K	0.37	0.08	0.24	9.80
Si K	1.11	0.08	0.71	4.60
Ca K	35.68	0.13	15.97	2.08
RCP | Area 2 | Selected Area 1				
C K	14.54	0.06	25.19	6.06
O K	38.49	0.07	50.07	7.74
Mg K	0.50	0.07	0.43	6.41
Al K	0.30	0.06	0.23	9.47
Si K	0.45	0.06	0.33	5.28
Ca K	45.72	0.11	23.74	1.98
RCP | Area 2 | Selected Area 2				
C K	12.74	0.09	24.17	6.14
O K	30.32	0.10	43.20	8.17
Mg K	0.12	0.08	0.11	20.67
Al K	0.13	0.07	0.11	22.85
Si K	0.65	0.07	0.52	5.54
Ca K	56.04	0.13	31.87	1.99

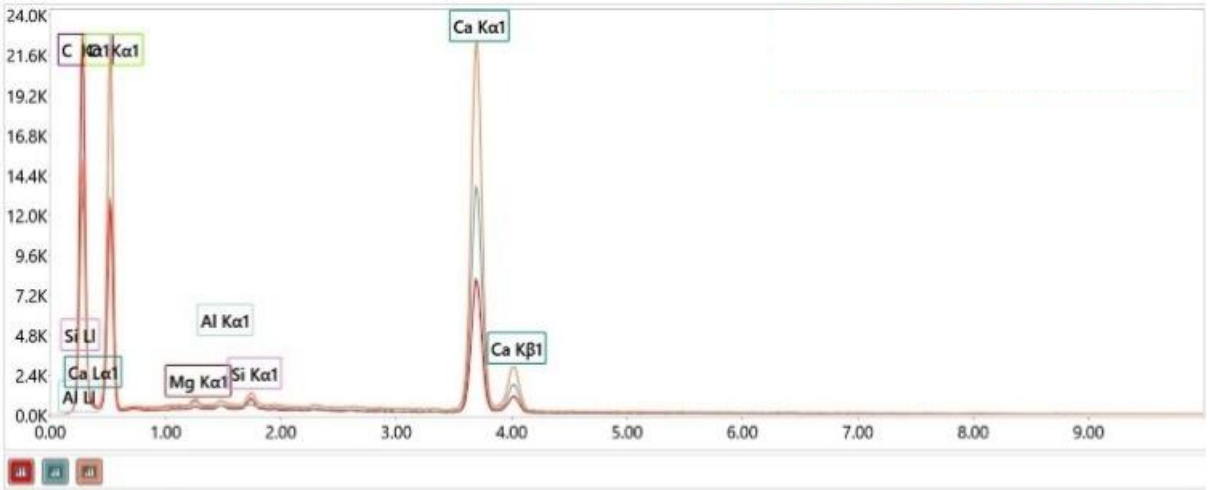

RCP-CaDC POWDER – EDS ANALYSIS

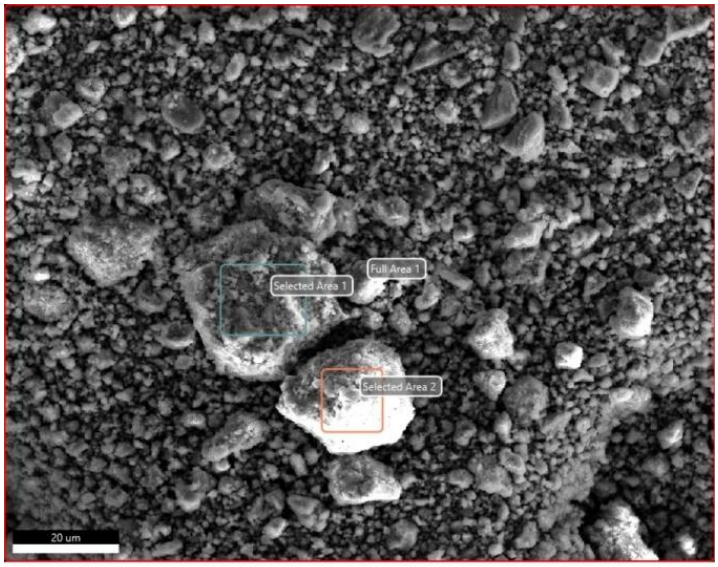

Element	Weight %	MDL	Atomic %	Error %
RCP_CaDC | Area 1 | Full Area 1				
C K	21.36	0.09	36.98	6.16
O K	27.66	0.11	35.94	8.11
Mg K	0.12	0.08	0.10	20.80
Al K	0.51	0.07	0.39	7.86
Si K	1.83	0.08	1.36	4.05
S K	0.53	0.09	0.34	8.47
Ca K	47.98	0.13	24.89	2.04
RCP_CaDC | Area 1 | Selected Area 1				
C K	17.28	0.09	31.14	6.83
O K	27.39	0.09	37.06	7.99
Mg K	0.16	0.07	0.14	13.24
Al K	1.55	0.06	1.24	4.38
Si K	5.79	0.07	4.46	2.91
S K	0.82	0.08	0.56	9.26
Cl K	0.29	0.08	0.18	15.48
Ca K	46.72	0.11	25.23	2.03
RCP_CaDC | Area 1 | Selected Area 2				
C K	17.67	0.08	32.28	6.61
O K	25.91	0.09	35.54	8.14
Mg K	0.14	0.07	0.13	16.73
Al K	1.00	0.07	0.81	5.46
Si K	3.44	0.07	2.69	3.32
S K	0.99	0.09	0.67	6.59
Cl K	0.40	0.09	0.25	9.33
Ca K	50.46	0.12	27.63	2.02

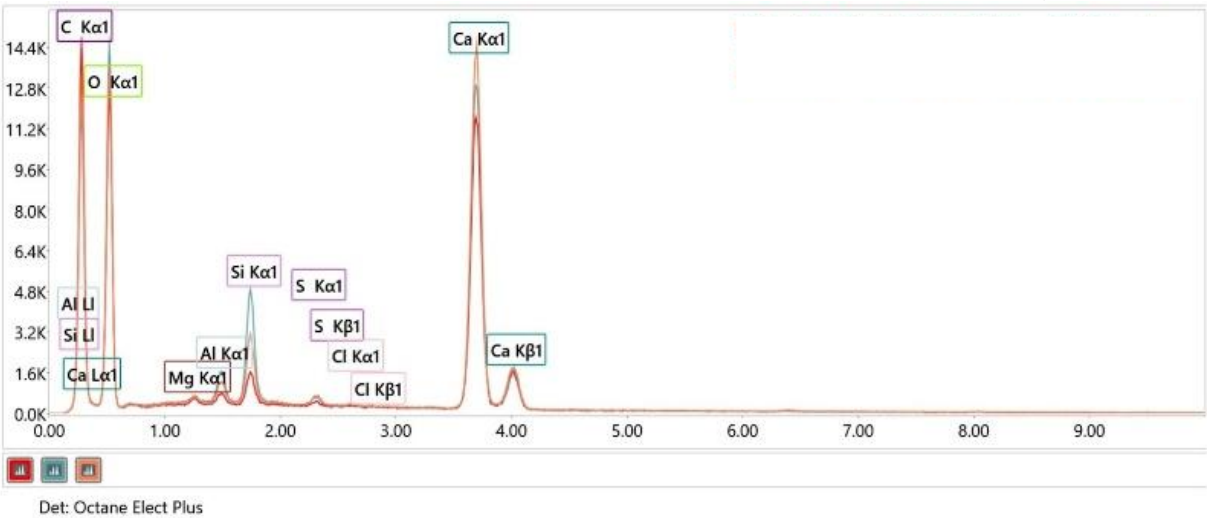

RCP-CaWC POWDER – EDS ANALYSIS

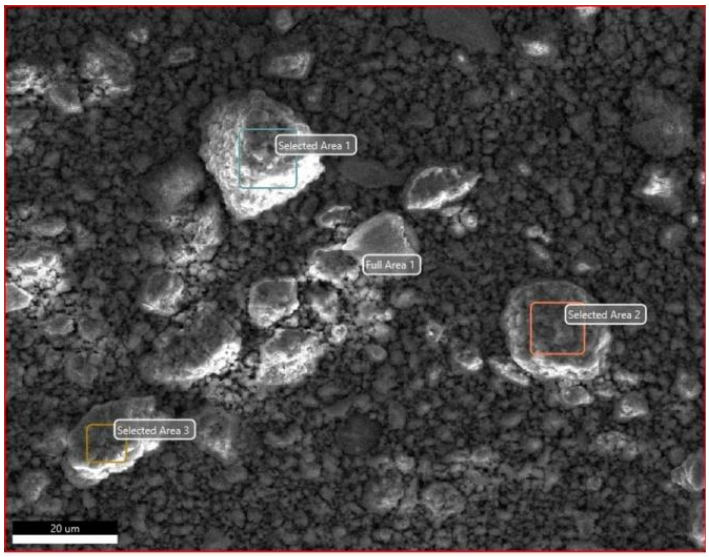

Element	Weight %	MDL	Atomic %	Error %
RCP_CaWC | Area 1 | Full Area 1				
C K	20.27	0.07	35.44	6.12
O K	28.20	0.12	37.01	8.12
Al K	0.48	0.07	0.37	7.94
Si K	1.92	0.07	1.43	4.06
Ca K	49.13	0.14	25.74	2.05
RCP_CaWC | Area 1 | Selected Area 1				
C K	17.17	0.08	29.95	6.34
O K	32.69	0.08	42.81	7.87
Mg K	0.24	0.04	0.21	8.96
Al K	1.11	0.04	0.86	4.78
Si K	3.00	0.05	2.24	3.23
Ca K	45.78	0.11	23.93	2.01
RCP_CaWC | Area 1 | Selected Area 2				
C K	14.89	0.07	27.96	6.22
O K	27.92	0.11	39.35	8.17
Al K	0.53	0.07	0.44	7.01
Si K	1.40	0.07	1.13	3.99
Cl K	0.31	0.09	0.20	12.03
Ca K	54.95	0.12	30.92	1.99
RCP_CaWC | Area 1 | Selected Area 3				
C K	16.67	0.06	29.54	5.91
O K	32.69	0.11	43.48	7.98
Mg K	0.12	0.06	0.10	20.24
Si K	0.26	0.07	0.20	15.32
Ca K	50.26	0.12	26.69	1.98

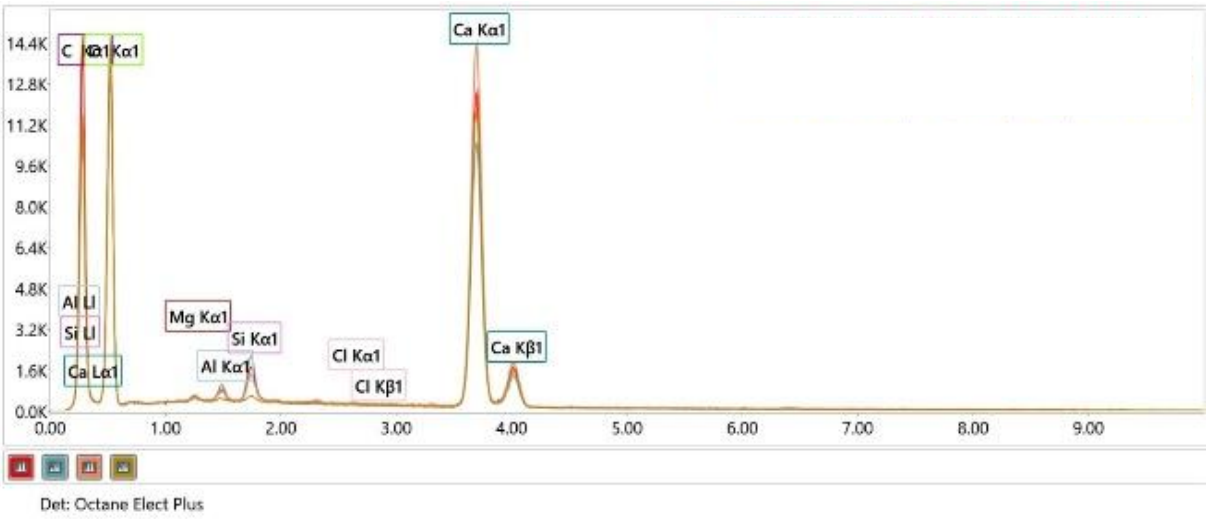

RCP-LDC POWDER – EDS ANALYSIS

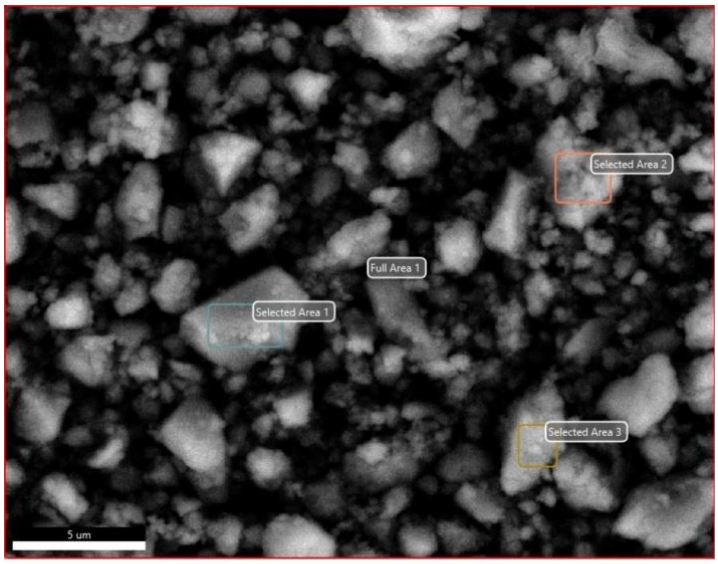

Element	Weight %	MDL	Atomic %	Error %
RCP_LDC | Area 1 | Full Area 1				
C K	34.79	0.08	51.62	5.71
O K	28.50	0.14	31.74	7.92
Al K	0.41	0.09	0.27	9.35
Si K	1.25	0.08	0.79	5.34
Ca K	35.05	0.15	15.58	2.10
RCP_LDC | Area 1 | Selected Area 1				
C K	19.06	0.07	32.26	5.84
O K	34.78	0.09	44.20	7.85
Al K	0.15	0.06	0.12	18.09
Si K	0.39	0.06	0.28	8.43
Ca K	45.62	0.11	23.14	2.00
RCP_LDC | Area 1 | Selected Area 2				
C K	22.98	0.05	36.95	6.00
O K	35.05	0.06	42.30	7.70
Mg K	0.38	0.06	0.31	6.53
Al K	0.63	0.06	0.45	6.15
Si K	0.99	0.07	0.68	4.11
S K	0.58	0.09	0.35	6.08
Ca K	39.38	0.11	18.97	2.00
RCP_LDC | Area 1 | Selected Area 3				
C K	19.53	0.05	31.96	6.04
O K	37.96	0.06	46.63	7.62
Mg K	0.72	0.06	0.58	6.05
Al K	0.51	0.06	0.37	6.39
Si K	0.83	0.06	0.58	4.25
S K	0.41	0.07	0.25	7.67
Ca K	40.04	0.11	19.63	2.00

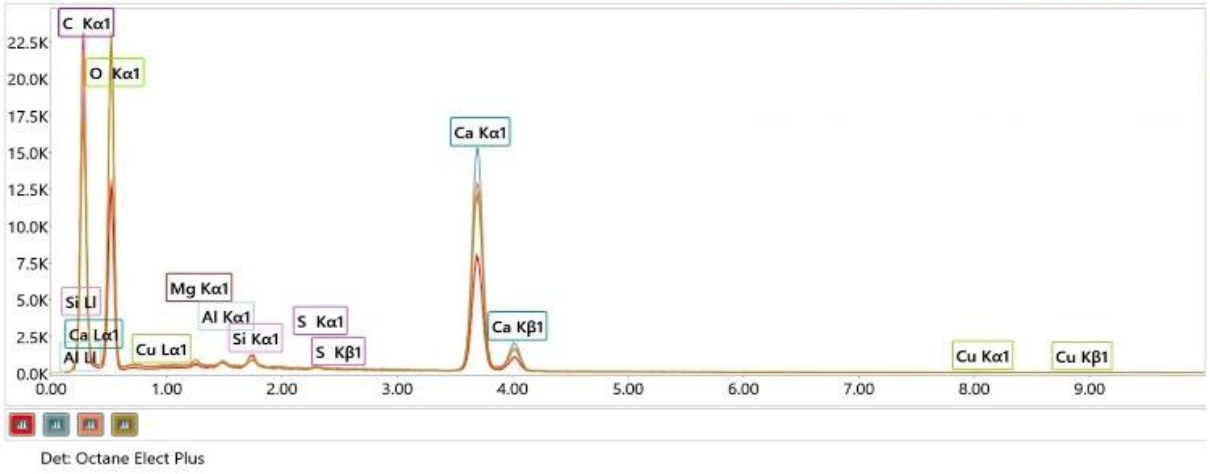

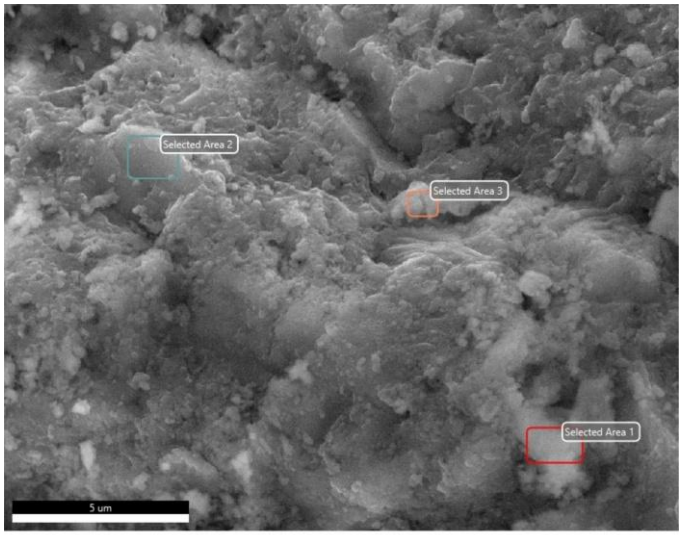

Element	Weight %	MDL	Atomic %	Error %
CEM_CON | Area 2 | Selected Area 1				
C K	5.86	0.12	11.46	7.56
O K	35.50	0.08	52.12	7.59
Mg K	0.61	0.07	0.59	6.15
Al K	3.20	0.06	2.78	3.75
Si K	5.54	0.06	4.63	3.01
S K	0.92	0.08	0.67	8.52
Cl K	0.21	0.08	0.14	21.11
K K	0.87	0.09	0.52	8.33
Ca K	43.41	0.11	25.44	2.06
Fe K	3.88	0.28	1.63	5.67
CEM_CON | Area 2 | Selected Area 2				
C K	5.61	0.12	11.32	7.22
O K	32.88	0.08	49.77	7.97
Mg K	0.36	0.07	0.36	8.58
Al K	0.84	0.06	0.76	5.85
Si K	4.74	0.07	4.09	3.02
S K	0.70	0.08	0.53	10.03
Cl K	0.19	0.09	0.13	19.92
K K	0.38	0.09	0.23	15.17
Ca K	54.30	0.12	32.81	1.98
CEM_CON | Area 2 | Selected Area 3				
C K	9.63	0.07	17.43	7.06
O K	38.69	0.06	52.55	7.58
Mg K	0.46	0.07	0.41	6.40
Al K	1.15	0.06	0.92	4.58
Si K	5.88	0.06	4.55	2.92
S K	1.23	0.09	0.84	3.93

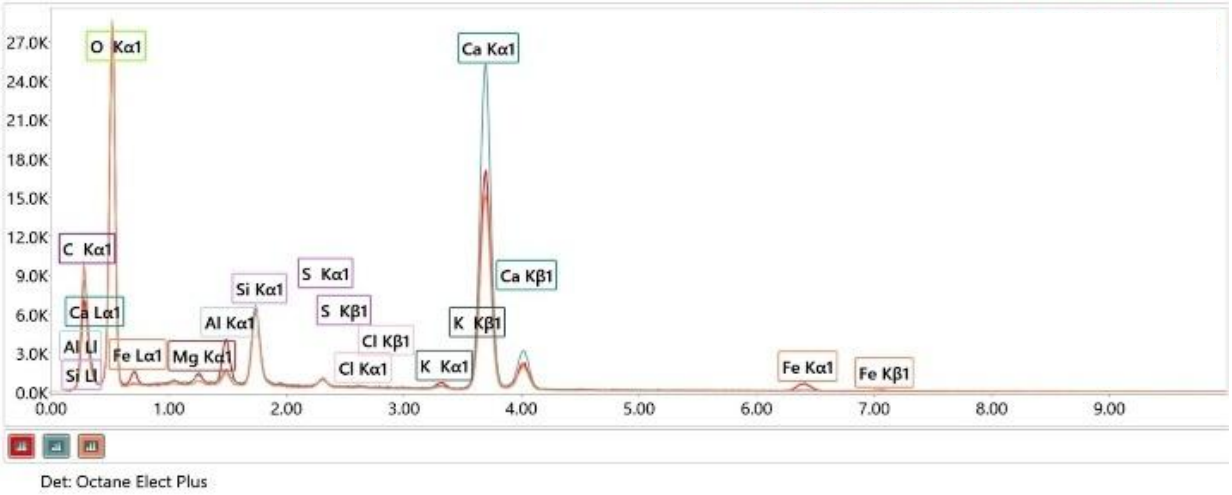

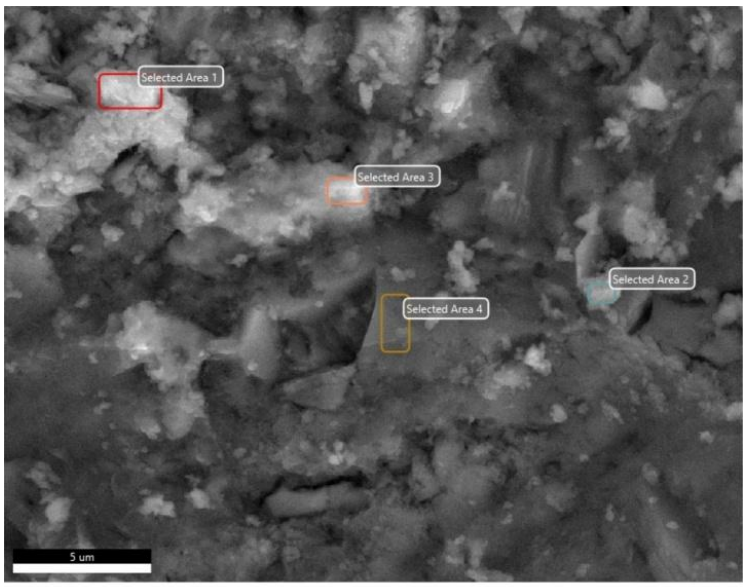

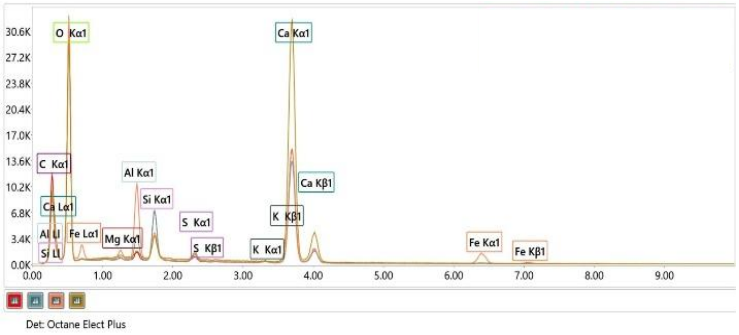

Element	Weight %	MDL	Atomic %	Error %
RCP_CaDC | Area 2 | Selected Area 1				
C K	10.72	0.09	18.94	7.08
O K	39.96	0.06	53.00	7.48
Mg K	0.37	0.06	0.32	7.44
Al K	1.17	0.06	0.92	4.49
Si K	6.33	0.06	4.78	2.88
S K	1.17	0.09	0.77	3.96
K K	0.61	0.09	0.33	10.38
Ca K	39.14	0.11	20.72	2.04
Fe K	0.54	0.27	0.21	22.19
RCP_CaDC | Area 2 | Selected Area 2				
C K	8.48	0.10	15.13	7.43
O K	41.21	0.06	55.21	7.35
Mg K	0.51	0.06	0.45	6.21
Al K	3.45	0.06	2.74	3.58
Si K	6.74	0.06	5.14	2.91
S K	1.55	0.08	1.04	3.76
K K	0.45	0.09	0.25	14.61
Ca K	37.09	0.11	19.84	2.05
Fe K	0.52	0.27	0.20	23.53
RCP_CaDC | Area 2 | Selected Area 3				
C K	7.54	0.08	14.55	7.71
O K	34.12	0.06	49.43	7.29
Mg K	0.89	0.06	0.84	5.49
Al K	8.30	0.06	7.13	3.28
Si K	3.25	0.06	2.68	3.47
S K	1.49	0.08	1.08	3.92
K K	0.28	0.09	0.17	17.09
Ca K	35.54	0.11	20.55	2.11
Fe K	8.59	0.27	3.56	3.72
RCP_CaDC | Area 2 | Selected Area 4				
C K	4.72	0.13	9.96	7.09
O K	30.33	0.08	47.97	8.16
Mg K	0.20	0.07	0.21	13.12
Al K	0.74	0.07	0.70	6.14
Si K	2.12	0.07	1.91	3.61
S K	1.13	0.10	0.89	4.06
Ca K	60.75	0.12	38.36	1.97

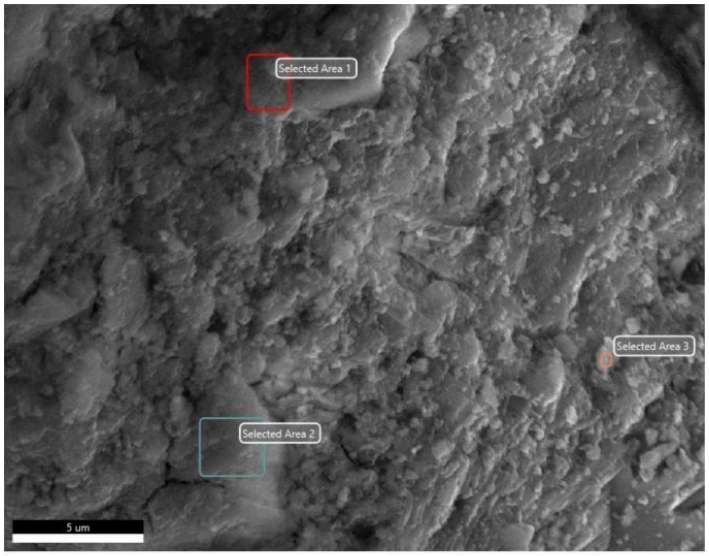

Element	Weight %	MDL	Atomic %	Error %
RCP_CaWC | Area 1 | Selected Area 1				
C K	6.94	0.11	13.72	7.84
O K	31.40	0.09	46.57	7.77
Mg K	0.37	0.08	0.36	8.57
Al K	2.52	0.06	2.21	3.93
Si K	9.23	0.06	7.80	2.87
S K	2.16	0.08	1.60	3.69
K K	0.56	0.10	0.34	13.76
Ca K	44.85	0.12	26.56	2.09
Fe K	1.97	0.27	0.84	10.45
RCP_CaWC | Area 1 | Selected Area 2				
C K	10.50	0.06	19.35	6.78
O K	35.88	0.08	49.66	7.78
Mg K	0.35	0.08	0.32	8.71
Al K	1.66	0.08	1.36	4.61
Si K	3.18	0.12	2.51	3.26
S K	0.88	0.14	0.61	4.60
K K	1.20	0.07	0.68	6.85
Ca K	45.76	0.11	25.28	2.04
Fe K	0.58	0.61	0.23	25.31
RCP_CaWC | Area 1 | Selected Area 3				
C K	8.21	0.12	15.04	7.49
O K	38.73	0.06	53.22	7.53
Mg K	0.48	0.06	0.44	6.33
Al K	1.63	0.07	1.33	4.32
Si K	7.76	0.05	6.07	2.81
S K	1.63	0.08	1.12	3.60
K K	0.31	0.18	0.17	18.30

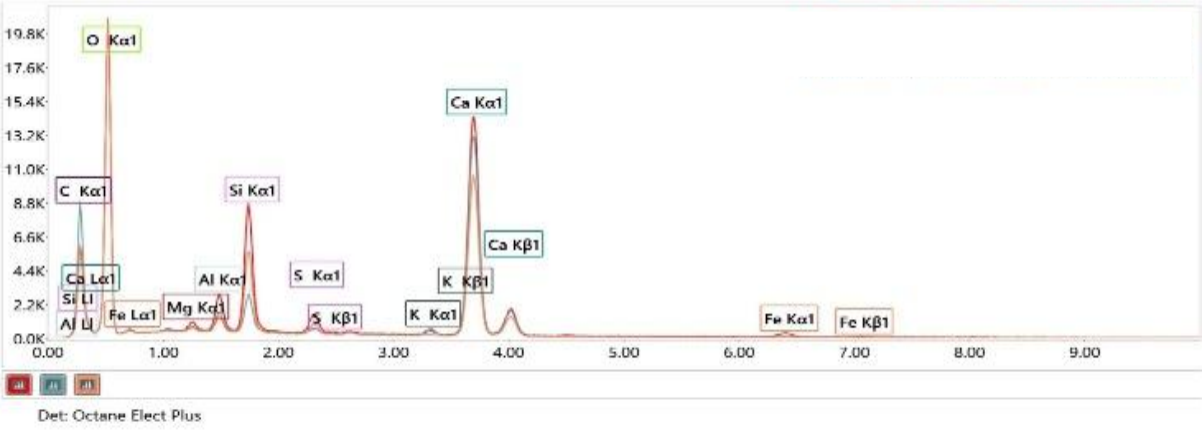

RCP-LDC PASTE – EDS ANALYSIS

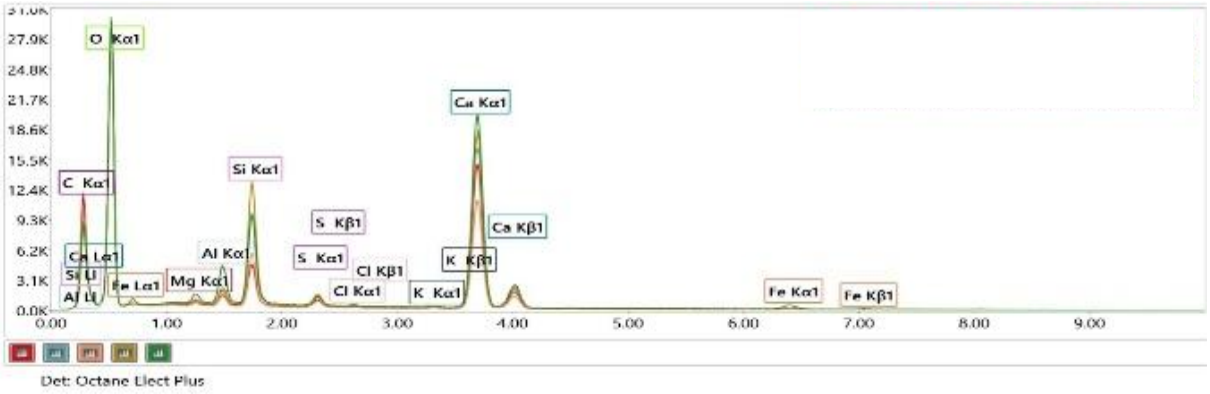

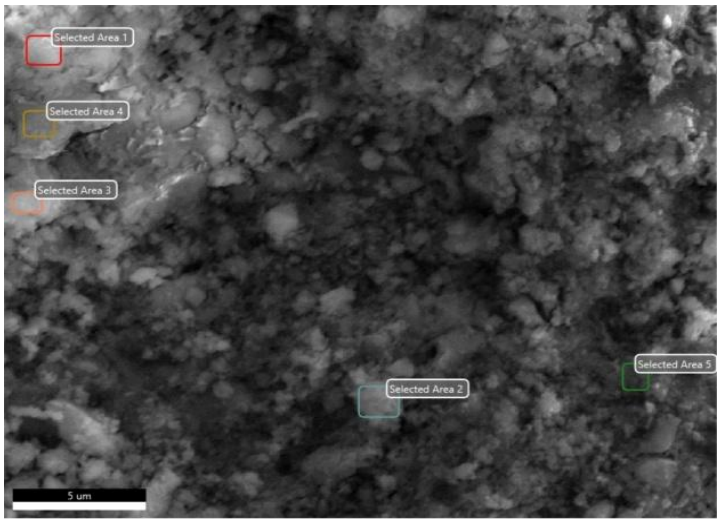

Element	Weight %	MDL	Atomic %	Error %
RCP_LDC | Area 1 | Selected Area 1				
C K	11.41	0.06	20.12	6.88
O K	39.66	0.07	52.49	7.54
Mg K	0.43	0.07	0.37	6.46
Al K	1.17	0.06	0.92	4.57
Si K	4.45	0.06	3.35	3.00
S K	1.23	0.09	0.81	3.89
K K	0.44	0.09	0.24	13.97
Ca K	40.66	0.11	21.48	2.04
Fe K	0.55	0.28	0.21	22.60
RCP_LDC | Area 1 | Selected Area 2				
C K	9.38	0.09	17.30	7.44
O K	36.03	0.07	49.90	7.61
Mg K	0.36	0.07	0.33	8.51
Al K	1.35	0.06	1.11	4.72
Si K	8.48	0.06	6.69	2.83
S K	1.58	0.08	1.09	4.36
Cl K	0.32	0.09	0.20	13.84
K K	0.42	0.09	0.24	15.72
Ca K	41.32	0.11	22.84	2.07
Fe K	0.77	0.34	0.30	18.42
RCP_LDC | Area 1 | Selected Area 3				
C K	10.89	0.09	18.66	7.20
O K	43.21	0.05	55.56	7.27
Mg K	0.57	0.06	0.48	6.17
Al K	1.47	0.06	1.12	4.35
Si K	6.44	0.06	4.72	2.81
S K	1.98	0.08	1.27	3.37
K K	0.40	0.08	0.21	14.69
Ca K	35.05	0.10	17.99	2.05

RCP_LDC | Area 1 | Selected Area 4			
7.55	0.09	14.39	7.79
34.23	0.07	49.02	7.66
0.31	0.09	0.29	8.61
1.49	0.07	1.27	4.57
10.84	0.06	8.84	2.74
1.74	0.10	1.24	3.86
0.38	0.10	0.22	15.87
42.76	0.11	24.44	2.08
0.70	1.25	0.29	20.08
RCP_LDC | Area 1 | Selected Area 5			
7.38	0.09	14.37	7.63
32.74	0.08	47.86	7.71
0.60	0.06	0.58	6.19
3.11	0.05	2.69	3.78
7.66	0.08	6.38	2.94
1.30	0.11	0.95	4.25
0.31	0.11	0.19	18.08
44.57	0.11	26.01	2.06
2.34	0.35	0.98	9.60

APPENDIX G – FLOW TABLE TEST

Flow Table - PASTE					
Mix Design	Diameter 1 *(mm)*	Diameter 2 *(mm)*	Mean Diameter *(mm)*	Standard Deviation	Standard Error
Cem Con	116.78	118.97	117.88	1.55	1.10
RCP	113.47	111.16	112.32	1.63	1.16
RCP-Ca	115.93	114.25	115.09	1.19	0.84
RCP-DC	112.49	109.91	111.20	1.82	1.29
RCP-WC	131.01	141.21	136.11	7.21	5.10
RCP-CaDC	125.26	124.62	124.94	0.45	0.32
RCP-CaWC	102.59	106.86	104.73	3.02	2.14
RCP-LDC	110.63	108.87	109.75	1.25	0.88

Flow Table - MORTAR					
Mix Design	Diameter 1 *(mm)*	Diameter 2 *(mm)*	Mean Diameter *(mm)*	Standard Deviation	Standard Error
Cem Con	196.79	195.97	196.38	0.580	0.41
RCP-CaDC	219.62	212.33	215.98	5.155	3.645
RCP-CaWC	207	209.88	208.44	2.036	1.44
RCP-LDC	226.55	231.93	229.24	3.804	2.69

APPENDIX H – COMPRESSIVE STRENGTH TEST

Compressive Strength - PASTE

7 Days									
Sample Type	Sample No.	Load *(kN)*	Length *(mm)*	Breadth *(mm)*	Area *(mm^2)*	Calc. Comp. Strength (*MPa)*	Average (*MPa)*	Comp. Strength *(MPa)*	Average *(MPa)*
Cem Con	Cube 1	25.90	19.99	19.79	395.60	65.47	67.53	64.74	69.39
	Cube 2	27.52	19.95	19.82	395.41	69.60		68.81	
	Cube 3	29.85	19.96	19.7	393.21	75.91		74.63	
RCP	Cube 1	28.40	19.97	19.55	390.41	72.74	70.81	71.01	74.34
	Cube 2	27.18	20.02	19.71	394.59	68.88		67.96	
	Cube 3	33.62	19.99	19.5	389.81	86.24		84.05	
RCP-Ca	Cube 1	27.85	20.05	19.78	396.59	70.22	71.01	69.63	63.42
	Cube 2	28.26	20.01	19.67	393.60	71.80		70.64	
	Cube 3	19.99	19.98	19.75	394.61	50.66		49.98	
RCP-DC	Cube 1	35.42	20.01	19.73	394.80	89.72	86.79	88.54	85.91
	Cube 2	33.38	20.01	19.89	397.99	83.8695		83.46	
	Cube 3	34.29	20.02	19.75	395.40	86.7234		85.73	
RCP-WC	Cube 1	33.68	20.03	19.82	396.99	84.84	53.80	84.2	63.69
	Cube 2	20.98	20	19.79	395.80	53.01		52.44	
	Cube 3	21.78	20.02	19.93	398.99	54.59		54.44	
RCP-CaDC	Cube 1	36.94	19.97	19.67	392.81	94.04	83.30	92.35	85.84
	Cube 2	33.14	20.04	19.75	395.79	83.73		82.85	
	Cube 3	32.93	20.02	19.85	397.40	82.86		82.32	
RCP-CaWC	Cube 1	28.82	20.00	19.62	392.40	73.45	78.90	72.04	72.49
	Cube 2	33.57	20.01	19.89	397.99	84.35		83.93	
	Cube 3	24.60	20.01	19.95	399.20	61.62		61.51	
RCP-LDC	Cube 1	38.6	20.00	19.88	397.60	97.08	94.54	96.50	89.99
	Cube 2	32.79	20.05	19.79	396.78	82.64		81.98	
	Cube 3	36.6	20.04	19.85	397.79	92.01		91.50	

21 Days									
Sample Type	Sample No.	Load *(kN)*	Length *(mm)*	Breadth *(mm)*	Area *(mm^2)*	Calc. Comp. Strength *(MPa)*	Average *(MPa)*	Comp. Strength *(MPa)*	Average (*MPa)*
Cem Con	Cube 1	38.40	20.04	19.78	396.39	96.87	110.47	94.89	104.65
	Cube 2	42.80	20.00	19.89	397.80	107.59		107.00	
	Cube 3	44.82	19.99	19.78	395.40	113.35		112.06	
RCP	Cube 1	42.67	20.06	19.75	396.18	107.70	103.08	106.67	101.90
	Cube 2	40.49	20.05	19.57	392.37	103.19		101.23	
	Cube 3	39.12	20.05	19.84	397.79	98.34		97.81	
RCP-Ca	Cube 1	41.53	20.06	19.88	398.79	104.14	83.20	103.84	89.61
	Cube 2	33.65	20.01	19.86	397.40	84.68		84.13	
	Cube 3	32.35	20.00	19.79	395.80	81.73		80.87	
RCP-DC	Cube 1	41.02	19.97	19.81	395.61	103.69	110.30	104.26	104.23
	Cube 2	36.48	20.05	19.84	397.79	91.70		91.52	
	Cube 3	46.74	20.06	19.93	399.80	116.91		116.91	
RCP-WC	Cube 1	37.16	20.06	19.66	394.38	94.22	95.27	92.89	93.81
	Cube 2	38.06	20.03	19.73	395.20	96.31		95.15	
	Cube 3	37.36	20.06	19.89	398.99	93.64		93.4	
RCP-CaDC	Cube 1	43.99	20.01	19.77	395.60	111.20	114.90	111.20	103.51
	Cube 2	47.13	20.05	19.82	397.39	118.60		118.60	
	Cube 3	31.76	20.04	19.63	393.39	80.73		80.74	
RCP-CaWC	Cube 1	40.85	20.08	19.92	399.99	102.13	106.64	102.13	101.26
	Cube 2	44.37	20.06	19.9	399.19	111.15		110.93	
	Cube 3	36.29	20	19.56	391.20	92.77		90.72	
RCP-LDC	Cube 1	22.89	20.02	19.55	391.39	58.48	87.04	59.09	77.55
	Cube 2	33.37	20.08	19.89	399.39	83.55		83.13	
	Cube 3	36.12	20	19.95	399.00	90.53		90.44	

Compressive Strength - MORTAR

7 Days							
Sample Type	Sample No.	Load *(kN)*	Length *(mm)*	Breadth *(mm)*	Area *(mm^2)*	Calc. Comp. Strength (*MPa)*	Average *(MPa)*
Cem Con	Cube 1	180.48	50.11	51.02	2556.61	70.59	72.18
	Cube 2	189.58	50.29	50.79	2554.23	74.22	
	Cube 3	179.90	49.88	50.29	2508.47	71.72	
RCP-CaDC	Cube 1	156.56	50.24	49.81	2502.45	62.56	60.32
	Cube 2	148.17	50.06	49.79	2492.49	59.45	
	Cube 3	147.55	50.10	49.96	2503.00	58.95	
RCP-CaWC	Cube 1	143.94	50.17	50.11	2514.02	57.25	55.95
	Cube 2	144.58	50.34	50.22	2528.07	57.19	
	Cube 3	136.73	50.84	50.35	2559.79	53.41	
RCP-LDC	Cube 1	136.18	50.57	50.17	2537.10	53.68	55.01
	Cube 2	147.07	50.35	50.14	2524.55	58.26	
	Cube 3	134.16	50.37	50.15	2526.06	53.11	

21 Days							
Sample Type	Sample No.	Load *(kN)*	Length *(mm)*	Breadth *(mm)*	Area *(mm^2)*	Calc. Comp. Strength *(MPa)*	Average *(MPa)*
Cem Con	Cube 1	190.32	49.86	50.21	2503.47	76.02	76.02
	Cube 2						
	Cube 3						
RCP-CaDC	Cube 1	168.41	50.63	49.57	2509.73	67.10	64.67
	Cube 2	159.18	50.20	49.64	2491.93	63.88	
	Cube 3	157.46	50.07	49.90	2498.49	63.02	
RCP-CaWC	Cube 1	136.90	50.17	50.50	2533.59	54.03	57.23
	Cube 2	150.94	50.22	50.15	2518.53	59.93	
	Cube 3	148.06	50.41	50.88	2564.86	57.73	
RCP-LDC	Cube 1	153.45	50.43	49.64	2503.35	61.30	57.33
	Cube 2	153.11	50.34	50.22	2528.07	60.56	
	Cube 3	126.71	50.43	50.13	2528.06	50.12	

APPENDIX I – VACUUM SATURATION POROSITY TEST

Vacuum Saturation Porosity Test - PASTE						
7 Days						
Sample Type	Sample No.	Oven-Dry Mass, W_d *(g)*	Buoyant Mass, W_b *(g)*	Saturated Surface-Dry Mass, W_s *(g)*	Permeable Porosity= $\frac{Ws-Wd}{Ws-Wb}$	Average Permeable Porosity
Cem Con	Cube 1	15.68	9.99	17.95	0.29	0.29
	Cube 2	15.36	9.79	17.58	0.28	
	Cube 3	15.70	10.00	18.01	0.29	
RCP	Cube 1	14.46	9.10	16.79	0.30	0.30
	Cube 2	14.46	9.12	16.79	0.30	
	Cube 3	14.39	9.08	16.74	0.31	
RCP-Ca	Cube 1	15.23	9.59	17.55	0.29	0.29
	Cube 2	14.93	9.35	17.17	0.29	
	Cube 3	14.99	9.43	17.27	0.29	
RCP-DC	Cube 1	14.68	9.28	16.95	0.30	0.30
	Cube 2	14.96	9.44	17.35	0.30	
	Cube 3	14.79	9.35	17.1	0.30	
RCP-WC	Cube 1	14.72	9.27	17.1	0.30	0.30
	Cube 2	14.53	9.12	16.87	0.30	
	Cube 3	14.90	9.37	17.31	0.30	
RCP-CaDC	Cube 1	14.74	9.42	16.98	0.30	0.30
	Cube 2	14.74	9.41	16.94	0.29	
	Cube 3	14.60	9.33	16.85	0.30	
RCP-CaWC	Cube 1	14.80	9.30	17.16	0.30	0.30
	Cube 2	14.55	9.16	16.92	0.30	
	Cube 3	14.63	9.19	16.98	0.30	
RCP-LDC	Cube 1	14.72	9.25	17.06	0.30	0.30
	Cube 2	14.63	9.21	16.93	0.30	
	Cube 3	14.6085	9.17	16.97	0.30	

21 Days						
Sample Type	Sample No.	Oven-Dry Mass, W_d *(g)*	Buoyant Mass, W_b *(g)*	Saturated Surface-Dry Mass, W_s *(g)*	Permeable Porosity= $\frac{Ws - Wd}{Ws - Wb}$	Average Permeable Porosity
Cem Con	Cube 1	15.54	9.84	17.69	0.27	0.27
	Cube 2	15.42	9.78	17.58	0.28	
	Cube 3	15.81	10.02	18.00	0.27	
RCP	Cube 1	15.32	9.67	17.53	0.28	0.28
	Cube 2	15.01	9.51	17.14	0.28	
	Cube 3	14.81	9.39	16.91	0.28	
RCP-Ca	Cube 1	14.90	9.31	17.09	0.28	0.28
	Cube 2	14.89	9.30	17.04	0.28	
	Cube 3	15.21	9.49	17.45	0.28	
RCP-DC	Cube 1	15.14	9.47	17.37	0.28	0.29
	Cube 2	15.10	9.42	17.39	0.29	
	Cube 3	15.24	9.51	17.53	0.29	
RCP-WC	Cube 1	14.76	9.25	17.04	0.29	0.29
	Cube 2	14.69	9.21	16.94	0.29	
	Cube 3	15.02	9.43	17.33	0.29	
RCP-CaDC	Cube 1	14.79	9.24	16.94	0.28	0.28
	Cube 2	15.00	9.35	17.17	0.28	
	Cube 3	15.05	9.42	17.21	0.28	
RCP-CaWC	Cube 1	14.39	9.00	16.55	0.29	0.29
	Cube 2	14.89	9.30	17.14	0.29	
	Cube 3	15.01	9.37	17.24	0.28	
RCP-LDC	Cube 1	14.65	9.18	16.86	0.29	0.28
	Cube 2	14.72	9.20	16.90	0.28	
	Cube 3	15.01	9.35	17.25	0.28	

Vacuum Saturation Porosity Test - MORTAR

7 Days						
Sample Type	Sample No.	Oven-Dry Mass, W_d *(g)*	Buoyant Mass, W_b *(g)*	Saturated Surface-Dry Mass, W_s *(g)*	Permeable Porosity= $\frac{Ws-Wd}{Ws-Wb}$	Average Permeable Porosity
Cem Con	Cube 1	291.34	185.36	309.91	284.66	0.15
	Cube 2	289.75	184.20	308.40	286.76	
	Cube 3	290.83	184.92	309.30	289.46	
RCP-CaDC	Cube 1	283.76	180.75	304.28	0.15	0.16
	Cube 2	280.04	178.54	300.16	0.15	
	Cube 3	284.5	181.51	304.00	0.15	
RCP-CaWC	Cube 1	284.66	181.35	305.06	0.16	0.16
	Cube 2	286.76	182.66	307.65	0.17	
	Cube 3	289.46	184.90	309.19	0.16	
RCP-LDC	Cube 1	284.66	181.35	305.06	281.49	0.17
	Cube 2	286.76	182.66	307.65	277.77	
	Cube 3	289.46	184.90	309.19	280.49	

21 Days						
Sample Type	Sample No.	Oven-Dry Mass, W_d *(g)*	Buoyant Mass, W_b *(g)*	Saturated Surface-Dry Mass, W_s *(g)*	Permeable Porosity= $\frac{Ws-Wd}{Ws-Wb}$	Average Permeable Porosity
Cem Con	Cube 1	290.25	185.13	307.71	0.14	0.14
	Cube 2	290.73	185.43	308.62	0.15	
	Cube 3	291.12	185.68	308.82	0.14	
RCP-CaDC	Cube 1	282.25	179.54	302.77	0.17	0.16
	Cube 2	285.53	181.78	305.35	0.16	
	Cube 3	284.17	180.88	303.95	0.16	
RCP-CaWC	Cube 1	282.81	179.94	302.85	0.16	0.17
	Cube 2	283.73	180.54	305.07	0.17	
	Cube 3	285.87	181.99	305.96	0.16	
RCP-LDC	Cube 1	278.15	177.12	298.04	0.16	0.16
	Cube 2	281.63	179.35	301.32	0.16	
	Cube 3	282.07	179.51	301.96	0.16	

APPENDIX J – DENSITY TEST

Density - PASTE

7 Days								
Sample Code	Sample No.	Length *(mm)*	Breadth *(mm)*	Height *(mm)*	Volume *(mm^3)*	Mass *(g)*	Density *(kg/m^3)*	Avg. Density *(kg/m^3)*
Cem Con	Cube 1	19.99	19.86	19.79	7856.66	16.85	2144.50	2165.50
	Cube 2	19.95	20.17	19.82	7975.40	17.26	2164.05	
	Cube 3	19.96	19.89	19.70	7820.99	17.11	2187.93	
RCP	Cube 1	19.97	19.92	19.55	7777.04	16.60	2134.51	2125.47
	Cube 2	20.02	20.03	19.71	7903.72	16.72	2115.84	
	Cube 3	19.99	19.97	19.50	7784.41	16.55	2126.07	
RCP-Ca	Cube 1	20.05	19.81	19.78	7856.43	16.40	2087.14	2117.51
	Cube 2	20.01	19.93	19.67	7844.38	16.71	2130.10	
	Cube 3	19.83	19.98	19.75	7825.02	16.71	2135.29	
RCP-DC	Cube 1	20.01	19.91	19.73	7860.41	16.82	2139.73	2127.86
	Cube 2	20.01	19.95	19.89	7940.08	16.94	2133.51	
	Cube 3	20.02	20.33	19.75	8038.38	16.96	2110.34	
RCP-WC	Cube 1	20.03	19.93	19.82	7912.10	16.68	2108.44	2114.67
	Cube 2	20.00	19.81	19.79	7840.80	16.80	2142.75	
	Cube 3	20.02	20.17	19.93	8047.80	16.84	2092.81	
RCP-CaDC	Cube 1	19.97	19.88	19.67	7809.06	16.90	2164.59	2160.70
	Cube 2	20.04	20.39	19.75	8070.16	17.23	2134.47	
	Cube 3	20.02	19.88	19.85	7900.25	17.25	2183.04	
RCP-CaWC	Cube 1	20.00	19.98	19.62	7840.15	16.95	2162.08	2158.68
	Cube 2	20.01	20.04	19.89	7975.90	16.99	2129.60	
	Cube 3	20.01	20.04	19.95	7999.96	17.47	2184.35	
RCP-LDC	Cube 1	20.00	20.07	19.88	7979.83	17.19	2154.14	2147.88
	Cube 2	20.05	20.12	19.79	7983.40	17.28	2164.82	
	Cube 3	20.04	20.10	19.85	7995.66	16.99	2124.69	

21 Days								
Sample Code	Sample No.	Length *(mm)*	Breadth *(mm)*	Height *(mm)*	Volume *(mm^3)*	Mass *(g)*	Density *(kg/m^3)*	Avg. Density *(kg/m^3)*
Cem Con	Cube 1	20.04	19.90	19.78	7888.18	17.37	2202.51	2184.52
	Cube 2	20.00	19.98	19.89	7948.04	17.32	2178.65	
	Cube 3	19.99	19.79	19.78	7825.01	17.00	2172.39	
RCP	Cube 1	20.06	20.06	19.75	7947.47	16.85	2120.41	2111.98
	Cube 2	20.05	19.99	19.57	7843.65	16.53	2108.06	
	Cube 3	20.05	20.02	19.84	7963.80	16.78	2107.46	
RCP-Ca	Cube 1	20.06	19.96	19.88	7959.90	17.21	2162.10	2168.18
	Cube 2	20.01	19.90	19.86	7908.23	17.36	2195.60	
	Cube 3	20.00	19.99	19.79	7912.04	16.99	2146.85	
RCP-DC	Cube 1	19.97	19.86	19.81	7856.73	17.07	2172.86	2173.90
	Cube 2	20.05	20.00	19.84	7955.84	17.32	2177.07	
	Cube 3	20.06	20.12	19.93	8043.89	17.47	2171.77	
RCP-WC	Cube 1	20.06	20.09	19.66	7923.09	17.32	2185.61	2169.90
	Cube 2	20.03	20.11	19.73	7947.31	17.15	2158.29	
	Cube 3	20.06	20.17	19.89	8047.70	17.43	2165.80	
RCP-CaDC	Cube 1	20.01	19.97	19.77	7900.09	17.24	2182.55	2182.85
	Cube 2	20.05	20.04	19.82	7963.72	17.50	2196.85	
	Cube 3	20.04	20.06	19.63	7891.31	17.12	2169.15	
RCP-CaWC	Cube 1	20.08	20.10	19.92	8039.87	17.46	2171.86	2165.93
	Cube 2	20.06	20.08	19.90	8015.82	17.48	2180.33	
	Cube 3	20.00	20.08	19.56	7855.30	16.85	2145.61	
RCP-LDC	Cube 1	20.02	20.01	19.55	7831.73	16.83	2149.49	2156.32
	Cube 2	20.08	20.01	19.89	7991.82	17.29	2163.41	
	Cube 3	20.00	20.04	19.95	7995.96	17.24	2156.05	

Density - MORTAR

7 Days								
Sample Type	Sample No.	Length *(mm)*	Breadth *(mm)*	Height *(mm)*	Volume *(mm^3)*	Mass *(g)*	Density *(kg/m^3)*	Avg. Density *(kg/m^3)*
Cem Con	Cube 1	50.33	50.00	50.64	127435.56	311.38	2443.43	2437.34
	Cube 2	50.29	50.11	50.51	127286.81	310.14	2436.54	
	Cube 3	50.03	50.33	50.76	127814.18	310.85	2432.05	
RCP-CaDC	Cube 1	50.17	50.52	49.82	126273.19	305.99	2423.24	2408.55
	Cube 2	50.17	50.81	49.34	125774.45	301.92	2400.49	
	Cube 3	50.26	50.71	49.86	127077.41	305.23	2401.92	
RCP-CaWC	Cube 1	50.21	50.92	49.84	127425.59	306.76	2407.37	2401.84
	Cube 2	50.74	50.96	49.81	128794.24	309.31	2401.58	
	Cube 3	50.35	50.64	50.82	129576.97	310.54	2396.57	
RCP-LDC	Cube 1	50.21	50.71	50.09	127536.61	303.22	2377.51	2390.97
	Cube 2	50.41	50.20	49.31	124783.00	298.85	2394.96	
	Cube 3	50.68	50.33	49.41	126031.29	302.53	2400.44	

21 Days								
Sample Type	Sample No.	Length *(mm)*	Breadth *(mm)*	Height *(mm)*	Volume *(mm^3)*	Mass *(g)*	Density *(kg/m^3)*	Avg. Density *(kg/m^3)*
Cem Con	Cube 1	50.30	50.21	50.11	126555.96	308.75	2439.63	2438.89
	Cube 2	50.01	50.45	50.59	127638.80	309.61	2425.67	
	Cube 3	50.14	50.19	50.20	126329.64	309.68	2451.36	
RCP-CaDC	Cube 1	50.13	50.82	49.55	126233.91	304.37	2411.16	2419.82
	Cube 2	50.82	50.26	49.35	126050.42	306.83	2434.18	
	Cube 3	50.89	50.17	49.56	126534.18	305.47	2414.13	
RCP-CaWC	Cube 1	50.54	50.17	49.97	126703.52	304.38	2402.30	2412.83
	Cube 2	50.76	50.25	49.69	126743.79	306.67	2419.61	
	Cube 3	50.63	50.42	49.84	127229.79	307.46	2416.57	
RCP-LDC	Cube 1	50.21	50.29	50.13	126581.30	299.53	2366.31	2391.15
	Cube 2	50.26	50.10	49.62	124944.45	302.93	2424.52	
	Cube 3	50.53	50.52	49.92	127434.56	303.63	2382.63	

APPENDIX K- SORPTIVITY

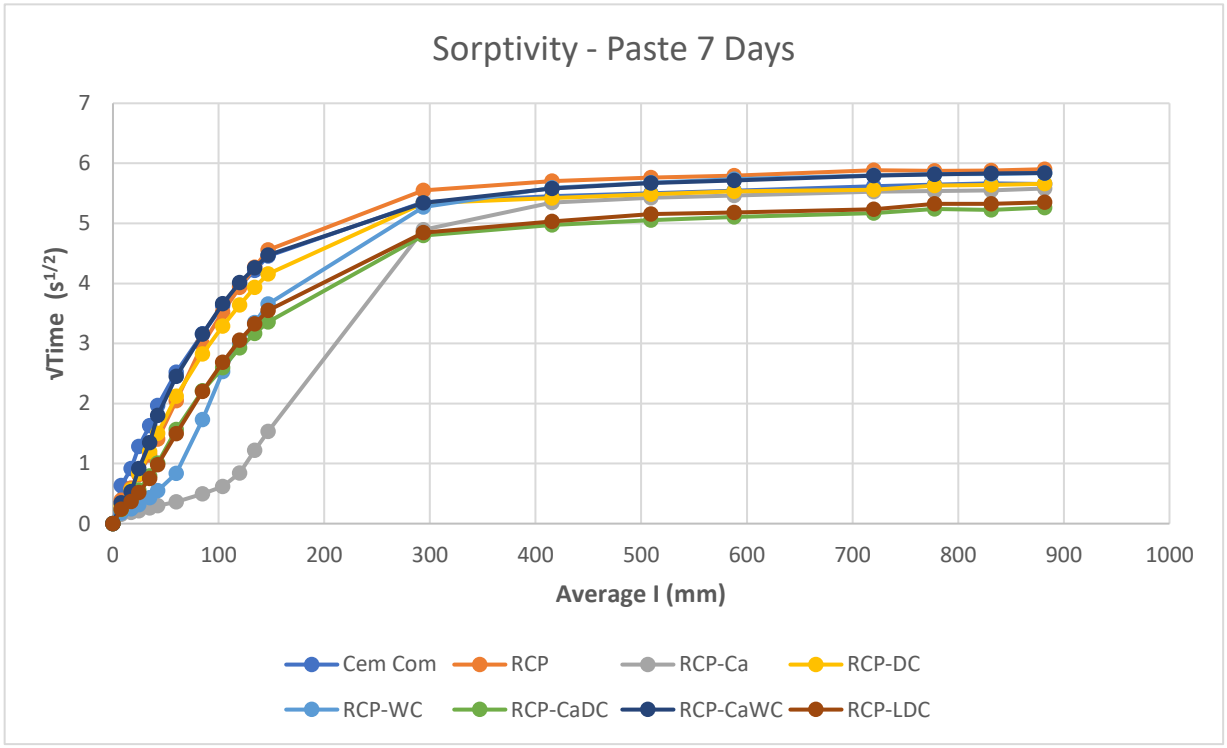
Sorptivity - Paste 7 Days
vTime (s^1/2)
Average I (mm)
Cem Com
RCP
RCP-Ca
RCP-DC
RCP-WC
RCP-CaDC
RCP-CaWC
RCP-LDC

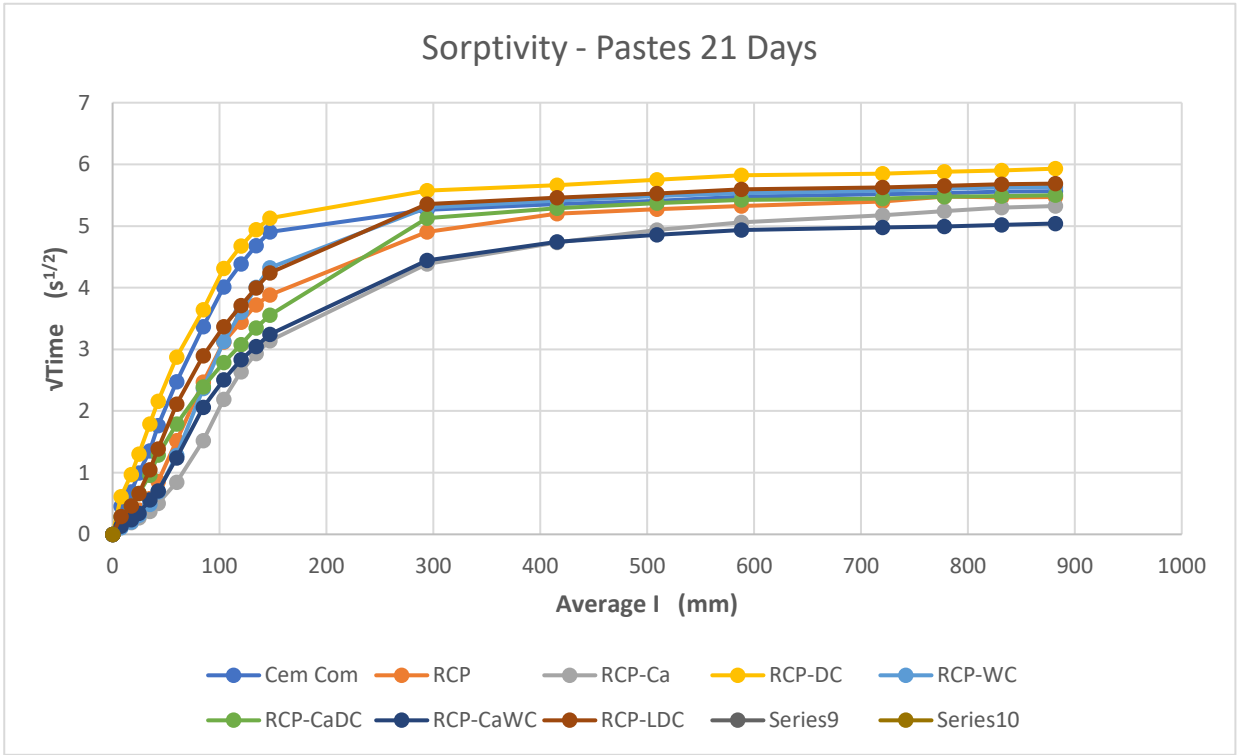
Sorptivity - Pastes 21 Days
vTime (s^1/2)
Average I (mm)
Cem Com
RCP
RCP-Ca
RCP-DC
RCP-WC
RCP-CaDC
RCP-CaWC
RCP-LDC
Series9
Series10

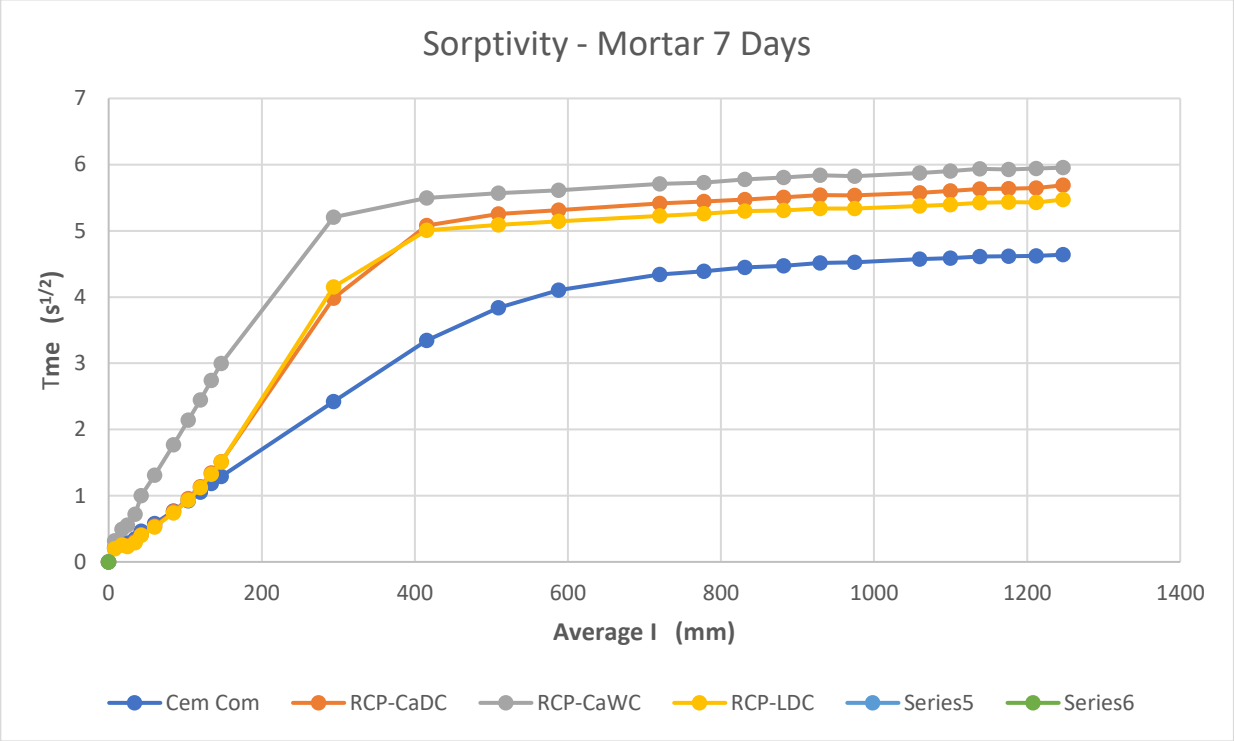
Sorptivity - Mortar 7 Days
Tme (s1/2)
Average I (mm)
0
1
2
3
4
5
6
7
0
200
400
600
800
1000
1200
1400
Cem Com
RCP-CaDC
RCP-CaWC
RCP-LDC
Series5
Series6

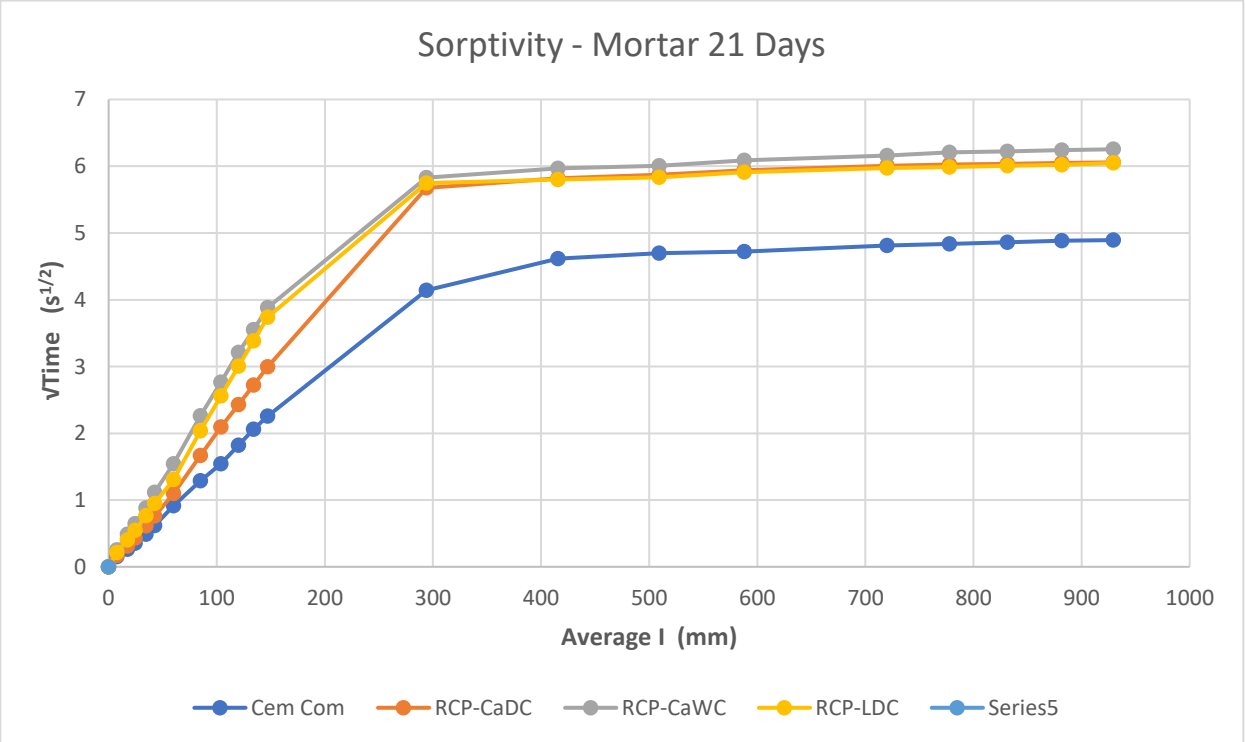
Sorptivity - Mortar 21 Days
√Time (s1/2)
Average I (mm)
0
1
2
3
4
5
6
7
0
100
200
300
400
500
600
700
800
900
1000
Cem Com
RCP-CaDC
RCP-CaWC
RCP-LDC
Series5

APPENDIX L – ULTRASONIC PULSE VELOCITY TEST

UPV - MORTAR

7 Days							
Sample Type	Sample No.	Path Length *(mm)*	Path Length *(km)*	Transit Time *(micro sec)*	Transit Time *(sec)*	Pulse Velocity *(km/s)*	Avrg. Pulse Velocity *(km/s)*
Cem Con	Cube 1	50.03	0.00	11.00	0.00	4.55	4.44
	Cube 2	50.01	0.00	10.80	0.00	4.63	
	Cube 3	49.72	0.00	12.00	0.00	4.14	
RCP-CaDC	Cube 1	50.45	0.00	10.90	0.00	4.63	4.62
	Cube 2	49.99	0.00	10.80	0.00	4.63	
	Cube 3	50.07	0.00	10.90	0.00	4.59	
RCP-CaWC	Cube 1	50.76	0.00	11.30	0.00	4.49	4.42
	Cube 2	50.68	0.00	11.50	0.00	4.41	
	Cube 3	50.00	0.00	11.50	0.00	4.35	
RCP-LDC	Cube 1	49.95	0.00	11.40	0.00	4.38	4.40
	Cube 2	49.97	0.00	11.40	0.00	4.38	
	Cube 3	50.54	0.00	11.40	0.00	4.43	

21 Days							
Sample Type	Sample No.	Path Length *(mm)*	Path Length *(km)*	Transit Time *(micro sec)*	Transit Time *(sec)*	Pulse Velocity *(km/s)*	Avrg. Pulse Velocity *(km/s)*
Cem Con	Cube 1	49.91	0.00	13.30	0.00	3.75	3.80
	Cube 2	-			0.00		
	Cube 3	50.05	0.00	13.00	0.00	3.85	
RCP-CaDC	Cube 1	50.19	0.00	11.60	0.00	4.33	4.26
	Cube 2	50.81	0.00	12.00	0.00	4.23	
	Cube 3	50.80	0.00	12.00	0.00	4.23	
RCP-CaWC	Cube 1	50.53	0.00	12.10	0.00	4.18	4.12
	Cube 2	50.65	0.00	11.90	0.00	4.26	
	Cube 3	50.57	0.00	12.90	0.00	3.92	
RCP-LDC	Cube 1	50.24	0.00	11.50	0.00	4.37	4.12
	Cube 2	50.43	0.00	12.70	0.00	3.97	
	Cube 3	50.48	0.00	12.60	0.00	4.01	